ADAR

Noncoding RNAs in Drug and Alcohol Research

Issue Editors

Stephanie Sillivan
Temple University,
United States

Sean Farris
University of Pittsburgh,
United States

frontiers | Publishing Partnerships

ADAR

Noncoding RNAs in Drug and Alcohol Research

ISSN 2674-0001
ISBN 978-2-8325-4295-8
DOI 10.3389/978-2-8325-4295-8

Noncoding RNAs have emerged as potent regulators of gene expression in the nervous system. Many noncoding RNAs are responsive to drug and alcohol exposure and manipulation of noncoding RNAs may impact drug seeking behavior. However, the field of noncoding RNAs in substance use disorder (SUD) is still understudied and many noncoding RNAs have not been examined in SUD patients or models of drug exposure. This Special Issue will feature studies that investigate noncoding RNAs in drug and alcohol research to highlight the mechanisms of noncoding RNA regulation that are associated with SUD. Examples include: noncoding RNAs in drug seeking phenotypes; noncoding RNAs as biomarkers; noncoding RNAs in HIV/SUD; and drug-induced regulation of noncoding RNAs. Work performed in model organisms, preclinical models or clinical populations is welcomed.

Table of contents

ADAR | Publishing Partnerships

TYPE Review
PUBLISHED 20 December 2022
DOI 10.3389/adar.2022.10807

OPEN ACCESS

EDITED BY
Stephanie Sillivan,
Temple University, United States

REVIEWED BY
Zheng-Xiong Xi,
National Institute on Drug Abuse (NIH), United States
Peter Hamilton,
Virginia Commonwealth University, United States

*CORRESPONDENCE
Gregory C. Sartor,
Gregory.sartor@uconn.edu

RECEIVED 29 July 2022
ACCEPTED 14 November 2022
PUBLISHED 20 December 2022

CITATION
Seyednejad SA and Sartor GC (2022), Noncoding RNA therapeutics for substance use disorder.
Adv. Drug. Alco. Res. 2:10807.
doi: 10.3389/adar.2022.10807

Noncoding RNA therapeutics for substance use disorder

Seyed Afshin Seyednejad[1,2] and Gregory C. Sartor[1,2]*

[1]Department of Pharmaceutical Sciences, University of Connecticut, Storrs, CT, United States, [2]Connecticut Institute for the Brain and Cognitive Sciences (CT IBACS), Storrs, CT, United States

Although noncoding RNAs (ncRNAs) have been shown to regulate maladaptive neuroadaptations that drive compulsive drug use, ncRNA-targeting therapeutics for substance use disorder (SUD) have yet to be clinically tested. Recent advances in RNA-based drugs have improved many therapeutic issues related to immune response, specificity, and delivery, leading to multiple successful clinical trials for other diseases. As the need for safe and effective treatments for SUD continues to grow, novel nucleic acid-based therapeutics represent an appealing approach to target ncRNA mechanisms in SUD. Here, we review ncRNA processes implicated in SUD, discuss recent therapeutic approaches for targeting ncRNAs, and highlight potential opportunities and challenges of ncRNA-targeting therapeutics for SUD.

KEYWORDS

microRNA, substance use disorder, noncoding RNA, lncRNA, SMIRNA, circRNA

Introduction

Substance use disorder (SUD) continues to be a worldwide public health crisis (1). Although many of the underlying mechanisms that drive compulsive drug use have been elucidated, the number of pharmacological agents that are approved to treat SUD remains stagnant (2). Current pharmacotherapies for SUD largely consist of small molecule modulation of neurotransmitter receptor activity (2). While these treatments have shown some clinical success, many promising therapeutic opportunities will likely be missed if this narrow focus continues. Thus, to move the field forward and to improve patient outcomes, novel pharmacological interventions for SUD are greatly needed.

As only 1%–2% of the human genome encodes for protein (3, 4) and many proteins lack druggable sites for small molecules (5), researchers are turning to nucleic acid-based treatments to target previously undruggable mechanisms. The recent progress in nucleic acid chemistry, bioinformatic approaches, and delivery systems has dramatically improved several issues associated with stability, specificity, and tolerability of RNA-targeting drugs (6). These advancements have resulted in successful clinical trials and recent approvals of nucleic acid-based therapeutics by the Food and Drug Administration (FDA) and the European Medicines Agency (EMA) for various disorders (7, 8). Additional factors contributing to the rising interest and growth in nucleic acid-based therapeutics include rationale design, rapid optimization and adaptability to evolving targets, high selectivity, and potentially longer half-life leading to infrequent administration (7, 8). While many of these initial therapies aimed to modulate protein-coding transcripts, more recently, there has been a rising interest in

developing nucleic acid-based drugs that target noncoding RNAs (ncRNAs), given their significant roles in cell type-specific biological processes in both health and disease (9).

In animal models of SUD, several ncRNAs have been shown to play functional roles in drug-seeking behaviors (10), and in humans, many genetic variants linked to SUD are located within noncoding regions of the genome (11). Thus, as the number of putative ncRNA targets in SUD continues to grow, nucleic acid-based therapeutics will likely be required to modulate these novel mechanisms. In this review, we describe different ncRNA classes involved in SUD, provide an overview of the modalities used to manipulate ncRNAs, and highlight ncRNA-based treatment strategies for SUD. We also discuss the ongoing challenges of ncRNA targeting and provide future perspectives for ncRNA-based therapeutics in SUD.

Noncoding RNAs in SUD

In humans and other primates, ncRNA expansion has fostered the intricate regulatory network required for brain evolution and cognitive advancement (12). ncRNAs are abundantly expressed in the central nervous system (CNS) where many are transcribed in a cell type-specific manner (13). In neuropsychiatric disorders, including SUD, changes in brain ncRNA expression have been associated with disease pathophysiology (13, 14), and several ncRNAs have been functionally examined in CNS disease models (15–17). In SUD, most of the research has focused on 3 classes of ncRNAs: microRNAs (miRs), long noncoding RNAs (lncRNAs), and more recently circular RNAs (circRNAs) (Table 1). In this section, we briefly review the mechanistic roles of miRs,

TABLE 1 Examples of ncRNA modulation in animal models of SUD.

ncRNA	Drug	Model	Region	Modality	Change	Reference
Let-7d	Alcohol	TBC	NAc	LV-let7d	↓ Intake	(18)
miR-30a-5p	Alcohol	TBC	mPFC	AdVs miR-30a-5p	↑ Intake	(19)
				LNA antimiR-30a-5p	↓ Intake	
miR-124a	Alcohol	TBC and CPP	DLS	LV-si124a	↓ Intake and CPP	(20)
				LV-miR124a	↑ Intake and CPP	
miR-137	Alcohol	EPM	AMG	LNA-antimiR-137	↓ Anxiety and consumption behaviors	(21)
miR-382	Alcohol	TBC	NAc	AdV-miR-382	↓ Intake	(22)
Let-7d	Cocaine	CPP	NAc	LV-silet7d	↑ CPP	(23)
				LV-miR-let7d	↓ CPP	
miR-124a	Cocaine	CPP	NAc	LV-si124	↑ CPP	(23)
				LV-miR-124	↓ CPP	
miR-181a	Cocaine	CPP	NAc	LV-si181a	↓ CPP	(23)
				LV-miR-181a	↑ CPP	
miR-206	Cocaine	CPP	NAc	AntagomiR-206	↑ CPP	(24)
miR-212	Cocaine	SA	DS	LV-miR212	↓ Intake	(25)
				LNA-antimiR-212	↑ Intake	
miR-495	Cocaine	SA	NAc	LV-miR495	↓ Seeking behavior	(26)
Gas5 lncRNA	Cocaine	CPP	NAc	AAV-Gas5 or HSV-Gas5	↓ Intake and CPP	(27)
circTmeff-1	Cocaine	CPP	NAc core	AAV-siR-circTmeff-1	↓ CPP	(24)
miR-29c	METH	OFT	NAc	AAV-miR-29c	↑ Locomotor activity	(28)
				AAV-antimiR-29c	↓ Locomotor activity	
miR-31-3p	METH	CPP	dHIP	AAV-miR-31-3p	↑ CPP	(29)
				AAV-antimiR-31-3p	↓ CPP	
miR-128	METH	OFT	NAc	AAV-miR128	↑Locomotor activity	(30)
				AAV-antimiR128	↓Locomotor activity	
miR-9	Oxycodone	SA	NAc	AAV-miR-9	↑ Intake	(31)
miR-132	Morphine	SA	DG	LV-miR-132	↑ Seeking behavior	(32)
circTmeff-1	Morphine	CPP	NAc core and shell	AAV-siR-circTmeff-1	↓ CPP	(33)
				AAV- circTmeff-1	No effect on CPP	
miR-221	Nicotine	EEM	mPFC	LV-miR-221	↑ Locomotor activity	(34)
BDNF-AS	Nicotine	SA	ILC	Anti BDNF-IV-AS ASO	↓ Drug-induced Reinstatement	(35)

AdV, adenoviral; AMG, amygdala; DG, dentate gyrus; DS, dorsal striatum; DLS, dorsolateral striatum; dHIP, dorsal hippocampus; EEM, enriched environment model; EPM, elevated plus maze; HSV, herpes simplex virus; ILC, infralimbic cortex; LV, Lentiviral; LNA, locked nucleic acid; METH, methamphetamine; mPFC, medial prefrontal cortex; OFT, open field test; SA, self-administering; siR, silencer; TBC, two-bottle choice.

lncRNAs, and circRNAs, and highlight potential therapeutic ncRNA targets in SUD.

MicroRNAs

MicroRNAs are a class of small noncoding RNAs with a highly conserved single-stranded sequence of approximately 22 nucleotides (36). Initially, miRs are transcribed into longer primary transcripts, called pri-miRs. The pri-miR is then cleaved by Drosha in the nucleus to produce the precursor miR (pre-miR) before being processed by Dicer in the cytosol to yield the mature miR. The mature miR is then loaded into the RNA-induced silencing complex (RISC) where it hybridizes to the three prime untranslated region (3′-UTR) of target mRNAs to mediate translational inhibition, cleavage, or degradation (36). With the ability to modulate 20%–50% of protein-coding genes, miRs are considered master regulators of many cellular activities (37–39). Notably, miRs play essential roles in brain development and neuroplasticity, and their dysregulation has been linked to the pathophysiology of most neuropsychiatric disorders (40–42).

In preclinical and clinical SUD studies, many miRs are dysregulated in reward-related brain regions following cocaine (25, 26, 43–48), amphetamine (49–51), methamphetamine (28–30, 52–57), nicotine (34, 58–63), opioid (31, 32, 64–71), and alcohol use (19, 20, 22, 72–83). SUD-associated miRs and their underlying mechanisms have been thoroughly reviewed elsewhere (14, 84). Of the miRs correlated with drug use, several have been shown to regulate the expression of known SUD targets that play important roles in maladaptive neuroplasticity and drug-seeking behaviors (e.g., *BDNF*, *CREB*, *MeCP2*, *CaMKIIa*) (14). In particular, miR-212, miR-132, miR-181, miR-9, and let-7 may be of interest for clinical targeting as altered expression of these miRs has been observed across multiple drugs of abuse in human and animal samples (14). In addition to miR activity in the brain, miR levels in SUD patient blood samples have been correlated with drug history and relapse (23, 85–94). Thus, circulating miRs may be a useful auxiliary measurement for diagnosis and treatment.

While there have been no clinical trials using miR-targeting therapeutics in SUD patients, several miRs have been explored functionally in preclinical SUD models (Table 1). For example, viral-mediated overexpression of miR-124a in the dorsolateral striatum enhanced alcohol-induced conditioned place preference (CPP) and increased alcohol intake, while silencing its expression attenuated CPP and alcohol consumption (20). In cocaine CPP experiments, overexpression of miR-124 and let-7d in the nucleus accumbens (NAc) attenuated cocaine CPP, whereas miR-181a overexpression enhanced CPP (95). The opposite effect on cocaine CPP was observed following knockdown of miR-124, let-7d, and miR-181a in the NAc. In self-administration studies, overexpression of miR-212 in the dorsal striatum attenuated compulsive cocaine intake in the extended-access self-administration procedure (25). Consistent with these observations, reduced levels of miR-212 in the striatum were associated with cocaine intake in addiction-prone but not addiction-resistant rats (96). In opioid self-administration experiments, overexpression of miR-132 in dentate gyrus increased morphine-seeking behaviors (32), while in a different study, overexpression of miR-9 in the NAc increased oxycodone intake and reduced inter-infusion interval (31). Overall, these results indicate that miRs are important therapeutic targets in SUD.

Long noncoding RNAs

Long noncoding RNAs (lncRNAs) are a diverse class of RNA molecules that are greater than 200 nucleotides in length and are generally classified based on their genomic location or function (e.g., intronic, intergenic, antisense, and enhancer) (97). Many lncRNAs are expressed in a cell-type and tissue-specific manner and play important regulatory roles in cells by acting as decoy, guide, scaffold, and/or signaling molecules (97, 98). For example, lncRNAs have been shown to mediate gene-specific epigenetic modifications by recruiting chromatin-modifying complexes to their targets (99, 100). At the post-transcriptional level, lncRNAs also fine-tune mRNA splicing, stability, and translation (97). In the mammalian nervous systems, many lncRNAs are highly enriched within the brain and play essential roles in the complex spatio-temporal gene expression mechanisms during brain development and neuroplasticity (98). Consequently, altered lncRNA expression is inherent to several brain diseases, including SUD (10).

One of the first attempts to examine a role for lncRNAs in SUD was made by analyzing lncRNA expression in the NAc of post-mortem heroin- and cocaine-using subjects (101). Relative to drug-free controls, an upregulation of *MIAT*, *NEAT1*, *MALAT1*, and *MEG3* lncRNAs was observed in the NAc of heroin-using subjects, and *MIAT*, *MALAT1*, *MEG3*, and *EMX2OS* upregulation was observed in the NAc of cocaine-using subjects. These well-studied lncRNAs contribute to various cellular processes, including GABA neuron neurogenesis, synapse formation, and cAMP signaling (102–104). In rodent studies, transcriptional profiling of lncRNAs in the NAc of methamphetamine-treated mice revealed thousands of lncRNAs that were altered, mostly downregulated by methamphetamine (105). Further bioinformatic analysis revealed that several of these lncRNAs act as potential cis- or trans-regulators of protein-coding genes involved in reward and

addiction pathways. In other experiments, lncRNAs, including *H19*, *Mirg*, *BC1*, *Lrap*, and *Gas5* have also been linked to SUDs (27, 106–110). Although most SUD-related lncRNA experiments have been limited to correlational data, Xu et al. recently revealed a functional role for the lncRNA *Gas5* in SUD models (111). In these studies, cocaine exposure (intraperitoneal injections and self-administration) reduced *Gas5* expression in the NAc, and in behavioral experiments, viral-mediated overexpression of *Gas5* in the NAc attenuated cocaine CPP and self-administration. At the transcriptomic level, *Gas5*-regulated gene expression patterns overlapped significantly with genes altered by cocaine exposure, an indication that *Gas5* regulates cocaine-induced transcriptional responses.

Natural antisense transcripts (NATs) are a class of lncRNAs that have also been implicated in SUD (112). NATs are transcribed from the opposite (antisense) strand of a coding gene and partially or completely overlap with the body, promoter, or enhancer region of the coding gene. Many genes involved in drug-induced neuroplasticity contain NATs (113), and the expression of multiple NATs such as *Bdnf-AS*, *Homer1-AS*, *Traf3ip2-AS1*, and *Prkcq-AS1* is altered by drugs of abuse (35, 113, 114). Therefore, NAT inhibition could be a particularly useful approach to increase the expression of SUD-related protein-coding genes. As a proof of concept, researchers have found that knockdown of *Bdnf-AS* in the infralimbic cortex *via* antisense oligonucleotides attenuated nicotine self-administration (115), and in other experiments, siRNA-mediated silencing of *Bdnf-AS* attenuated ketamine-induced neurotoxicity (116). Thus, with their high target specificity and their emerging roles in drug-seeking behaviors, lncRNAs are promising therapeutic targets for SUD.

Circular RNAs

Circular RNAs (circRNAs) are single-stranded noncoding RNA molecules produced from pre-mRNAs by a non-canonical splicing process called back-splicing, resulting in covalently closed RNA loops. Approximately 20% of mammalian genes express circRNAs, and while these ncRNAs are present in various organs, their enriched expression in the brain makes them an appealing target for the treatment of neuropsychiatric disorders (117, 118). circRNAs play important roles as transcriptional, post-transcriptional, and/or translational regulators through various mechanisms, most notably as a sponge for miRs (119). Compared to linear RNAs, circRNAs are highly stable (120), and thus may also mediate long-term effects in several disease states.

In several recent papers, a role for circRNAs in SUD has been explored. For example, RNA-sequencing analysis of post-mortem human NAc samples identified several circRNA–miR interactions that were associated with alcohol dependence (121), and in rodent studies, prenatal alcohol exposure was shown to alter the expression of brain circRNAs in a sex-specific manner (122). circRNAs are also dysregulated by opioids (24, 33, 123). In particular, CircTmeff-1, a sponge of miR-541-5p and miR-6934-3p, was observed to be functionally important for morphine CPP (24) and more recently for the reconsolidation of cocaine CPP (124). In other psychostimulant studies, 90 mouse striatal circRNAs were differentially expressed following cocaine self-administration (125), and 41 differentially expressed circRNAs were discovered in the dorsolateral prefrontal cortex of post-mortem human subjects with cocaine use disorder (126). Finally, in methamphetamine-induced neurotoxicity models, numerous circRNAs were significantly altered following methamphetamine treatment (127), and knockdown of circHomer1 alleviated methamphetamine-induced toxicity (128). Together, these initial experiments indicate an important and emerging role for circRNAs in drug-induced neuroadaptations.

Categories of ncRNA-targeting drugs

Due to significant improvements in safety, selectivity and delivery, RNA-based pharmaceuticals have received considerable attention and 14 RNA-based drugs have received FDA or EMA approval since 2015. See reference (129) for a comprehensive review of current FDA-approved RNA therapeutics. In addition to using nucleic acids to target RNAs, researchers have also developed small molecules that target RNA transcripts, termed small molecules interacting with RNA (SMIRNAs) (130). While the initial strategies to target RNAs focused on coding genes, many preclinical and clinical studies are now using similar approaches to target ncRNAs (Figure 1). In this section, we will briefly review the major categories of ncRNA-targeting drugs and highlight potential therapeutic opportunities for each platform in the context of SUD.

Antisense oligonucleotides

Antisense oligonucleotides (ASOs) are small, synthetic single-stranded nucleic acid molecules that hybridize with the target RNA to alter splicing or translation *via* steric block or RNA degradation (7). The smaller size and stringent binding specificity give ASOs a therapeutic advantage in CNS-related diseases compared to other nucleic acid drugs (Table 2). Indeed, several ASOs that are in clinical trials are being used to treat CNS-related diseases (131). Also, unlike siRNAs, ASOs are able to increase target protein expression by promoting alternative splicing, a strategy that is used clinically for Duchenne muscular dystrophy and spinal muscular atrophy (132).

Unmodified or naked ASOs display significant immunogenicity, low stability, and are rapidly cleared from circulation (133). Thus, chemical modifications are necessary to improve pharmacokinetics and pharmacodynamics of ASO

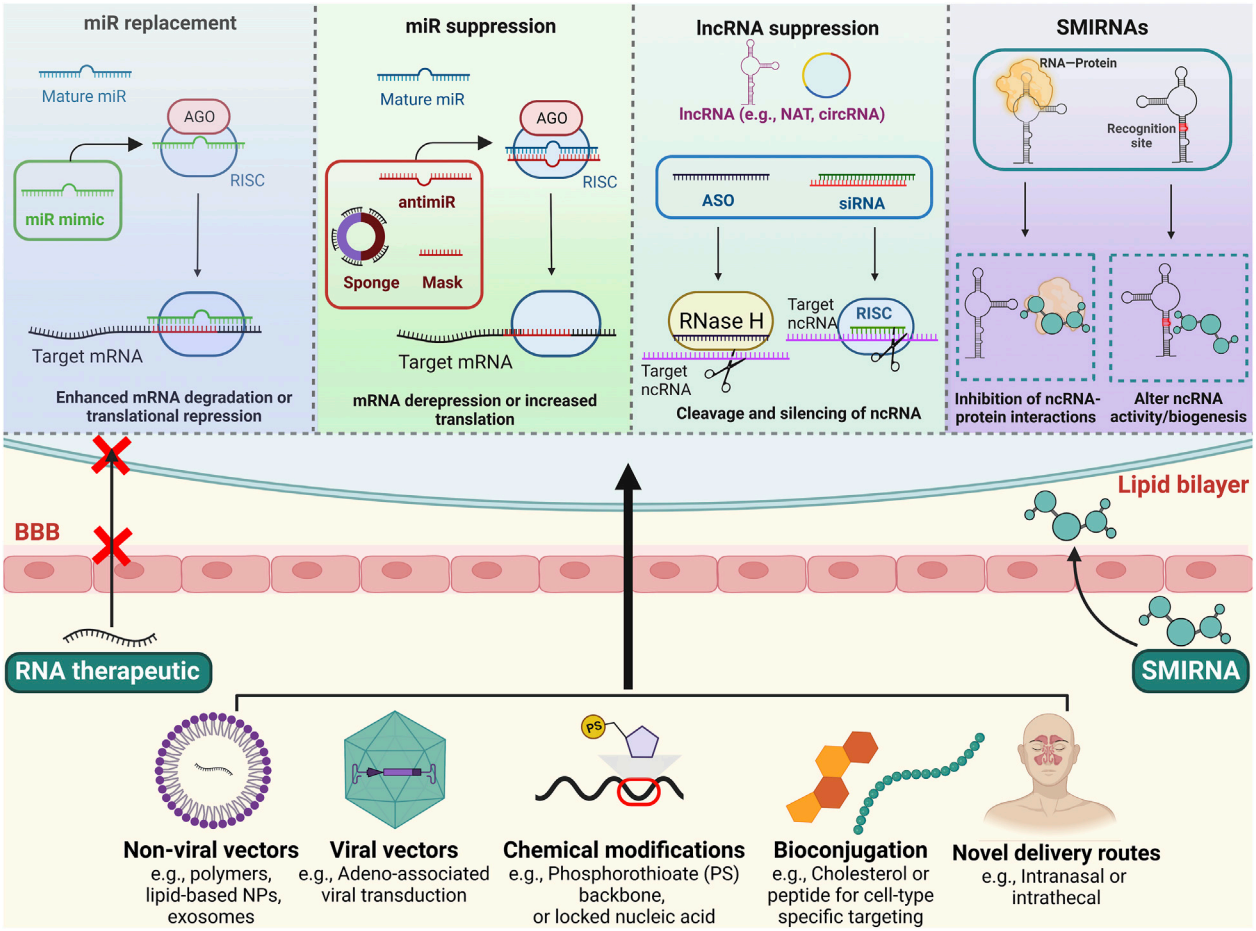

FIGURE 1
Schematic overview of RNA-targeting therapeutics and strategies to improve CNS delivery. Top: Multiple approaches exist for targeting ncRNAs. For miR replacement, miR mimics are used to imitate endogenous miRs activity, whereas antimiRs, miR masks and sponges inhibit endogenous miR activity. lncRNAs can be targeted with ASOs and siRNAs, leading to their degradation and silencing. SMIRNAs are small molecules that directly bind to ncRNAs or interfere with ncRNA-protein interactions. Bottom: Nanoparticles, viral vectors, chemical modifications, and/or bioconjugations can facilitate stability, cellular uptake, and brain delivery of the ncRNA therapeutics. Novel delivery routes, such as intranasal and intrathecal administration, may also promote CNS delivery and limit systemic toxicities. Some drug-like SMIRNAs are able to cross the blood-brain barrier without a delivery system *via* passive diffusion. Figure created using BioRender.

TABLE 2 Characteristics of RNA-targeting drugs for CNS indications.

Characteristics	ASOs	siRNAs	SMIRNAs
Target	Nucleic acid	Nucleic acid	Nucleic acid or protein
Effect on ncRNA	Increase/decrease activity	Decrease activity	Increase/decrease activity
Duration of effect	Days to weeks	Days to weeks	Hours
Specificity and Strength	Specific and potent	Specific and potent	Specificity and potency vary
Lead optimization	Rapid	Rapid	Slow
Drug-likeness	Chemical modifications needed	Chemical modifications and/or delivery systems needed	Drug-like
Route of Administration	Usually intrathecal	Usually intrathecal	Usually oral
Manufacturing cost	High cost but lower than siRNAs	High cost	Lower cost

pharmaceuticals (for a comprehensive review see (134)). Common ASO modifications include substitution of a phosphorothioate (PS) backbone and sugar moiety modifications at 2′ position (e.g., 2′-O-methyl, locked nucleic acid, LNA) (134). Though each type of chemically modified ASOs has advantages and disadvantages, in general, these modifications increase safety, stability, and affinity while reducing the need for delivery systems. However, because most ASOs and other nucleic acids are unable to cross the blood-brain barrier, intrathecal or intranasal administration is typically required to target the CNS (135). Currently, there is at least one ncRNA-targeting ASO undergoing clinical testing for Angelman syndrome (NCT05127226) after successful *in vitro* and *in vivo* investigations (136). A few SUD-associated lncRNAs (e.g., *MALAT1*, *MIAT*, and *BDNF-AS*) have been successfully targeted using ASOs in other preclinical disease models (137–141), but additional work is needed to determine if these or other ncRNA-targeting ASO formulations are effective in SUD models.

siRNAs

SiRNAs are short double-stranded RNAs that attach to RISC, unfold, and form Watson-Crick base pairing with the target RNA, leading to argonaute-induced degradation of the transcript (129). Like ASOs, chemical modifications to siRNAs have improved their safety and efficacy (142–144) and currently 5 siRNA-based drugs have received FDA or EMA approval (Patisiran, Givosiran, Lumasiran, Inclisiran, Vutrisiran). However, in contrast to some ASOs, siRNA platforms depend on the intracellular machinery for their effects, which may restrict the type and number of chemical modifications to the siRNA. Also, in some instances, siRNAs are not as effective at targeting nuclear RNAs compared to ASOs (145), and because of their larger size and negative charge, unmodified siRNAs require the use of a delivery agent to enter the cell (Table 2). To combat some of these limitations, researchers have developed siRNA prodrugs (siRibonucleic neutrals, siRNNs) that disguise the siRNAs' negative charge by replacing phosphodiesters with charge-neutral phosphotriesters (146). These siRNA prodrugs are able to cross the lipid bilayer, and once in the cell, the phosphotriester group is cleaved off by thioesterases, allowing for the knockdown to occur.

While most FDA-approved siRNA drugs target the liver, there has been a growing interest in using novel siRNA formulations to treat CNS-related disorders. For example, Regeneron Pharmaceuticals and Alnylam Pharmaceuticals recently announced a billion-dollar collaboration to develop siRNA-based drugs for CNS indications (147). Further supporting the usefulness of siRNA-based drugs for CNS uses, recent preclinical experiments identified novel, chemically modified siRNAs that exhibited safe, potent, and long-lasting gene silencing in the brain of rodents and nonhuman primates following intrathecal administration (148). Using systemic or direct brain injections, siRNA-targeting of ncRNAs has been achieved in animal models of SUD (124, 149, 150), Parkinson's disease (151, 152), Alzheimer's disease (153–155), epilepsy (156, 157) and stroke (158, 159). Thus, with recent FDA approvals, multiple ongoing, late-stage clinical tests, and promising preclinical data, siRNA-based therapeutics appear to have a promising future, but more testing of siRNA formulations for CNS indications is needed.

miR replacement/suppression

MiR targeting has been achieved using RNA interference approaches. For example, miR mimics are modified double-stranded RNA molecules that imitate endogenous miR activity and bind to the 3′UTR region of the target mRNAs (37). This approach leads to a downregulation of the target mRNAs *via* translational inhibition. On the other hand, antimiRs, miR sponges, and miR masking techniques are used to reduce miR activity. Structurally similar to ASOs, miR inhibitors or antimiRs prevent an endogenous miRs interaction with its target genes. These single-stranded molecules are usually modified using locked nucleic acid, peptide nucleic acids, or cholesterol (i.e., antagomiR) to improve stability, cellular uptake, and *in vivo* delivery (134, 160). To inhibit a family of miRs, miR sponges, synthetic transcripts that contain various complementary sequences that recognize the seed sequences of multiple miRs, have also been employed in preclinical studies (161–163). Finally, in a technique called miR masking, ASOs bind to 3′UTR sites on a specific mRNA and prevent its interaction with a complementary miR (21) (Figure 1).

In preclinical studies, researchers have demonstrated the effectiveness of antimiRs in animal models of alcohol (19, 164–166), cocaine (25, 124), and opioid (167) use disorders *via* intrathecal or direct brain injections. In other disease models, SUD-relevant miRs (miR-34, miR-145, miR-212) have been targeted with miR mimics (168–170). Although miR-based therapeutics have yet to be tested clinically in SUD patients, several miR mimic and antimiR formulations are being tested in animals or clinical trials for other diseases (171–175). To move the field of miR-targeted SUD therapeutics forward, researchers are encouraged to identify miRs that drive relapse and craving (rather than acquisition of drug-seeking behaviors) and test clinically relevant miR-targeted formulations in sophisticated SUD models.

Small molecules interacting with RNAs

Emerging research indicates that the three-dimensional structure of RNA, which creates well-defined recognition sites

and motifs, can be selectively targeted with small molecules (176). Other than directly binding to specific RNAs (including ncRNAs), SMIRNAs are also able to indirectly affect the RNA functions by interfering with RNA biogenesis or RNA-protein interactions (177–179) (Figure 1). Unlike nucleic acid-based treatments, many SMIRNAs have low molecular weights (usually <1 KDa) and may be administered orally (180), important factors for translational applications (Table 2). However, the likelihood of discovering a small molecule with favorable drug-like characteristics depends on the selected RNA target (181). In other words, the RNA must contain a unique recognition site with considerable structural complexity, differentiating it from other RNAs to avoid non-specific binding and side effects. Also, the abundance of the RNA may influence the efficacy of SMIRNAs (182), a potential issue when targeting very low expressing lncRNAs.

Despite the aforementioned challenges, several SMIRNAs have been identified and validated in preclinical studies (183–189), and in 2020 Risdiplam (an orally available, non-antibiotic SMIRNA) received FDA approval for the treatment of spinal muscular atrophy (190). ncRNAs have also been successfully targeted with SMIRNAs. For example, two studies have identified SMIRNAs for MALAT1 (191, 192), a lncRNA that is altered in the brain of heroin and cocaine users and in rats treated with morphine (101, 193). In other studies, a first-in-class, clinical-stage quinolone compound, ABX464, was found to increase the expression of miR-124, a target that has been well-studied in SUD models (194). This molecule has passed phase I dose safety trial and phase IIa clinical studies, and although ABX464 has been mainly studied in HIV and Ulcerative Colitis, it could also be used to upregulate miR-124 expression in the brain to reduce drug-induced neurobehavioral adaptations (194). NP-C86 is another SMIRNA that stabilizes the lncRNA *Gas5* (195), a lncRNA that has been associated to cocaine-seeking behaviors (111). Finally, the *let-7* family, miRs with a known link to SUD, are suppressed by RNA-binding proteins called LIN28. Recently, Wang et al. successfully identified six small molecule disruptors of LIN28 and subsequently *let-7* suppression (179). Together, these studies indicate that targeting ncRNAs with SMIRNAs is a feasible approach and may have potential utility in SUD.

Delivery systems for ncRNA therapeutics

Despite several advances, treating CNS diseases with nucleic acids-based platforms remains a major challenge due to the blood-brain barrier. Comprised of tight junctions between brain capillary endothelial cells, the blood-brain barrier prevents large molecule therapeutics from entering the brain parenchyma. To circumvent this issue, researchers have developed several RNA delivery systems that are capable of entering the brain *via* intravenous, intrathecal, or intranasal routes of administration (131, 196–200). Viral vectors and nanoparticle carrier systems are some of the most promising strategies for delivering ncRNA therapeutics to the brain and are discussed below.

Viral vectors

In preclinical studies, viral vectors are widely used to transfer nucleic acids to brain cells with high efficiency (201). The most commonly used viral vectors for delivering nucleic acids are adenovirus, adeno-associated virus (AAV), and lentivirus vectors (202–204). In neuroscience research, AAVs are especially popular as different serotypes allow for transduction of distinct brain cells (205) and projection-specific pathways (206). Another advantage of viral vectors is the ability to target disease-related brain cells, using cell type-specific promoters (207, 208). However, the vast majority of SUD-related studies that have used viral vectors to manipulate ncRNAs have done so by direct brain injections, an approach that may have limited clinical utility. More recently, researchers have developed viral vectors that are capable of targeting the brain *via* more feasible routes of administration. For example, intrathecal injection of an AAV that expresses an artificial miR resulted in robust gene silencing with no observed side effects in nonhuman primates (209). Using the same approach, a case study in ALS patients also generated promising results (210). In animal models of Huntington's disease, intravenous injection of a novel AAV encoding an artificial miR that targets the huntingtin (HTT) gene yielded extensive knockdown of HTT across multiple brain regions with the highest transduction observed in the striatum (199). Several other studies have also explored viral-mediated CNS delivery of ncRNAs *via* intrathecal or intravenous routes of administration (211–215) and multiple clinical trials using AAVs in Parkinson's disease, Alzheimer's disease, Batten disease, and Canavan disease patients have been conducted or in progress (216). In summary, nonpathogenic viral vectors offer a powerful option for ncRNA-targeted brain delivery and should be further pursued in SUD patients.

Nanoparticles

Nanoparticle-mediated delivery of ncRNA therapeutics is a promising approach for the treatment of SUD (217). Nanoparticles have several appealing properties including, tunable release rate, biocompatibility, limited toxicity, brain penetrating capabilities, and adjustable surface modifications for cell type-specific delivery (218). Many different classes of nanocarriers have been successfully tested in CNS disease models, including polymeric, inorganic, exosome, and lipid-based nanoparticles (219–229), and as an indication of their safety and efficacy across multiple disease states, several

nanoparticle formulations have received FDA approval, including the recent approvals of the Pfizer-BioNTech and Moderna COVID-19 vaccines (both use lipid nanoparticles for mRNA delivery) and the siRNA drug Patisiran (230).

Although nanoparticle-mediated brain delivery *via* systemic administration remains an ongoing challenge, miR mimic and antimiR encapsulated nanoparticles have successfully targeted the brain in multiple CNS disease models following systemic administration (231–233). For example, intranasal delivery of extracellular vesicles loaded with miR-124 to cocaine-treated mice resulted in successful brain uptake and abrogation of inflammatory markers (234). A more recent strategy for the delivery of nucleic acids to the brain is to add surface modifications to the nanoparticles that facilitate transport across the blood-brain barrier. For example, using sugar-coated polymeric nanoparticles that bind a major glucose transporter in the brain called GLUT-1, researchers successfully targeted coding and noncoding transcripts in the brain following intravenous administration (225, 235). In other studies, exosomes with a transferrin binding ligand attached to the surface effectively delivered antimiRs into the rat brain after an intravenous injection. Systemic delivery of nucleic acid payloads to the brain has also been accomplished using rabies virus glycoprotein (RVG) exosomes and liposomes (236–238), transferrin-targeted cyclodextrins (239), angiopep-2-targeted lipid- and polymer-based nanoparticles (240, 241), and calcium phosphate lipid nanoparticles (242). Thus, as the number of nanoformulations capable of delivering nucleic acids to the brain continues to improve, ncRNA nanocarrier systems warrant further research in SUD models.

Ongoing challenges and outlook

The lipid bilayer is a billion-year-old barrier that prevents large, charged molecules like RNAs from entering the cell. In addition to this barrier, there are other formidable obstacles that protect cells from RNAs including, RNases, the innate immune system, and for neurons, the blood-brain barrier (243). Despite these natural defenses, decades of basic science and clinical research have recently led to multiple FDA-approved nucleic acid-based therapeutics for various indications (244). However, it is clear that we are still in the early days of ncRNA therapeutic development, particularly for SUD, and several issues need to be addressed to move the field forward. First, most preclinical and all clinical experiments exploring ncRNAs in SUD are correlational studies. Additional functional studies that target conserved ncRNAs in sophisticated SUD models will be essential to identify the ncRNA targets with the highest translational potential. Also, as low-quality sequence data have incorrectly annotated some ncRNAs (245, 246), SUD-associated ncRNAs should be thoroughly characterized and validated as true ncRNAs before being pursued therapeutically. To facilitate therapeutic developoment, multiple bioinformatic tools have been created to predict ncRNA targets and assist with characterization and safety (245, 247). Second, rather than studying the ncRNAs involved in the acquisition of drug-seeking, researchers should focus on ncRNA mechanisms that drive drug craving, relapse, and withdrawal, as such targets are likely more relevant to promote abstinence and recovery in humans. Also, as different cells and circuits may exert contrasting effects in the context of SUD, additional cell-type specific studies are needed to identify the most promising ncRNA targets. Third, instead of injecting RNA-based therapeutics directly into the brain in preclinical models, researchers are encouraged to test clinically relevant routes of administration for ncRNA treatments. For example, multiple studies have demonstrated the promise of intranasal administration as a way to bypass the blood-brain barrier (196, 197, 231, 248–253). Intrathecal injections of modified ASOs and siRNAs and nanoparticle-containing nucleic acids have also achieved high brain uptake in preclinical and clinical studies (131, 200, 254) and should also be employed in SUD experiments. Finally, using nucleic acids, nanoparticles, and/or AAVs that contain ligands or surface modifications to promote brain and/or cell type-specific delivery is an approach to enhance CNS uptake and avoid potential side effects (7, 217, 247, 255–257). N-acetylgalactosamine (GalNac), a biomolecule conjugate that promotes liver-specific uptake of RNA-targeted therapeutics, is a prime example of how such modifications can facilitate tissue-specific uptake. Additional research is needed to determine whether similar opportunities exist to enhance CNS-specific delivery.

An additional strategy to move the field forward is to repurpose or test clinical-stage nucleic acid-based therapeutics that may also have relevance to SUD. For example, several companies have developed miR mimics or antimiR that target miRs linked to SUD (28, 53, 64, 73, 74, 82, 83, 258–260). Also, SMIRNA databases (e.g., R-BIND, infoRNA) (261, 262) could be used to identify compounds that target SUD-relevant ncRNAs, an appealing translational approach as small molecules typically have a better physicochemical profile compared to nucleic acids. These databases also consist of clinically tested small molecules, providing drug repurposing opportunities for rapid translational applications. Additionally, the abused substance itself may create opportunities for nucleic acid-based treatments. For example, the disrupted blood-brain barrier caused by chronic methamphetamine use (263) may allow for RNA-based drug delivery *via* less invasive routes of administration, a hypothesis that merits further exploration.

Although many promising opportunities are listed above, multiple clinical trials using RNA-based treatments have been withdrawn due to severe side effects or limited efficacy (18, 247, 264). These failures may serve as lessons learned for future SUD therapeutics. For instance, in preclinical studies, MRX34, a liposome-delivered miR-34a mimic for treatment of solid

tumors, showed favorable efficacy and safety profile (265, 266). However, when injected systemically in humans, MRX34 induced severe immune-related side effects and death in some patients causing the clinical trial to be terminated (264). MRX34 was designed to target the low-pH environment in tumors, but preclinical studies indicated that it also accumulates in the bone marrow and other organs, potentially impacting immune cell activity (267). This incident highlights the need for a thorough risk assessment of all organ systems following systemic administration of RNA therapeutics. In another example, oblimersen, a phosphothiorate-modified ASO targeting *BCL2* mRNA, showed promise in preclinical experiments but lacked efficacy in multiple clinical trials (268, 269). Further analyses revealed that several off-target effects of oblimersen were related to the phosphothiorate modification, as these off-target effects were not observed with the same ASO that lacked this modification (270–272). On a related note, the RNA payload may also alter the efficacy of the delivery vehicle. For example, nanoparticle tropism has been shown to change based on the type of cargo (273). Thus, going forward, each RNA modification along with the delivery vehicle should be carefully assessed for efficacy and safety before moving to human subjects.

Dosing is another major issue that needs to be addressed in ncRNA-targeting therapeutics, as many ncRNA studies have used supraphysiological concentrations that may lead to unpredictable side effects (247, 274). For example, high doses of miR mimics can cause off-target effects by saturating RISC, potentially blocking the activity of unrelated miRs and triggering a cascade of side effects. As a prerequisite for clinical studies, future experiments should establish dose-dependent on- and off-target effects of the ncRNA therapeutic in both control and pathological conditions. To address dose-dependent toxicities, metronomic ncRNA therapy is an approach used in cancer in which frequent low doses of the ncRNA therapy are administered (usually in combination with conventional treatments) to avoid excessive toxicity or immunogenicity (275). Similar strategies could also be investigated for efficacy and safety in SUD studies. Finally, the exorbitant price of RNA-based therapeutics is a continuing issue that needs to be addressed, particularly for SUD patients that may lack sufficient means to purchase these costly drugs. Ongoing efforts to address these concerns will open the door for ncRNA SUD therapeutics.

Author contributions

SAS wrote the manuscript with edits and feedback from GCS.

Funding

This publication was supported by National Institute on Drug Abuse grants R00DA040744 and U18DA052394.

Conflict of interest

The authors declare that the research was conducted in the absence of any commercial or financial relationships that could be construed as a potential conflict of interest.

References

1. Degenhardt L, Charlson F, Ferrari A, Santomauro D, Erskine H, Mantilla-Herrara A, et al. The global burden of disease attributable to alcohol and drug use in 195 countries and territories, 1990–2016: A systematic analysis for the global burden of disease study 2016. *Lancet Psychiatry* (2018) 5(12):987–1012. doi:10.1016/S2215-0366(18)30337-7

2. Butelman ER, Kreek MJ. Medications for substance use disorders (SUD): Emerging approaches. *Expert Opin Emerg Drugs* (2017) 22:301–15. doi:10.1080/14728214.2017.1395855

3. Clamp M, Fry B, Kamal M, Xie X, Cuff J, Lin MF, et al. Distinguishing protein-coding and noncoding genes in the human genome. *Proc Natl Acad Sci U S A* (2007) 104(49):19428–33. doi:10.1073/pnas.0709013104

4. Ezkurdia I, Juan D, Rodriguez JM, Frankish A, Diekhans M, Harrow J, et al. Multiple evidence strands suggest that theremay be as few as 19 000 human protein-coding genes. *Hum Mol Genet* (2014) 23(22):5866–78. doi:10.1093/hmg/ddu309

5. Hopkins A, Colin G. The druggable genome. *Nat Rev Drug Discov* (2002) 1:727–30. doi:10.1038/nrd892

6. Dammes N, Peer D. Paving the road for RNA therapeutics. *Trends Pharmacol Sci* (2020) 41:755–75. doi:10.1016/j.tips.2020.08.004

7. Kulkarni JA, Witzigmann D, Thomson SB, Chen S, Leavitt BR, Cullis PR, et al. Author Correction: The current landscape of nucleic acid therapeutics. *Nat Nanotechnol* (2021) 16:841. doi:10.1038/s41565-021-00937-w

8. Damase TR, Sukhovershin R, Boada C, Taraballi F, Pettigrew RI, Cooke JP. The limitless future of RNA therapeutics. *Front Bioeng Biotechnol* (2021) 9:628137. doi:10.3389/fbioe.2021.628137

9. Cech TR, Steitz JA. The noncoding RNA revolution - trashing old rules to forge new ones. *Cell* (2014) 157:77–94. doi:10.1016/j.cell.2014.03.008

10. Kyzar EJ, Bohnsack JP, Pandey SC. Current and future perspectives of noncoding RNAs in brain function and neuropsychiatric disease. *Biol Psychiatry* (2022) 91:183–93. doi:10.1016/j.biopsych.2021.08.013

11. Srinivasan C, Phan BN, Lawler AJ, Ramamurthy E, Kleyman M, Brown AR, et al. Addiction-associated genetic variants implicate brain cell type- and region-specific cis-regulatory elements in addiction neurobiology. *J Neurosci* (2021) 41(43):9008–30. doi:10.1523/JNEUROSCI.2534-20.2021

12. Ponting CP, Oliver PL, Reik W. Evolution and functions of long noncoding RNAs. *Cell* (2009) 136:629–41. doi:10.1016/j.cell.2009.02.006

13. Nie JH, Li TX, Zhang XQ, Liu J. Roles of non-coding RNAs in normal human brain development, brain tumor, and neuropsychiatric disorders. *Noncoding RNA* (2019) 5:E36. doi:10.3390/ncrna5020036

14. Gowen AM, Odegaard KE, Hernandez J, Chand S, Koul S, Pendyala G, et al. *Role of microRNAs in the pathophysiology of addiction*, 12. Wiley Interdisciplinary Reviews: RNA (2021).

15. Liu J, Zhou F, Guan Y, Meng F, Zhao Z, Su Q, et al. The biogenesis of miRNAs and their role in the development of amyotrophic lateral sclerosis. *Cells* (2022) 11:572. doi:10.3390/cells11030572

16. Nakamori M, Junn E, Mochizuki H, Mouradian MM. Nucleic acid–based therapeutics for Parkinson's disease. *Neurotherapeutics* (2019) 16:287–98. doi:10.1007/s13311-019-00714-7

17. Riscado M, Baptista B, Sousa F. New rna-based breakthroughs in alzheimer's disease diagnosis and therapeutics. *Pharmaceutics* (2021) 13:1397. doi:10.3390/pharmaceutics13091397

18. Anastasiadou E, Seto AG, Beatty X, Hermreck M, Gilles ME, Stroopinsky D, et al. Cobomarsen, an oligonucleotide inhibitor of miR-155, slows DLBCL tumor cell growth *in vitro* and *in vivo*. *Clin Cancer Res* (2021) 27(4):1139–49. doi:10.1158/1078-0432.CCR-20-3139

19. Darcq E, Warnault V, Phamluong K, Besserer GM, Liu F, Ron D. MicroRNA-30a-5p in the prefrontal cortex controls the transition from moderate to excessive alcohol consumption. *Mol Psychiatry* (2015) 20(10):1219–31. doi:10.1038/mp.2014.120

20. Bahi A, Dreyer JL. Striatal modulation of BDNF expression using microRNA124a-expressing lentiviral vectors impairs ethanol-induced conditioned-place preference and voluntary alcohol consumption. *Eur J Neurosci* (2013) 38(2):2328–37. doi:10.1111/ejn.12228

21. Wang Z. The principles of MiRNA-masking antisense oligonucleotides technology. *Methods Mol Biol* (2011) 676:43–9. doi:10.1007/978-1-60761-863-8_3

22. Li J, Li J, Liu X, Qin S, Guan Y, Liu Y, et al. MicroRNA expression profile and functional analysis reveal that miR-382 is a critical novel gene of alcohol addiction. *EMBO Mol Med* (2013) 5(9):1402–14. doi:10.1002/emmm.201201900

23. Xu W, Zhao M, Lin Z, Liu H, Ma H, Hong Q, et al. Increased expression of plasma hsa-miR-181a in male patients with heroin addiction use disorder. *J Clin Lab Anal* (2020) 34(11):e23486. doi:10.1002/jcla.23486

24. Yu H, Xie B, Zhang J, Luo Y, Galaj E, Zhang X, et al. The role of circTmeff-1 in incubation of context-induced morphine craving. *Pharmacol Res* (2021) 170:105722. doi:10.1016/j.phrs.2021.105722

25. Hollander JA, Im HI, Amelio AL, Kocerha J, Bali P, Lu Q, et al. Striatal microRNA controls cocaine intake through CREB signalling. *Nature* (2010) 466(7303):197–202. doi:10.1038/nature09202

26. Bastle RM, Oliver RJ, Gardiner AS, Pentkowski NS, Bolognani F, Allan AM, et al. *In silico* identification and *in vivo* validation of miR-495 as a novel regulator of motivation for cocaine that targets multiple addiction-related networks in the nucleus accumbens. *Mol Psychiatry* (2018) 23(2):434–43. doi:10.1038/mp.2016.238

27. Farris SP, Dayne Mayfield R. RNA-seq reveals novel transcriptional reorganization in human alcoholic brain. *Int Rev Neurobiol* (2014) 116:275–300. doi:10.1016/B978-0-12-801105-8.00011-4

28. Su H, Zhu L, Li J, Wang R, Liu D, Han W, et al. Regulation of microRNA-29c in the nucleus accumbens modulates methamphetamine -induced locomotor sensitization in mice. *Neuropharmacology* (2019) 148:160–8. doi:10.1016/j.neuropharm.2019.01.007

29. Qian H, Shang Q, Liang M, Gao B, Xiao J, Wang J, et al. MicroRNA-31-3p/RhoA signaling in the dorsal hippocampus modulates methamphetamine-induced conditioned place preference in mice. *Psychopharmacology (Berl)* (2021) 238:3207–19. doi:10.1007/s00213-021-05936-2

30. Li J, Zhu L, Su H, Liu D, Yan Z, Ni T, et al. Regulation of miR-128 in the nucleus accumbens affects methamphetamine-induced behavioral sensitization by modulating proteins involved in neuroplasticity. *Addict Biol* (2021) 26(1):e12881. doi:10.1111/adb.12881

31. Mavrikaki M, Anastasiadou E, Ozdemir RA, Potter D, Helmholz C, Slack FJ, et al. Overexpression of miR-9 in the nucleus accumbens increases oxycodone self-administration. *Int J Neuropsychopharmacol* (2019) 22(6):383–93. doi:10.1093/ijnp/pyz015

32. Jia M, Wang X, Zhang H, Ye C, Ma H, Yang M, et al. MicroRNA-132 in the adult dentate gyrus is involved in opioid addiction via modifying the differentiation of neural stem cells. *Neurosci Bull* (2019) 35(3):486–96. doi:10.1007/s12264-019-00338-z

33. Irie T, Shum R, Deni I, Hunkele A, le Rouzic V, Xu J, et al. Identification of abundant and evolutionarily conserved opioid receptor circular RNAs in the nervous system modulated by morphine. *Mol Pharmacol* (2019) 96(2):247–58. doi:10.1124/mol.118.113977

34. Gomez AM, Altomare D, Sun WL, Midde NM, Ji H, Shtutman M, et al. Prefrontal microRNA-221 mediates environmental enrichment-induced increase of locomotor sensitivity to nicotine. *Int J Neuropsychopharmacol* (2016) 19(1):pyv090. doi:10.1093/ijnp/pyv090

35. Bannon MJ, Savonen CL, Jia H, Dachet F, Halter SD, Schmidt CJ, et al. Identification of long noncoding RNAs dysregulated in the midbrain of human cocaine abusers. *J Neurochem* (2015) 135(1):50–9. doi:10.1111/jnc.13255

36. Ha M, Kim VN. Regulation of microRNA biogenesis. *Nat Rev Mol Cel Biol.* (2014) 15:509–24. doi:10.1038/nrm3838

37. Rooij E, Kauppinen S. Development of micro RNA therapeutics is coming of age. *EMBO Mol Med* (2014) 6(7):851–64. doi:10.15252/emmm.201100899

38. O'Brien J, Hayder H, Zayed Y, Peng C. Overview of microRNA biogenesis, mechanisms of actions, and circulation. *Front Endocrinol* (2018) 9:402. doi:10.3389/fendo.2018.00402

39. Saliminejad K, Khorram Khorshid HR, Soleymani Fard S, Ghaffari SH. An overview of microRNAs: Biology, functions, therapeutics, and analysis methods. *J Cel Physiol.* (2019) 234:5451–65. doi:10.1002/jcp.27486

40. Yapijakis C. Regulatory role of MicroRNAs in brain development and function. In: *Advances in Experimental Medicine and Biology* (2020).

41. Gui YX, Liu H, Zhang LS, Lv W, Hu XY. Altered microRNA profiles in cerebrospinal fluid exosome in Parkinson disease and Alzheimer disease. *Oncotarget* (2015) 6(35):37043–53. doi:10.18632/oncotarget.6158

42. Briggs CE, Wang Y, Kong B, Woo TUW, Iyer LK, Sonntag KC. Midbrain dopamine neurons in Parkinson's disease exhibit a dysregulated miRNA and target-gene network. *Brain Res* (2015) 1618:111–21. doi:10.1016/j.brainres.2015.05.021

43. Im HI, Hollander JA, Bali P, Kenny PJ. MeCP2 controls BDNF expression and cocaine intake through homeostatic interactions with microRNA-212. *Nat Neurosci* (2010) 13(9):1120–7. doi:10.1038/nn.2615

44. Eipper-Mains JE, Kiraly DD, Palakodeti D, Mains RE, Eipper BA, Graveley BR. microRNA-Seq reveals cocaine-regulated expression of striatal microRNAs. *RNA* (2011) 17(8):1529–43. doi:10.1261/rna.2775511

45. Chen CL, Liu H, Guan X. Changes in microRNA expression profile in hippocampus during the acquisition and extinction of cocaine-induced conditioned place preference in rats. *J Biomed Sci* (2013) 20(1):96. doi:10.1186/1423-0127-20-96

46. Cabana-Domínguez J, Arenas C, Cormand B, Fernàndez-Castillo N. MiR-9, miR-153 and miR-124 are down-regulated by acute exposure to cocaine in a dopaminergic cell model and may contribute to cocaine dependence. *Transl Psychiatry* (2018) 8(1):173. doi:10.1038/s41398-018-0224-5

47. Guo ML, Periyasamy P, Liao K, Kook YH, Niu F, Callen SE, et al. Cocaine-mediated downregulation of microglial miR-124 expression involves promoter DNA methylation. *Epigenetics* (2016) 11(11):819–30. doi:10.1080/15592294.2016.1232233

48. Sessa F, Maglietta F, Bertozzi G, Salerno M, di Mizio G, Messina G, et al. Human brain injury and mirnas: An experimental study. *Int J Mol Sci* (2019) 20(7):E1546. doi:10.3390/ijms20071546

49. Sequeira-Cordero A, Brenes JC. Time-dependent changes in striatal monoamine levels and gene expression following single and repeated amphetamine administration in rats. *Eur J Pharmacol* (2021) 904:174148. doi:10.1016/j.ejphar.2021.174148

50. Cuesta S, Restrepo-Lozano JM, Popescu C, He S, Reynolds LM, Israel S, et al. DCC-related developmental effects of abused- versus therapeutic-like amphetamine doses in adolescence. *Addict Biol* (2020) 25(4):e12791. doi:10.1111/adb.12791

51. Cuesta S, Restrepo-Lozano JM, Silvestrin S, Nouel D, Torres-Berrío A, Reynolds LM, et al. Non-contingent exposure to amphetamine in adolescence recruits miR-218 to regulate dcc expression in the VTA. *Neuropsychopharmacology* (2018) 43(4):900–11. doi:10.1038/npp.2017.284

52. Zhu L, Li J, Dong N, Guan F, Liu Y, Ma D, et al. MRNA changes in nucleus accumbens related to methamphetamine addiction in mice. *Sci Rep* (2016) 6:36993. doi:10.1038/srep36993

53. Bosch PJ, Benton MC, Macartney-Coxson D, Kivell BM. mRNA and microRNA analysis reveals modulation of biochemical pathways related to addiction in the ventral tegmental area of methamphetamine self-administering rats. *BMC Neurosci* (2015) 16(1):43. doi:10.1186/s12868-015-0186-y

54. Du HY, Cao DN, Chen Y, Wang L, Wu N, Li J. Alterations of prefrontal cortical microRNAs in methamphetamine self-administering rats: From controlled drug intake to escalated drug intake. *Neurosci Lett* (2016) 611:21–7. doi:10.1016/j.neulet.2015.11.016

55. Sim MS, Soga T, Pandy V, Wu YS, Parhar IS, Mohamed Z. MicroRNA expression signature of methamphetamine use and addiction in the rat nucleus accumbens. *Metab Brain Dis* (2017) 32(6):1767–83. doi:10.1007/s11011-017-0061-x

56. Ni T, Li Y, Wang R, Hu T, Guan F, Zhu L, et al. The potential involvement of miR-204-3p-axon guidance network in methamphetamine-induced locomotor sensitization of mice. *Neurosci Lett* (2019) 707:134303. doi:10.1016/j.neulet.2019.134303

57. Chand S, Gowen A, Savine M, Moore D, Clark A, Huynh W, et al. A comprehensive study to delineate the role of an extracellular vesicle-associated microRNA-29a in chronic methamphetamine use disorder. *J Extracell Vesicles* (2021) 10(14):e12177. doi:10.1002/jev2.12177

58. Lallai V, Grimes N, Fowler JP, Sequeira PA, Cartagena P, Limon A, et al. Nicotine acts on cholinergic signaling mechanisms to directly modulate choroid plexus function. *eNeuro* (2019) 6(2):0051–19. doi:10.1523/ENEURO.0051-19.2019

59. Rauthan M, Gong J, Liu J, Li Z, Wescott SA, Liu J, et al. MicroRNA regulation of nAChR expression and nicotine-dependent behavior in *C. elegans*. *Cell Rep.* (2017) 21(6):1434–41. doi:10.1016/j.celrep.2017.10.043

60. Keller RF, Dragomir A, Yantao F, Akay YM, Akay M. Investigating the genetic profile of dopaminergic neurons in the VTA in response to perinatal nicotine exposure using mRNA-miRNA analyses. *Sci Rep* (2018) 8(1):13769. doi:10.1038/s41598-018-31882-9

61. Pittenger ST, Schaal VL, Moore D, Guda RS, Koul S, Yelamanchili Sv., et al. MicroRNA cluster miR199a/214 are differentially expressed in female and male rats following nicotine self-administration. *Sci Rep* (2018) 8(1):17464. doi:10.1038/s41598-018-35747-z

62. Lippi G, Steinert JR, Marczylo EL, D'Oro S, Fiore R, Forsythe ID, et al. Targeting of the Arpc3 actin nucleation factor by miR-29a/b regulates dendritic spine morphology. *J Cel Biol.* (2011) 194(6):889–904. doi:10.1083/jcb.201103006

63. Lee S, Woo J, Kim YS, Im HI. Integrated miRNA-mRNA analysis in the habenula nuclei of mice intravenously self-administering nicotine. *Sci Rep* (2015) 5:12909. doi:10.1038/srep12909

64. Kim J, Im HI, Moon C. Intravenous morphine self-administration alters accumbal microRNA profiles in the mouse brain. *Neural Regen Res* (2018) 13(1):77–85. doi:10.4103/1673-5374.224374

65. Tapocik JD, Ceniccola K, Mayo CL, Schwandt ML, Solomon M, Wang BD, et al. MicroRNAs are involved in the development of morphine-induced analgesic tolerance and regulate functionally relevant changes in serpini1. *Front Mol Neurosci* (2016) 9(MAR):20. doi:10.3389/fnmol.2016.00020

66. He Y, Yang C, Kirkmire CM, Wang ZJ. Regulation of opioid tolerance by let-7 family microRNA targeting the μ opioid receptor. *J Neurosci* (2010) 30(30):10251–8. doi:10.1523/JNEUROSCI.2419-10.2010

67. Tapocik JD, Luu Tv., Mayo CL, Wang BD, Doyle E, Lee AD, et al. Neuroplasticity, axonal guidance and micro-RNA genes are associated with morphine self-administration behavior. *Addict Biol* (2013) 18(3):480–95. doi:10.1111/j.1369-1600.2012.00470.x

68. Xu W, Hong Q, Lin Z, Ma H, Chen W, Zhuang D, et al. Role of nucleus accumbens microRNA-181a and MeCP2 in incubation of heroin craving in male rats. *Psychopharmacology (Berl)* (2021) 238(8):2313–24. doi:10.1007/s00213-021-05854-3

69. Yan B, Hu Z, Yao W, Le Q, Xu B, Liu X, et al. MiR-218 targets MeCP2 and inhibits heroin seeking behavior. *Sci Rep* (2017) 7:40413. doi:10.1038/srep40413

70. Wu Q, Hwang CK, Zheng H, Wagley Y, Lin HY, Kim DK, et al. MicroRNA 339 down-regulates μ-opioid receptor at the post-transcriptional level in response to opioid treatment. *FASEB J* (2013) 27(2):522–35. doi:10.1096/fj.12-213439

71. Shi X, Li Y, Yan P, Shi Y, Lai J. Weighted gene co-expression network analysis to explore the mechanism of heroin addiction in human nucleus accumbens. *J Cel Biochem.* (2020) 121(2):1870–9. doi:10.1002/jcb.29422

72. Pietrzykowski AZ, Friesen RM, Martin GE, Puig SI, Nowak CL, Wynne PM, et al. Posttranscriptional regulation of BK channel splice variant stability by miR-9 underlies neuroadaptation to alcohol. *Neuron* (2008) 59(2):274–87. doi:10.1016/j.neuron.2008.05.032

73. Gorini G, Nunez YO, Mayfield RD. Integration of miRNA and protein profiling reveals coordinated neuroadaptations in the alcohol-dependent mouse brain. *PLoS One* (2013) 8(12):e82565. doi:10.1371/journal.pone.0082565

74. Asimes AD, Kim CK, Rao YS, Bartelt K, Pak TR. microRNA expression profiles in the ventral hippocampus during pubertal development and the impact of peri-pubertal binge alcohol exposure. *Noncoding RNA* (2019) 5(1):E21. doi:10.3390/ncrna5010021

75. Tapocik JD, Barbier E, Flanigan M, Solomon M, Pincus A, Pilling A, et al. MicroRNA-206 in rat medial prefrontal cortex regulates BDNF expression and alcohol drinking. *J Neurosci* (2014) 34(13):4581–8. doi:10.1523/JNEUROSCI.0445-14.2014

76. Santos-Bezerra DP, Cavaleiro AM, Santos AS, Suemoto CK, Pasqualucci CA, Jacob-Filho W, et al. Alcohol use disorder is associated with upregulation of MicroRNA-34a and MicroRNA-34c in hippocampal postmortem tissue. *Alcohol Clin Exp Res* (2021) 45(1):64–8. doi:10.1111/acer.14505

77. Manzardo AM, Gunewardena S, Butler MG. Over-expression of the miRNA cluster at chromosome 14q32 in the alcoholic brain correlates with suppression of predicted target mRNA required for oligodendrocyte proliferation. *Gene* (2013) 526(2):356–63. doi:10.1016/j.gene.2013.05.052

78. Zhang H, Wang F, Xu H, Liu Y, Liu J, Zhao H, et al. Differentially co-expressed genes in postmortem prefrontal cortex of individuals with alcohol use disorders: Influence on alcohol metabolism-related pathways. *Hum Genet* (2014) 133(11):1383–94. doi:10.1007/s00439-014-1473-x

79. Zhang JG, Gelernter J, Zhang H. Differential expression of miR-130a in postmortem prefrontal cortex of subjects with alcohol use disorders. *J Addict Res Ther* (2013) 04(04):18179. doi:10.4172/2155-6105.1000155

80. Vornholt E, Drake J, Mamdani M, McMichael G, Taylor ZN, Bacanu SA, et al. Network preservation reveals shared and unique biological processes associated with chronic alcohol abuse in NAc and PFC. *PLoS One* (2020) 15(12):e0243857. doi:10.1371/journal.pone.0243857

81. Lim Y, Beane-Ebel JE, Tanaka Y, Ning B, Husted CR, Henderson DC, et al. Exploration of alcohol use disorder-associated brain miRNA–mRNA regulatory networks. *Transl Psychiatry* (2021) 11(1):504. doi:10.1038/s41398-021-01635-w

82. Lewohl JM, Nunez YO, Dodd PR, Tiwari GR, Harris RA, Mayfield RD. Up-regulation of microRNAs in brain of human alcoholics. *Alcohol Clin Exp Res* (2011) 35(11):1928–37. doi:10.1111/j.1530-0277.2011.01544.x

83. Mamdani M, Williamson V, McMichael GO, Blevins T, Aliev F, Adkins A, et al. Integrating mRNA and miRNA weighted gene co-expression networks with eQTLs in the nucleus accumbens of subjects with alcohol dependence. *PLoS One* (2015) 10(9):e0137671. doi:10.1371/journal.pone.0137671

84. Zhao Y, Qin F, Han S, Li S, Zhao Y, Wang H, et al. MicroRNAs in drug addiction: Current status and future perspectives. *Pharmacol Ther* (2022) 236:108215. doi:10.1016/j.pharmthera.2022.108215

85. Liu H, Xu W, Feng J, Ma H, Zhang J, Xie X, et al. Corrigendum: Increased expression of plasma miRNA-320a and let-7b-5p in heroin-dependent patients and its clinical significance. *Front Psychiatry* (2021) 12:733293. doi:10.3389/fpsyt.2021.733293

86. Hsu CW, Huang TL, Tsai MC. Decreased level of blood microRNA-133b in men with opioid use disorder on methadone maintenance therapy. *J Clin Med* (2019) 8(8):E1105. doi:10.3390/jcm8081105

87. Toyama K, Kiyosawa N, Watanabe K, Ishizuka H. Identification of circulating miRNAs differentially regulated by opioid treatment. *Int J Mol Sci* (2017) 18(9):E1991. doi:10.3390/ijms18091991

88. Zhao Y, Zhang K, Jiang H, Du J, Na Z, Hao W, et al. Decreased expression of plasma MicroRNA in patients with methamphetamine (MA) use disorder. *J Neuroimmune Pharmacol* (2016) 11(3):542–8. doi:10.1007/s11481-016-9671-z

89. Gu WJ, Zhang C, Zhong Y, Luo J, Zhang CY, Zhang C, et al. Altered serum microRNA expression profile in subjects with heroin and methamphetamine use disorder. *Biomed Pharmacother* (2020) 125.

90. Ignacio C, Hicks SD, Burke P, Lewis L, Szombathyne-Meszaros Z, Middleton FA. Alterations in serum microRNA in humans with alcohol use disorders impact cell proliferation and cell death pathways and predict structural and functional changes in brain. *BMC Neurosci* (2015) 16(1):55. doi:10.1186/s12868-015-0195-x

91. ten Berg PW, Shaffer J, Vliegenthart ADB, McCrae J, Sharkey N, Webb DJ, et al. Attending a social event and consuming alcohol is associated with changes in serum microRNA: A before and after study in healthy adults. *Biomarkers* (2018) 23(8):781–6. doi:10.1080/1354750X.2018.1499128

92. Sugiura T, Dohi Y, Yamashita S, Iwaki S, Ito S, Sanagawa A, et al. Circulating level of microRNA-126 may be a potential biomarker for recovery from smoking-related vascular damage in middle-aged habitual smokers. *Int J Cardiol Heart Vasc* (2015) 7:83–7. doi:10.1016/j.ijcha.2015.02.012

93. Kim B, Tag SH, Kim YS, Cho SN, Im HI. Circulating microRNA miR-137 as a stable biomarker for methamphetamine abstinence. *Psychopharmacology (Berl)* (2022) 239(3):831–40. doi:10.1007/s00213-022-06074-z

94. Viola TW, Heberle BA, Zaparte A, Sanvicente-Vieira B, Wainer LM, Fries GR, et al. Peripheral blood microRNA levels in females with cocaine use disorder. *J Psychiatr Res* (2019) 114:48–54. doi:10.1016/j.jpsychires.2019.03.028

95. Chandrasekar V, Dreyer JL. Regulation of MiR-124, Let-7d, and MiR-181a in the accumbens affects the expression, extinction, and reinstatement of cocaine-induced conditioned place preference. *Neuropsychopharmacology* (2011) 36(6):1149–64. doi:10.1038/npp.2010.250

96. Quinn RK, Brown AL, Goldie BJ, Levi EM, Dickson PW, Smith DW, et al. Distinct miRNA expression in dorsal striatal subregions is associated with risk for addiction in rats. *Transl Psychiatry* (2015) 5(2):e503. doi:10.1038/tp.2014.144

97. Briggs JA, Wolvetang EJ, Mattick JS, Rinn JL, Barry G. Mechanisms of long non-coding RNAs in mammalian nervous system development, plasticity, disease, and evolution. *Plasticity, Dis EvolutionNeuron* (2015) 88:861–77. doi:10.1016/j.neuron.2015.09.045

98. Andersen RE, Lim DA. Forging our understanding of lncRNAs in the brain. *Cell Tissue Res.* (2018) 371:55–71. doi:10.1007/s00441-017-2711-z

99. Begolli R, Sideris N, Giakountis A. Lncrnas as chromatin regulators in cancer: From molecular function to clinical potential. *Cancers* (2019) 11:E1524. doi:10.3390/cancers11101524

100. Khalil AM, Guttman M, Huarte M, Garber M, Raj A, Morales DR, et al. Many human large intergenic noncoding RNAs associate with chromatin-modifying complexes and affect gene expression. *Proc Natl Acad Sci U S A* (2009) 106(28):11667–72. doi:10.1073/pnas.0904715106

101. Michelhaugh SK, Lipovich L, Blythe J, Jia H, Kapatos G, Bannon MJ. Mining Affymetrix microarray data for long non-coding RNAs: Altered expression in the nucleus accumbens of heroin abusers. *J Neurochem* (2011) 116(3):459–66. doi:10.1111/j.1471-4159.2010.07126.x

102. Mercer TR, Qureshi IA, Gokhan S, Dinger ME, Li G, Mattick JS, et al. Long noncoding RNAs in neuronal-glial fate specification and oligodendrocyte lineage maturation. *BMC Neurosci* (2010) 11:14. doi:10.1186/1471-2202-11-14

103. Zhang X, Hamblin MH, Yin KJ. The long noncoding RNA Malat1: Its physiological and pathophysiological functions. *RNA Biol* (2017) 14:1705–14. doi:10.1080/15476286.2017.1358347

104. Zhao J, Zhang X, Zhou Y, Ansell PJ, Klibanski A. Cyclic AMP stimulates MEG3 gene expression in cells through a cAMP-response element (CRE) in the MEG3 proximal promoter region. *Int J Biochem Cel Biol.* (2006) 38(10):1808–20. doi:10.1016/j.biocel.2006.05.004

105. Zhu L, Zhu J, Liu Y, Chen Y, Li Y, Huang L, et al. Methamphetamine induces alterations in the long non-coding RNAs expression profile in the nucleus accumbens of the mouse. *BMC Neurosci* (2015) 16(1):18. doi:10.1186/s12868-015-0157-3

106. Ribeiro EA, Scarpa JR, Garamszegi SP, Kasarskis A, Mash DC, Nestler EJ. Gene network dysregulation in dorsolateral prefrontal cortex neurons of humans with cocaine use disorder. *Sci Rep* (2017) 7(1):5412. doi:10.1038/s41598-017-05720-3

107. Saad MH, Rumschlag M, Guerra MH, Savonen CL, Jaster AM, Olson PD, et al. Differentially expressed gene networks, biomarkers, long noncoding RNAs, and shared responses with cocaine identified in the midbrains of human opioid abusers. *Sci Rep* (2019) 9(1):1534. doi:10.1038/s41598-018-38209-8

108. Farris SP, Arasappan D, Hunicke-Smith S, Harris RA, Mayfield RD. Transcriptome organization for chronic alcohol abuse in human brain. *Mol Psychiatry* (2015) 20(11):1438–47. doi:10.1038/mp.2014.159

109. van Booven D, Li M, Sunil Rao J, Blokhin IO, Dayne Mayfield R, Barbier E, et al. Alcohol use disorder causes global changes in splicing in the human brain. *Transl Psychiatry* (2021) 11(1):2. doi:10.1038/s41398-020-01163-z

110. Drake J, McMichael GO, Vornholt ES, Cresswell K, Williamson V, Chatzinakos C, et al. Assessing the role of long noncoding RNA in nucleus accumbens in subjects with alcohol dependence. *Alcohol Clin Exp Res* (2020) 44(12):2468–80. doi:10.1111/acer.14479

111. Xu H, Brown AN, Waddell NJ, Liu X, Kaplan GJ, Chitaman JM, et al. Role of long noncoding RNA Gas5 in cocaine action. *Biol Psychiatry* (2020) 88(10):758–66. doi:10.1016/j.biopsych.2020.05.004

112. Sartor GC, stLaurent G, Wahlestedt C. The emerging role of non-coding RNAs in drug addiction. *Front Genet* (2012) 3:106. doi:10.3389/fgene.2012.00106

113. Sartor GC, Powell SK, Velmeshev D, Lin DY, Magistri M, Wiedner HJ, et al. Cocaine alters Homer1 natural antisense transcript in the nucleus accumbens. *Mol Cel Neurosci.* (2017) 85:183–9. doi:10.1016/j.mcn.2017.10.003

114. Bohnsack JP, Teppen T, Kyzar EJ, Dzitoyeva S, Pandey SC. The lncRNA BDNF-AS is an epigenetic regulator in the human amygdala in early onset alcohol use disorders. *Transl Psychiatry* (2019) 9(1):34. doi:10.1038/s41398-019-0367-z

115. Youngson NA, Castino MR, Stuart A, Kershaw KA, Holmes NM, Heffernan EC, et al. A role for a novel natural antisense-BDNF in the maintenance of nicotine-seeking. *Addict Neurosci* (2022) 2:100010. doi:10.1016/j.addicn.2022.100010

116. Zheng X, Lin C, Li Y, Ye J, Zhou J, Guo P. Long noncoding RNA BDNF-AS regulates ketamine-induced neurotoxicity in neural stem cell derived neurons. *Biomed Pharmacother* (2016) 82:722–8. doi:10.1016/j.biopha.2016.05.050

117. Mahmoudi E, Cairns MJ. Circular RNAs are temporospatially regulated throughout development and ageing in the rat. *Sci Rep* (2019) 9(1):2564. doi:10.1038/s41598-019-38860-9

118. You X, Vlatkovic I, Babic A, Will T, Epstein I, Tushev G, et al. Neural circular RNAs are derived from synaptic genes and regulated by development and plasticity. *Nat Neurosci* (2015) 18(4):603–10. doi:10.1038/nn.3975

119. Chen X, Zhou M, Yant L, Huang C. Circular RNA in disease: Basic properties and biomedical relevance. *Wiley Interdiscip Rev RNA* (2022) 22:e1723. n/a(n/a). doi:10.1002/wrna.1723

120. Holdt LM, Kohlmaier A, Teupser D. Circular RNAs as therapeutic agents and targets. *Front Physiol* (2018) 9:1262. doi:10.3389/fphys.2018.01262

121. Vornholt E, Drake J, Mamdani M, McMichael G, Taylor ZN, Bacanu SA, et al. Identifying a novel biological mechanism for alcohol addiction associated with circRNA networks acting as potential miRNA sponges. *Addict Biol* (2021) 26:e13071. doi:10.1111/adb.13071

122. Paudel P, Pierotti C, Lozano E, Amoah SK, Gardiner AS, Caldwell KK, et al. Prenatal alcohol exposure results in sex-specific alterations in circular RNA expression in the developing mouse brain. *Front Neurosci* (2020) 14:581895. doi:10.3389/fnins.2020.581895

123. Floris G, Gillespie A, Zanda MT, Dabrowski KR, Sillivan SE. Heroin regulates orbitofrontal circular RNAs. *Int J Mol Sci* (2022) 23(3):1453. doi:10.3390/ijms23031453

124. Shen Q, Xie B, Galaj E, Yu H, Li X, Lu Y, et al. CircTmeff-1 in the nucleus accumbens regulates the reconsolidation of cocaine-associated memory. *Brain Res Bull* (2022) 185:64–73. Internet. doi:10.1016/j.brainresbull.2022.04.010

125. Bu Q, Long H, Shao X, Gu H, Kong J, Luo L, et al. Cocaine induces differential circular RNA expression in striatum. *Transl Psychiatry* (2019) 9(1):199. doi:10.1038/s41398-019-0527-1

126. Chen Y, Li X, Meng S, Huang S, Chang S, Shi J. Identification of functional CircRNA-miRNA-mRNA regulatory network in dorsolateral prefrontal cortex neurons of patients with cocaine use disorder. *Front Mol Neurosci* (2022) 15. doi:10.3389/fnmol.2022.839233

127. Li J, Shi Q, Wang Q, Tan X, Pang K, Liu X, et al. Profiling circular RNA in methamphetamine-treated primary cortical neurons identified novel circRNAs related to methamphetamine addiction. *Neurosci Lett* (2019) 701:146–53. doi:10.1016/j.neulet.2019.02.032

128. Li J, Sun Q, Zhu S, Xi K, Shi Q, Pang K, et al. Knockdown of circHomer1 ameliorates METH-induced neuronal injury through inhibiting Bbc3 expression. *Neurosci Lett* (2020) 732:135050. doi:10.1016/j.neulet.2020.135050

129. Zogg H, Singh R, Ro S. Current advances in RNA therapeutics for human diseases. *Int J Mol Sci* (2022) 23:2736. doi:10.3390/ijms23052736

130. Disney MD. Targeting RNA with small molecules to capture opportunities at the intersection of chemistry, biology, and medicine. *J Am Chem Soc* (2019) 141:6776–90. doi:10.1021/jacs.8b13419

131. Khorkova O, Hsiao J, Wahlestedt C. Nucleic acid–based therapeutics in orphan neurological disorders: Recent developments. *Front Mol Biosci* (2021) 8:643681. doi:10.3389/fmolb.2021.643681

132. Relizani K, Goyenvalle A. Use of tricyclo-DNA antisense oligonucleotides for exon skipping. *Methods Mol Biol* (2018) 1828:381–94. doi:10.1007/978-1-4939-8651-4_24

133. Crooke ST, Bennett CF. Progress in antisense oligonucleotide therapeutics. *Annu Rev Pharmacol Toxicol* (1996) 36:107–29. doi:10.1146/annurev.pa.36.040196.000543

134. Ochoa S, Milam VT. Modified nucleic acids: Expanding the capabilities of functional oligonucleotides. *Molecules* (2020) 25:E4659. doi:10.3390/molecules25204659

135. Hersh DS, Wadajkar AS, Roberts N, Perez JG, Connolly NP, Frenkel V, et al. Evolving drug delivery strategies to overcome the blood brain barrier. *Curr Pharm Des* (2016) 22(9):1177–93. doi:10.2174/1381612822666151221150733

136. Meng L, Ward AJ, Chun S, Bennett CF, Beaudet AL, Rigo F. Towards a therapy for Angelman syndrome by targeting a long non-coding RNA. *Nature* (2015) 518(7539):409–12. doi:10.1038/nature13975

137. Barry G, Briggs JA, Vanichkina DP, Poth EM, Beveridge NJ, Ratnu VS, et al. The long non-coding RNA Gomafu is acutely regulated in response to neuronal activation and involved in schizophrenia-associated alternative splicing. *Mol Psychiatry* (2014) 19(4):486–94. doi:10.1038/mp.2013.45

138. Zhang X, Tang X, Liu K, Hamblin MH, Yin KJ. Long noncoding RNA malat1 regulates cerebrovascular pathologies in ischemic stroke. *J Neurosci* (2017) 37(7):1797–806. doi:10.1523/JNEUROSCI.3389-16.2017

139. Michalik KM, You X, Manavski Y, Doddaballapur A, Zörnig M, Braun T, et al. Long noncoding RNA MALAT1 regulates endothelial cell function and vessel growth. *Circ Res* (2014) 114(9):1389–97. doi:10.1161/CIRCRESAHA.114.303265

140. Amodio N, Stamato MA, Juli G, Morelli E, Fulciniti M, Manzoni M, et al. Drugging the lncRNA MALAT1 via LNA gapmeR ASO inhibits gene expression of proteasome subunits and triggers anti-multiple myeloma activity. *Leukemia* (2018) 32(9):1948–57. doi:10.1038/s41375-018-0067-3

141. Modarresi F, Faghihi MA, Lopez-Toledano MA, Fatemi RP, Magistri M, Brothers SP, et al. Inhibition of natural antisense transcripts *in vivo* results in gene-specific transcriptional upregulation. *Nat Biotechnol* (2012) 30(5):453–9. doi:10.1038/nbt.2158

142. Shum K, Rossi J. In: *Methods in Molecular Biology*, 1364 (2016).*SiRNA Delivery Methods: Methods and Protocols*

143. Snead NM, Escamilla-Powers JR, Rossi JJ, McCaffrey AP. 5′ unlocked nucleic acid modification improves siRNA targeting. *Mol Ther Nucleic Acids* (2013) 2:e103. doi:10.1038/mtna.2013.36

144. Robbins M, Judge A, Liang L, McClintock K, Yaworski E, MacLachlan I. 2′-O-methyl-modified RNAs act as TLR7 antagonists. *Mol Ther* (2007) 15(9):1663–9. doi:10.1038/sj.mt.6300240

145. Lennox KA, Behlke MA. Cellular localization of long non-coding RNAs affects silencing by RNAi more than by antisense oligonucleotides. *Nucleic Acids Res* (2016) 44(2):863–77. doi:10.1093/nar/gkv1206

146. Hamil AS, Dowdy SF. Synthesis and conjugation of small interfering ribonucleic neutral siRNNs. *Methods Mol Biol* (2016) 1364:1–9. doi:10.1007/978-1-4939-3112-5_1

147. Sheridan C. Billion-dollar deal propels RNAi to CNS frontier. *Nat Biotechnol* (2019) 37:702–4. doi:10.1038/d41587-019-00014-7

148. Brown KM, Nair JK, Janas MM, Anglero-Rodriguez YI, Dang LTH, Peng H, et al. Expanding RNAi therapeutics to extrahepatic tissues with lipophilic conjugates. *Nat Biotechnol* (2022) 40:1500–8. Internet. doi:10.1038/s41587-022-01334-x

149. Deng M, Zhang Z, Xing M, Liang X, Li Z, Wu J, et al. LncRNA MRAK159688 facilitates morphine tolerance by promoting REST-mediated inhibition of mu opioid receptor in rats. *Neuropharmacology* (2022) 206:108938. doi:10.1016/j.neuropharm.2021.108938

150. Huang R, Zhang Y, Han B, Bai Y, Zhou R, Gan G, et al. Circular RNA HIPK2 regulates astrocyte activation via cooperation of autophagy and ER stress by targeting MIR124–2HG. *Autophagy* (2017) 13(10):1722–41. doi:10.1080/15548627.2017.1356975

151. Liu S, Cui B, Dai Z-X, Shi P-k, Wang Z-H, Guo Y-Y. Long non-coding RNA HOTAIR promotes Parkinson';s disease induced by MPTP through up-regulating the expression of LRRK2. *Curr Neurovasc Res* (2016) 13(2):115–20. doi:10.2174/1567202613666160316155228

152. Cai L, Tu L, Li T, Yang X, Ren Y, Gu R, et al. Downregulation of lncRNA UCA1 ameliorates the damage of dopaminergic neurons, reduces oxidative stress and inflammation in Parkinson's disease through the inhibition of the PI3K/Akt signaling pathway. *Int Immunopharmacol* (2019) 75:105734. doi:10.1016/j.intimp.2019.105734

153. Lopez-Toledano MA, Modarresi F, Faghihi MA, Patel NS, Sahagan BG, Wahlestedt C. Knockdown of BACE1-AS nonprotein-coding transcript modulates beta-amyloid-related hippocampal neurogenesis. *Int J Alzheimers Dis* (2011) 2011:929042. doi:10.4061/2011/929042

154. Zhang W, Zhao H, Wu Q, Xu W, Xia M. Knockdown of BACE1-AS by siRNA improves memory and learning behaviors in Alzheimer's disease animal model. *Exp Ther Med* (2018) 16(3):2080–6. doi:10.3892/etm.2018.6359

155. Li F, Wang Y, Yang H, Xu Y, Zhou X, Zhang X, et al. The effect of BACE1-AS on β-amyloid generation by regulating BACE1 mRNA expression. *BMC Mol Biol* (2019) 20(1):23. doi:10.1186/s12867-019-0140-0

156. Shao L, Jiang G-T, Yang X-L, Zeng M-L, Cheng J-J, Kong S, et al. Silencing of circIgf1r plays a protective role in neuronal injury via regulating astrocyte polarization during epilepsy. *FASEB J* (2021) 35(2):e21330. doi:10.1096/fj.202001737RR

157. Wu Q, Yi X. Down-regulation of long noncoding RNA MALAT1 protects hippocampal neurons against excessive autophagy and apoptosis via the PI3K/akt signaling pathway in rats with epilepsy. *J Mol Neurosci* (2018) 65(2):234–45. doi:10.1007/s12031-018-1093-3

158. Zhao JH, Wang B, Wang XH, Wang JR, Xu CW. Influence of lncRNA ANRIL on neuronal apoptosis in rats with cerebral infarction by regulating the NF-κB signaling pathway. *Eur Rev Med Pharmacol Sci* (2019) 23(22):10092–100. doi:10.26355/eurrev_201911_19577

159. Zhao JH, Wang B, Wang XH, Xu CW. Effect of lncRNA GAS5 on the apoptosis of neurons via the notch1 signaling pathway in rats with cerebral infarction. *Eur Rev Med Pharmacol Sci* (2019) 23(22):10083–91. doi:10.26355/eurrev_201911_19576

160. Rupaimoole R, Slack FJ. MicroRNA therapeutics: Towards a new era for the management of cancer and other diseases. *Nat Rev Drug Discov* (2017) 16:203–22. doi:10.1038/nrd.2016.246

161. Jung J, Yeom C, Choi YS, Kim S, Lee EJ, Park MJ, et al. Simultaneous inhibition of multiple oncogenic miRNAs by a multi-potent microRNA sponge. *Oncotarget* (2015) 6(24):20370–87. doi:10.18632/oncotarget.4827

162. Das S, Kohr M, Dunkerly-Eyring B, Lee DI, Bedja D, Kent OA, et al. Divergent effects of miR-181 family members on myocardial function through protective cytosolic and detrimental mitochondrial microRNA targets. *J Am Heart Assoc* (2017) 6(3):e004694. doi:10.1161/JAHA.116.004694

163. Bernardo BC, Gregorevic P, Ritchie RH, McMullen JR. Generation of MicroRNA-34 sponges and tough decoys for the heart: Developments and challenges. *Front Pharmacol* (2018) 9:1090. doi:10.3389/fphar.2018.01090

164. Kyzar EJ, Bohnsack JP, Zhang H, Pandey SC. MicroRNA-137 drives epigenetic reprogramming in the adult amygdala and behavioral changes after adolescent alcohol exposure. *eNeuro* (2019) 6(6):0401–19. doi:10.1523/ENEURO.0401-19.2019

165. Most D, Salem NA, Tiwari GR, Blednov YA, Mayfield RD, Harris RA. Silencing synaptic MicroRNA-411 reduces voluntary alcohol consumption in mice. *Addict Biol* (2019) 24(4):604–16. doi:10.1111/adb.12625

166. Teppen TL, Krishnan HR, Zhang H, Sakharkar AJ, Pandey SC. The potential role of amygdaloid MicroRNA-494 in alcohol-induced anxiolysis. *Biol Psychiatry* (2016) 80(9):711–9. doi:10.1016/j.biopsych.2015.10.028

167. Huang J, Liang X, Wang J, Kong Y, Zhang Z, Ding Z, et al. miR-873a-5p targets A20 to facilitate morphine tolerance in mice. *Front Neurosci* (2019) 13(APR):347. doi:10.3389/fnins.2019.00347

168. Perumal N, Kanchan RK, Doss D, Bastola N, Atri P, Chirravuri-Venkata R, et al. MiR-212-3p functions as a tumor suppressor gene in group 3 medulloblastoma via targeting nuclear factor I/B (NFIB). *Acta Neuropathol Commun* (2021) 9(1):195. doi:10.1186/s40478-021-01299-z

169. Vázquez-Ríos AJ, Molina-Crespo Á, Bouzo BL, López-López R, Moreno-Bueno G, de la Fuente M. Exosome-mimetic nanoplatforms for targeted cancer drug delivery. *J Nanobiotechnology* (2019) 17(1):85. doi:10.1186/s12951-019-0517-8

170. Ofek P, Calderón M, Mehrabadi FS, Krivitsky A, Ferber S, Tiram G, et al. Restoring the oncosuppressor activity of microRNA-34a in glioblastoma using a polyglycerol-based polyplex. *Nanomedicine* (2016) 12(7):2201–14. doi:10.1016/j.nano.2016.05.016

171. Janssen HLA, Reesink HW, Lawitz EJ, Zeuzem S, Rodriguez-Torres M, Patel K, et al. Treatment of HCV infection by targeting MicroRNA. *N Engl J Med* (2013) 368(18):1685–94. doi:10.1056/NEJMoa1209026

172. van der Ree MH, de Vree JM, Stelma F, Willemse S, van der Valk M, Rietdijk S, et al. Safety, tolerability, and antiviral effect of RG-101 in patients with chronic hepatitis C: A phase 1B, double-blind, randomised controlled trial. *Lancet* (2017) 389(10070):709–17. doi:10.1016/S0140-6736(16)31715-9

173. Reid G, Pel ME, Kirschner MB, Cheng YY, Mugridge N, Weiss J, et al. Restoring expression of miR-16: A novel approach to therapy for malignant pleural mesothelioma. *Ann Oncol* (2013) 24(12):3128–35. doi:10.1093/annonc/mdt412

174. Chakraborty C, Sharma AR, Sharma G, Lee SS. Therapeutic advances of miRNAs: A preclinical and clinical update. *J Adv Res* (2021) 28:127–38. doi:10.1016/j.jare.2020.08.012

175. Romano G, Acunzo M, Nana-Sinkam P. Micrornas as novel therapeutics in cancer. *Cancers* (2021) 13:1526. doi:10.3390/cancers13071526

176. Falese JP, Donlic A, Hargrove AE. Targeting RNA with small molecules: From fundamental principles towards the clinic. *Chem Soc Rev* (2021) 50:2224–43. doi:10.1039/d0cs01261k

177. Costales MG, Haga CL, Velagapudi SP, Childs-Disney JL, Phinney DG, Disney MD. Small molecule inhibition of microRNA-210 reprograms an oncogenic hypoxic circuit. *J Am Chem Soc* (2017) 139(9):3446–55. doi:10.1021/jacs.6b11273

178. Costales MG, Aikawa H, Li Y, Childs-Disney JL, Abegg D, Hoch DG, et al. Small-molecule targeted recruitment of a nuclease to cleave an oncogenic RNA in a mouse model of metastatic cancer. *Proc Natl Acad Sci U S A* (2020) 117(5):2406–11. doi:10.1073/pnas.1914286117

179. Wang L, Rowe RG, Jaimes A, Yu C, Nam Y, Pearson DS, et al. Small-molecule inhibitors disrupt let-7 oligouridylation and release the selective blockade of let-7 processing by LIN28. *Cel Rep.* (2018) 23(10):3091–101. doi:10.1016/j.celrep.2018.04.116

180. Chhabra M. Biological therapeutic modalities. In: *Translational Biotechnology: A Journey from Laboratory to Clinics* (2021).

181. Warner KD, Hajdin CE, Weeks KM. Principles for targeting RNA with drug-like small molecules. *Nat Rev Drug Discov* (2018) 17(8):547–58. doi:10.1038/nrd.2018.93

182. Sztuba-Solinska J, Chavez-Calvillo G, Cline SE. Unveiling the druggable RNA targets and small molecule therapeutics. *Bioorg Med Chem* (2019) 27:2149–65. doi:10.1016/j.bmc.2019.03.057

183. Luo Y, Disney MD. Bottom-up design of small molecules that stimulate exon 10 skipping in mutant MAPT pre-mRNA. *ChemBioChem* (2015) 16(17):2041–4. doi:10.1002/cbic.201402069

184. Keller CG, Shin Y, Monteys AM, Renaud N, Beibel M, Teider N, et al. An orally available, brain penetrant, small molecule lowers huntingtin levels by enhancing pseudoexon inclusion. *Nat Commun* (2022) 13(1):1150. doi:10.1038/s41467-022-28653-6

185. Disney MD, Liu B, Yang WY, Sellier C, Tran T, Charlet-Berguerand N, et al. A small molecule that targets r(CGG)exp and improves defects in fragile X-associated tremor ataxia syndrome. *ACS Chem Biol* (2012) 7(10):1711–8. doi:10.1021/cb300135h

186. Yang WY, He F, Strack RL, Oh SY, Frazer M, Jaffrey SR, et al. Small molecule recognition and tools to study modulation of r(CGG)exp in fragile X-associated tremor ataxia syndrome. *ACS Chem Biol* (2016) 11(9):2456–65. doi:10.1021/acschembio.6b00147

187. Yang WY, Gao R, Southern M, Sarkar PS, Disney MD. Design of a bioactive small molecule that targets r(AUUCU) repeats in spinocerebellar ataxia 10. *Nat Commun* (2016) 7:11647. doi:10.1038/ncomms11647

188. Rzuczek SG, Colgan LA, Nakai Y, Cameron MD, Furling D, Yasuda R, et al. Precise small-molecule recognition of a toxic CUG RNA repeat expansion. *Nat Chem Biol* (2017) 13(2):188–93. doi:10.1038/nchembio.2251

189. di Giorgio A, Duca M. Synthetic small-molecule RNA ligands: Future prospects as therapeutic agents. *MedChemComm* (2019) 10(8):1242–55. doi:10.1039/c9md00195f

190. Dhillon S. Risdiplam: First approval. *Drugs* (2020) 80(17):1853–8. doi:10.1007/s40265-020-01410-z

191. Donlic A, Zafferani M, Padroni G, Puri M, Hargrove AE. Regulation of MALAT1 triple helix stability and *in vitro* degradation by diphenylfurans. *Nucleic Acids Res* (2020) 48(14):7653–64. doi:10.1093/nar/gkaa585

192. Donlic A, Morgan BS, Xu JL, Liu A, Roble C, Hargrove AE. Discovery of small molecule ligands for MALAT1 by tuning an RNA-binding scaffold. *Angew Chem Int Ed Engl* (2018) 57(40):13242–7. doi:10.1002/anie.201808823

193. Ahmadi S, Zobeiri M, Mohammadi Talvar S, Masoudi K, Khanizad A, Fotouhi S, et al. Differential expression of H19, BC1, MIAT1, and MALAT1 long non-coding RNAs within key brain reward regions after repeated morphine treatment. *Behav Brain Res* (2021) 414:113478. doi:10.1016/j.bbr.2021.113478

194. Tazi J, Begon-Pescia C, Campos N, Apolit C, Garcel A, Scherrer D. Specific and selective induction of miR-124 in immune cells by the quinoline ABX464: A transformative therapy for inflammatory diseases. *Drug Discov Today* (2021) 26:1030–9. doi:10.1016/j.drudis.2020.12.019

195. Shi Y, Parag S, Patel R, Lui A, Murr M, Cai J, et al. Stabilization of lncRNA GAS5 by a small molecule and its implications in diabetic adipocytes. *Cell Chem. Biol.* (2019) 26(3):319–30. doi:10.1016/j.chembiol.2018.11.012

196. Padmakumar S, Jones G, Khorkova O, Hsiao J, Kim J, Bleier BS, et al. Osmotic core-shell polymeric implant for sustained BDNF AntagoNAT delivery in CNS using minimally invasive nasal depot (MIND) approach. *Biomaterials* (2021) 276:120989. doi:10.1016/j.biomaterials.2021.120989

197. Padmakumar S, Jones G, Pawar G, Khorkova O, Hsiao J, Kim J, et al. Minimally invasive nasal depot (MIND) technique for direct BDNF AntagoNAT delivery to the brain. *J Controlled Release* (2021) 331:176–86. doi:10.1016/j.jconrel.2021.01.027

198. Deverman BE, Pravdo PL, Simpson BP, Kumar SR, Chan KY, Banerjee A, et al. Cre-dependent selection yields AAV variants for widespread gene transfer to the adult brain. *Nat Biotechnol* (2016) 34(2):204–9. doi:10.1038/nbt.3440

199. Choudhury SR, Harris AF, Cabral DJ, Keeler AM, Sapp E, Ferreira JS, et al. Widespread central nervous system gene transfer and silencing after systemic delivery of novel AAV-AS vector. *Mol Ther* (2016) 24(4):726–35. doi:10.1038/mt.2015.231

200. Talbot K, Wood MJA. Wrangling RNA: Antisense oligonucleotides for neurological disorders. *Sci Transl Med* (2019) 11(511):eaay2069. doi:10.1126/scitranslmed.aay2069

201. Nectow AR, Nestler EJ. Viral tools for neuroscience. *Nat Rev Neurosci* (2020) 21:669–81. doi:10.1038/s41583-020-00382-z

202. Imbert M, Dias-Florencio G, Goyenvalle A. Viral vector-mediated antisense therapy for genetic diseases. *Genes* (2017) 8:E51. doi:10.3390/genes8020051

203. Fu Y, Chen J, Huang Z. Recent progress in microrna-based delivery systems for the treatment of human disease. *ExRNA* (2019) 1:24. doi:10.1186/s41544-019-0024-y

204. Lundstrom K. Viral vectors applied for RNAi-based antiviral therapy. *Viruses* (2020) 12:924. doi:10.3390/v12090924

205. Komatsu H. Innovative therapeutic approaches for Huntington's disease: From nucleic acids to GPCR-targeting small molecules. *Front Cel Neurosci.* (2021) 15:785703. doi:10.3389/fncel.2021.785703

206. Koshimizu Y, Isa K, Kobayashi K, Isa T. Double viral vector technology for selective manipulation of neural pathways with higher level of efficiency and safety. *Gene Ther* (2021) 28(6):339–50. doi:10.1038/s41434-020-00212-y

207. Jüttner J, Szabo A, Gross-Scherf B, Morikawa RK, Rompani SB, Hantz P, et al. Targeting neuronal and glial cell types with synthetic promoter AAVs in mice, non-human primates and humans. *Nat Neurosci* (2019) 22(8):1345–56. doi:10.1038/s41593-019-0431-2

208. Bedbrook CN, Deverman BE, Gradinaru V. Viral strategies for targeting the central and peripheral nervous systems. *Annu Rev Neurosci* (2018) 41:323–48. doi:10.1146/annurev-neuro-080317-062048

209. Borel F, Gernoux G, Sun H, Stock R, Blackwood M, Brown RH, et al. Safe and effective superoxide dismutase 1 silencing using artificial microRNA in macaques. *Sci Transl Med* (2018) 10(465):eaau6414. doi:10.1126/scitranslmed.aau6414

210. Mueller C, Berry JD, McKenna-Yasek DM, Gernoux G, Owegi MA, Pothier LM, et al. SOD1 suppression with adeno-associated virus and MicroRNA in familial ALS. *N Engl J Med* (2020) 383(2):151–8. doi:10.1056/NEJMoa2005056

211. Yang B, Li S, Wang H, Guo Y, Gessler DJ, Cao C, et al. Global CNS transduction of adult mice by intravenously delivered rAAVrh.8 and rAAVrh.10 and nonhuman primates by rAAVrh.10. *Mol Ther* (2014) 2:1299–309. doi:10.1038/mt.2014.68

212. Tung YT, Peng KC, Chen YC, Yen YP, Chang M, Thams S, et al. Mir-17~92 confers motor neuron subtype differential resistance to ALS-associated degeneration. *Cell Stem Cell* (2019) 25(2):193–209. doi:10.1016/j.stem.2019.04.016

213. Dirren E, Aebischer J, Rochat C, Towne C, Schneider BL, Aebischer P. SOD1 silencing in motoneurons or glia rescues neuromuscular function in ALS mice. *Ann Clin Transl Neurol* (2015) 2(2):167–84. doi:10.1002/acn3.162

214. Martier R, Sogorb-Gonzalez M, Stricker-Shaver J, Hübener-Schmid J, Keskin S, Klima J, et al. Development of an AAV-based MicroRNA gene therapy to treat machado-joseph disease. *Mol Ther Methods Clin Dev* (2019) 15:343–58. doi:10.1016/j.omtm.2019.10.008

215. Borel F, Gernoux G, Cardozo B, Metterville JP, Toro Cabreja GC, Song L, et al. Therapeutic rAAVrh10 mediated SOD1 silencing in adult SOD1G93A mice and nonhuman primates. *Hum Gene Ther* (2016) 27(1):19–31. doi:10.1089/hum.2015.122

216. Hudry E, Vandenberghe LH. Therapeutic AAV gene transfer to the nervous system. *A Clin RealityNeuron* (2019) 101:839–62. doi:10.1016/j.neuron.2019.02.017:

217. Mendonça MCP, Kont A, Aburto MR, Cryan JF, O'Driscoll CM. Advances in the design of (Nano)Formulations for delivery of antisense oligonucleotides and small interfering RNA: Focus on the central nervous system. *Mol Pharmaceutics* (2021) 18(4):1491–506. doi:10.1021/acs.molpharmaceut.0c01238

218. Ross KA, Brenza TM, Binnebose AM, Phanse Y, Kanthasamy AG, Gendelman HE, et al. Nano-enabled delivery of diverse payloads across complex biological barriers. *J Controlled Release* (2015) 219:548–59. doi:10.1016/j.jconrel.2015.08.039

219. Yang J, Luo S, Zhang J, Yu T, Fu Z, Zheng Y, et al. Exosome-mediated delivery of antisense oligonucleotides targeting α-synuclein ameliorates the pathology in a mouse model of Parkinson's disease. *Neurobiol Dis* (2021) 148:105218. doi:10.1016/j.nbd.2020.105218

220. Mendonça MCP, Cronin MF, Cryan JF, O'Driscoll CM. Modified cyclodextrin-based nanoparticles mediated delivery of siRNA for huntingtin gene silencing across an *in vitro* BBB model. *Eur J Pharmaceutics Biopharmaceutics* (2021) 169:309–18. doi:10.1016/j.ejpb.2021.11.003

221. Wei T, Cheng Q, Min YL, Olson EN, Siegwart DJ. Systemic nanoparticle delivery of CRISPR-Cas9 ribonucleoproteins for effective tissue specific genome editing. *Nat Commun* (2020) 11(1):3232. doi:10.1038/s41467-020-17029-3

222. Rungta RL, Choi HB, Lin PJC, Ko RWY, Ashby D, Nair J, et al. Lipid nanoparticle delivery of sirna to silence neuronal gene expression in the brain. *Mol Ther Nucleic Acids* (2013) 2:e136. doi:10.1038/mtna.2013.65

223. Yoshida S, Duong C, Oestergaard M, Fazio M, Chen C, Peralta R, et al. MXD3 antisense oligonucleotide with superparamagnetic iron oxide nanoparticles: A new targeted approach for neuroblastoma. *Nanomedicine* (2020) 24:102127. doi:10.1016/j.nano.2019.102127

224. Wang P, Zheng X, Guo Q, Yang P, Pang X, Qian K, et al. Systemic delivery of BACE1 siRNA through neuron-targeted nanocomplexes for treatment of Alzheimer's disease. *J Controlled Release* (2018) 279:220–33. doi:10.1016/j.jconrel.2018.04.034

225. Min HS, Kim HJ, Naito M, Ogura S, Toh K, Hayashi K, et al. Systemic brain delivery of antisense oligonucleotides across the blood–brain barrier with a glucose-coated polymeric nanocarrier. *Angew Chem Int Ed Engl* (2020) 59(21):8173–80. doi:10.1002/anie.201914751

226. Shilo M, Motiei M, Hana P, Popovtzer R. Transport of nanoparticles through the blood-brain barrier for imaging and therapeutic applications. *Nanoscale* (2014) 6(4):2146–52. doi:10.1039/c3nr04878k

227. Sela H, Cohen H, Elia P, Zach R, Karpas Z, Zeiri Y. Spontaneous penetration of gold nanoparticles through the blood brain barrier (BBB). *J Nanobiotechnology* (2015) 13(1):71. doi:10.1186/s12951-015-0133-1

228. Fatima N, Gromnicova R, Loughlin J, Sharrack B, Male D. Gold nanocarriers for transport of oligonucleotides across brain endothelial cells. *PLoS One* (2020) 15(9):e0236611. doi:10.1371/journal.pone.0236611

229. Male D, Gromnicova R. Nanocarriers for delivery of oligonucleotides to the CNS. *Int J Mol Sci* (2022) 23:760. doi:10.3390/ijms23020760

230. Anselmo AC, Mitragotri S. Nanoparticles in the clinic: An update post COVID-19 vaccines. *Bioeng Translational Med* (2021) 6(3):e10246. doi:10.1002/btm2.10246

231. Sukumar UK, Bose RJC, Malhotra M, Babikir HA, Afjei R, Robinson E, et al. Intranasal delivery of targeted polyfunctional gold–iron oxide nanoparticles loaded with therapeutic microRNAs for combined theranostic multimodality imaging and presensitization of glioblastoma to temozolomide. *Biomaterials* (2019) 218:119342. doi:10.1016/j.biomaterials.2019.119342

232. Costa PM, Cardoso AL, Custódia C, Cunha P, Pereira De Almeida L, Pedroso De Lima MC. MiRNA-21 silencing mediated by tumor-targeted nanoparticles combined with sunitinib: A new multimodal gene therapy approach for glioblastoma. *J Controlled Release* (2015) 207:31–9. doi:10.1016/j.jconrel.2015.04.002

233. Dhuri K, Vyas RN, Blumenfeld L, Verma R, Bahal R. Nanoparticle delivered anti-mir-141-3p for stroke therapy. *Cells* (2021) 10(5):1011. doi:10.3390/cells10051011

234. Chivero ET, Liao K, Niu F, Tripathi A, Tian C, Buch S, et al. Engineered extracellular vesicles loaded with miR-124 attenuate cocaine-mediated activation of microglia. *Front Cel Dev. Biol.* (2020) 8:573. doi:10.3389/fcell.2020.00573

235. Zhou Y, Zhu F, Liu Y, Zheng M, Wang Y, Zhang D, et al. Blood-brain barrier-penetrating siRNA nanomedicine for Alzheimer's disease therapy. *Sci Adv* (2020) 6(41):7031. doi:10.1126/sciadv.abc7031

236. Grafals-Ruiz N, Rios-Vicil CI, Lozada-Delgado EL, Quiñones-Díaz BI, Noriega-Rivera RA, Martínez-Zayas G, et al. Brain targeted gold liposomes improve rnai delivery for glioblastoma. *Int J Nanomedicine* (2020) 15:2809–28. doi:10.2147/IJN.S241055

237. Conceição M, Mendonça L, Nóbrega C, Gomes C, Costa P, Hirai H, et al. Intravenous administration of brain-targeted stable nucleic acid lipid particles alleviates Machado-Joseph disease neurological phenotype. *Biomaterials* (2016) 82: 124–37. doi:10.1016/j.biomaterials.2015.12.021

238. Alvarez-Erviti L, Seow Y, Yin H, Betts C, Lakhal S, Wood MJA. Delivery of siRNA to the mouse brain by systemic injection of targeted exosomes. *Nat Biotechnol* (2011) 29(4):341–5. doi:10.1038/nbt.1807

239. Heidel JD, Yu Z, Liu JYC, Rele SM, Liang Y, Zeidan RK, et al. Administration in non-human primates of escalating intravenous doses of targeted nanoparticles containing ribonucleotide reductase subunit M2 siRNA. *Proc Natl Acad Sci U S A* (2007) 104(14):5715–21. doi:10.1073/pnas.0701458104

240. Yuan Z, Zhao L, Zhang Y, Li S, Pan B, Hua L, et al. Inhibition of glioma growth by a GOLPH3 siRNA-loaded cationic liposomes. *J Neurooncol* (2018) 140(2):249–60. doi:10.1007/s11060-018-2966-6

241. Ye C, Pan B, Xu H, Zhao Z, Shen J, Lu J, et al. Co-delivery of GOLPH3 siRNA and gefitinib by cationic lipid-PLGA nanoparticles improves EGFR-targeted therapy for glioma. *J Mol Med* (2019) 97(11):1575–88. doi:10.1007/s00109-019-01843-4

242. Chen L, Watson C, Morsch M, Cole NJ, Chung RS, Saunders DN, et al. Improving the delivery of SOD1 antisense oligonucleotides to motor neurons using calcium phosphate-lipid nanoparticles. *Front Neurosci* (2017) 11(AUG):476. doi:10.3389/fnins.2017.00476

243. Dowdy SF. Overcoming cellular barriers for RNA therapeutics. *Nat Biotechnol* (2017) 35:222–9. doi:10.1038/nbt.3802

244. Yamada Y. Nucleic acid drugs—current status, issues, and expectations for exosomes. *Cancers* (2021) 13:5002. doi:10.3390/cancers13195002

245. Kilikevicius A, Meister G, Corey DR. Reexamining assumptions about miRNA-guided gene silencing. *Nucleic Acids Res* (2022) 50:617–34. doi:10.1093/nar/gkab1256

246. Alles J, Fehlmann T, Fischer U, Backes C, Galata V, Minet M, et al. An estimate of the total number of true human miRNAs. *Nucleic Acids Res* (2019) 47(7):3353–64. doi:10.1093/nar/gkz097

247. Diener C, Keller A, Meese E. Emerging concepts of miRNA therapeutics: From cells to clinic. *Trends Genet* (2022) 38:613–26. doi:10.1016/j.tig.2022.02.006

248. Kim M, Lee Y, Lee M, Yoo J, Kim JS. Sequence-dependent twist-bend coupling in DNA minicircles. *Nanoscale* (2021) 13(33):20186–96. doi:10.1039/d1nr04672a

249. Wang K, Kumar US, Sadeghipour N, Massoud TF, Paulmurugan R. A microfluidics-based scalable approach to generate extracellular vesicles with enhanced therapeutic MicroRNA loading for intranasal delivery to mouse glioblastomas. *ACS Nano* (2021) 15(11):18327–46. doi:10.1021/acsnano.1c07587

250. Yang YL, Zhang XY, Wu SW, Zhang R, Zhou BL, Zhang XY, et al. Enhanced nose-to-brain delivery of siRNA using hyaluronan-enveloped nanomicelles for glioma therapy. *J Controlled Release* (2022) 342:66–80. doi:10.1016/j.jconrel.2021.12.034

251. Hao R, Sun B, Yang L, Ma C, Li S. RVG29-modified microRNA-loaded nanoparticles improve ischemic brain injury by nasal delivery. *Drug Deliv* (2020) 27(1):772–81. doi:10.1080/10717544.2020.1760960

252. Rassu G, Soddu E, Posadino AM, Pintus G, Sarmento B, Giunchedi P, et al. Nose-to-brain delivery of BACE1 siRNA loaded in solid lipid nanoparticles for Alzheimer's therapy. *Colloids Surf B Biointerfaces* (2017) 152:296–301. doi:10.1016/j.colsurfb.2017.01.031

253. Borgonetti V, Galeotti N. Intranasal delivery of an antisense oligonucleotide to the RNA-binding protein HuR relieves nerve injury-induced neuropathic pain. *Pain* (2021) 162(5):1500–10. doi:10.1097/j.pain.0000000000002154

254. Holm A, Hansen SN, Klitgaard H, Kauppinen S. Clinical advances of RNA therapeutics for treatment of neurological and neuromuscular diseases. *RNA Biol* (2022) 19(1):594–608. doi:10.1080/15476286.2022.2066334

255. Kasina V, Mownn RJ, Bahal R, Sartor GC. Nanoparticle delivery systems for substance use disorder. *Neuropsychopharmacology* (2022) 47:1431–9. doi:10.1038/s41386-022-01311-7

256. Shabanpoor F, Hammond SM, Abendroth F, Hazell G, Wood MJA, Gait MJ. Identification of a peptide for systemic brain delivery of a morpholino oligonucleotide in mouse models of spinal muscular atrophy. *Nucleic Acid Ther* (2017) 27(3):130–43. doi:10.1089/nat.2016.0652

257. Kim G, Kim M, Lee Y, Byun JW, Hwang DW, Lee M. Systemic delivery of microRNA-21 antisense oligonucleotides to the brain using T7-peptide decorated exosomes. *J Controlled Release* (2020) 317:273–81. doi:10.1016/j.jconrel.2019.11.009

258. Mizuo K, Okazaki S. Acute ethanol administration increases mir-124 expression via histone acetylation in the brain. *J Alcohol Drug Depend* (2016) 04(02). doi:10.4172/2329-6488.1000232

259. Sadakierska-Chudy A, Frankowska M, Miszkiel J, Wydra K, Jastrzębska J, Filip M. Prolonged induction of miR-212/132 and REST expression in rat striatum following cocaine self-administration. *Mol Neurobiol* (2017) 54(3):2241–54. doi:10.1007/s12035-016-9817-2

260. Nunez YO, Truitt JM, Gorini G, Ponomareva ON, Blednov YA, Harris RA, et al. Positively correlated miRNA-mRNA regulatory networks in mouse frontal cortex during early stages of alcohol dependence. *BMC Genomics* (2013) 14(1):725. doi:10.1186/1471-2164-14-725

261. Morgan BS, Sanaba BG, Donlic A, Karloff DB, Forte JE, Zhang Y, et al. R-BIND: An interactive database for exploring and developing RNA-targeted chemical probes. *ACS Chem Biol* (2019) 14(12):2691–700. doi:10.1021/acschembio.9b00631

262. Disney MD, Winkelsas AM, Velagapudi SP, Southern M, Fallahi M, Childs-Disney JL. Inforna 2.0: A platform for the sequence-based design of small molecules targeting structured RNAs. *ACS Chem Biol* (2016) 11(6):1720–8. doi:10.1021/acschembio.6b00001

263. Turowski P, Kenny BA. The blood-brain barrier and methamphetamine: Open sesame? *Front Neurosci* (2015) 9:156. doi:10.3389/fnins.2015.00156

264. Hong DS, Kang YK, Borad M, Sachdev J, Ejadi S, Lim HY, et al. Phase 1 study of MRX34, a liposomal miR-34a mimic, in patients with advanced solid tumours. *Br J Cancer* (2020) 122(11):1630–7. doi:10.1038/s41416-020-0802-1

265. Liu C, Kelnar K, Liu B, Chen X, Calhoun-Davis T, Li H, et al. The microRNA miR-34a inhibits prostate cancer stem cells and metastasis by directly repressing CD44. *Nat Med* (2011) 17(2):211–5. doi:10.1038/nm.2284

266. Bader AG. MiR-34 - a microRNA replacement therapy is headed to the clinic. *Front Genet* (2012) 3(JUL):120. doi:10.3389/fgene.2012.00120

267. Kelnar K, Bader AG. A qRT-PCR method for determining the biodistribution profi le of a miR-34a mimic. *Methods Mol Biol* (2015) 1317: 125–33. doi:10.1007/978-1-4939-2727-2_8

268. Moulder SL, Symmans WF, Booser DJ, Madden TL, Lipsanen C, Yuan L, et al. Phase I/II study of G3139 (Bcl-2 antisense oligonucleotide) in combination with doxorubicin and docetaxel in breast cancer. *Clin Cancer Res* (2008) 14(23): 7909–16. doi:10.1158/1078-0432.CCR-08-1104

269. Sternberg CN, Dumez H, van Poppel H, Skoneczna I, Sella A, Daugaard G, et al. Docetaxel plus oblimersen sodium (Bcl-2 antisense oligonucleotide): An EORTC multicenter, randomized phase II study in patients with castration-resistant prostate cancer. *Ann Oncol* (2009) 20(7):1264–9. doi:10.1093/annonc/mdn784

270. Anderson EM, Miller P, Ilsley D, Marshall W, Khvorova A, Stein CA, et al. Gene profiling study of G3139- and Bcl-2-targeting siRNAs identifies a unique G3139 molecular signature. *Cancer Gene Ther* (2006) 13(4):406–14. doi:10.1038/sj.cgt.7700901

271. Lai JC, Tan W, Benimetskaya L, Miller P, Colombini M, Stein CA. A pharmacologic target of G3139 in melanoma cells may be the mitochondrial VDAC. *Proc Natl Acad Sci U S A* (2006) 103(19):7494–9. doi:10.1073/pnas.0602217103

272. Pisano M, Baldinu P, Sini MC, Ascierto PA, Tanda F, Palmieri G. Targeting Bcl-2 protein in treatment of melanoma still requires further clarifications. *Ann Oncol* (2008) 19:2092–3. doi:10.1093/annonc/mdn672

273. Sago CD, Lokugamage MP, Paunovska K, Vanover DA, Monaco CM, Shah NN, et al. High-throughput *in vivo* screen of functional mRNA delivery identifies nanoparticles for endothelial cell gene editing. *Proc Natl Acad Sci U S A* (2018) 115(42):E9944–E9952. doi:10.1073/pnas.1811276115

274. Shu J, Xia Z, Li L, Liang ET, Slipek N, Shen D, et al. Dose-dependent differential mRNA target selection and regulation by let-7a-7f and miR-17-92 cluster microRNAs. *RNA Biol* (2012) 9(10):1275–87. doi:10.4161/rna.21998

275. Winkle M, El-Daly SM, Fabbri M, Calin GA. Noncoding RNA therapeutics — challenges and potential solutions. *Nat Rev Drug Discov* (2021) 20:629–51. doi:10.1038/s41573-021-00219-z

ADAR | Publishing Partnerships

TYPE Original Research
PUBLISHED 05 December 2022
DOI 10.3389/adar.2022.10831

OPEN ACCESS

EDITED BY
Emmanuel Onaivi,
William Paterson University,
United States

REVIEWED BY
Z. Carl Lin,
Harvard Medical School, United States
Berhanu Geresu Kibret,
William Paterson University,
United States

*CORRESPONDENCE
Gregg E. Homanics,
homanicsge@upmc.edu

RECEIVED 10 August 2022
ACCEPTED 14 November 2022
PUBLISHED 05 December 2022

CITATION
Plasil SL, Collins VJ, Baratta AM, Farris SP and Homanics GE (2022), Hippocampal ceRNA networks from chronic intermittent ethanol vapor-exposed male mice and functional analysis of top-ranked lncRNA genes for ethanol drinking phenotypes.
Adv. Drug. Alco. Res. 2:10831.
doi: 10.3389/adar.2022.10831

Hippocampal ceRNA networks from chronic intermittent ethanol vapor-exposed male mice and functional analysis of top-ranked lncRNA genes for ethanol drinking phenotypes

Sonja L. Plasil[1], Valerie J. Collins[1], Annalisa M. Baratta[2], Sean P. Farris[2,3,4] and Gregg E. Homanics[1,2,3,5]*

[1]Department of Pharmacology and Chemical Biology, School of Medicine, University of Pittsburgh, Pittsburgh, PA, United States, [2]Center for Neuroscience, School of Medicine, University of Pittsburgh, Pittsburgh, PA, United States, [3]Department of Anesthesiology and Perioperative Medicine, School of Medicine, University of Pittsburgh, Pittsburgh, PA, United States, [4]Department of Biomedical Informatics, School of Medicine, University of Pittsburgh, Pittsburgh, PA, United States, [5]Department of Neurobiology, School of Medicine, University of Pittsburgh, Pittsburgh, PA, United States

The molecular mechanisms regulating the development and progression of alcohol use disorder (AUD) are largely unknown. While noncoding RNAs have previously been implicated as playing key roles in AUD, long-noncoding RNA (lncRNA) remains understudied in relation to AUD. In this study, we first identified ethanol-responsive lncRNAs in the mouse hippocampus that are transcriptional network hub genes. Microarray analysis of lncRNA, miRNA, circular RNA, and protein coding gene expression in the hippocampus from chronic intermittent ethanol vapor- or air- (control) exposed mice was used to identify ethanol-responsive competing endogenous RNA (ceRNA) networks. Highly interconnected lncRNAs (genes that had the strongest overall correlation to all other dysregulated genes identified) were ranked. The top four lncRNAs were novel, previously uncharacterized genes named *Gm42575*, *4930413E15Rik*, *Gm15767*, and *Gm33447*, hereafter referred to as Pitt1, Pitt2, Pitt3, and Pitt4, respectively. We subsequently tested the hypothesis that CRISPR/Cas9 mutagenesis of the putative promoter and first exon of these lncRNAs in C57BL/6J mice would alter ethanol drinking behavior. The Drinking in the Dark (DID) assay was used to examine binge-like drinking behavior, and the Every-Other-Day Two-Bottle Choice (EOD-2BC) assay was used to examine intermittent ethanol consumption and preference. No significant differences between control and mutant mice were observed in the DID assay. Female-specific reductions in ethanol consumption were observed in the EOD-2BC assay for Pitt1, Pitt3, and Pitt4 mutant mice compared to controls. Male-specific alterations in ethanol preference were observed for Pitt1 and Pitt2. Female-specific increases in ethanol preference were observed for Pitt3 and Pitt4. Total fluid consumption was reduced in Pitt1 and Pitt2 mutants at 15% v/v ethanol and in Pitt3 and Pitt4 at 20% v/v ethanol in females only. We conclude that all lncRNAs targeted altered ethanol drinking

behavior, and that lncRNAs Pitt1, Pitt3, and Pitt4 influenced ethanol consumption in a sex-specific manner. Further research is necessary to elucidate the biological mechanisms for these effects. These findings add to the literature implicating noncoding RNAs in AUD and suggest lncRNAs also play an important regulatory role in the disease.

KEYWORDS

alcohol use disorder, ethanol consumption, CRISPR/Cas9, long-noncoding RNA, transcriptome, knockout, mutagenesis, epigenetics

Introduction

Alcohol use disorder (AUD) is a chronic and debilitating neurological disorder that has extensive global, social, and economic burdens. In the United States AUD is one of the leading risk factors for premature death and disability (1) and has an annual estimated socioeconomic cost of ~$250 billion (2). Many consequences of chronic alcohol misuse are attributed to alcohol's effect on the brain (3, 4), and alcohol acts in part by altering neural gene expression (4–8). Deciphering alcohol's impact on gene expression within discrete brain regions and subsequent downstream effects offers an opportunity to identify novel pharmacological targets that could prevent sustained alcohol-induced alterations from occurring in humans.

The hippocampus is an important ethanol-sensitive brain region involved in the transition to AUD (9–11). The hippocampus is susceptible to the detrimental impacts of excessive alcohol exposure (12–14), and binge-like ethanol consumption has been shown to significantly impact neuroimmune functions within the hippocampus in mice (15). Neuroimmune, transcriptional, and epigenetic cell signaling changes are shown to underly the loss of hippocampal neurogenesis (15, 17–20) and plasticity (9, 19, 21) following both exposure to ethanol and other drugs of abuse (17, 19, 22, 23). This supports the concept that hippocampal neuroadaptations are critical targets to understand ethanol withdrawal and consumption.

The noncoding RNA (ncRNA) transcriptome acts as epigenetic regulators controlling cellular homeostasis (24). Evidence supports important roles for ncRNA in the progression of AUD (7, 8, 25–27). Functional studies targeting specific RNAs in animal models for AUD have shown that the ethanol-responsive RNA transcriptome is involved in ethanol consumption, withdrawal, and the progression of addiction. Transcriptome data gathered from both humans and animals chronically exposed to ethanol has revealed mass dysregulation of multiple RNA subtypes in the brain (7, 8), such as mRNAs and their coded proteins (28–34), miRNAs (7, 35–39), circular RNAs (circRNA) (40), and long noncoding RNAs (lncRNAs) (4, 41–43). LncRNAs are an abundant and diverse subclass of ncRNAs defined as transcripts exceeding 200 nucleotides (nts) that do not encode protein (7, 44). There are over 100,000 different lncRNA transcripts (45–49), with many showing brain-specific expression (50). LncRNAs are known for their roles in epigenetic regulation (44, 50–53), such as impacting chromatin modifications, RNA processing events, modulation of miRNAs, gene silencing, regulation of neighboring genes, synaptic plasticity (44) and molecular networks by acting and interacting as central hubs (8, 54). Those that have been studied largely function by regulating gene expression through *cis*- and *trans*-mechanisms (55, 56). LncRNA expression can be developmentally regulated, can show tissue- and cell-type specific expression, and can be involved in numerous cellular pathways critical to normal development and physiology (50–53, 57–59). The dysregulation of lncRNAs has been linked to the pathophysiology of several disease states (7, 8, 41, 44, 53, 60–66) including AUD (41, 67, 68), drug addiction (63, 69–71), psychiatric disorders (72, 73), and stress responses (74, 75). Identifying and directly testing lncRNAs that regulate ethanol consumption and related behaviors is important to fully understand the initiation and progression of AUD. Here, we hypothesize that specific ethanol-responsive lncRNAs are critical hubs of molecular networks that act as key determinants of ethanol consumption. Targeting specific ethanol-responsive lncRNAs for genetic modulation that have strong correlations to other ethanol-responsive RNAs may help discern transcriptomic network alterations that can impact ethanol drinking phenotypes.

To shed light on how ncRNAs interact with each other *in vivo*, competing endogenous RNA (ceRNA) networks can be bioinformatically generated from transcriptome data sets (76–81). LncRNA, circRNA, and miRNA are all known as ncRNA epigenetic regulators, which work in concert to coordinate mRNA expression, protein levels, and homeostasis *via* such functions as transcription factors, molecular sponges, scaffolds, decoys, and guides (for reviews, see: (7,24, 44, 51, 53, 54, 63). These networks provide insight into discrete clusters of RNAs that interact and/or compete with each other to maintain the network's function (76–81). These correlated RNAs can then be intertwined and linked together computationally to either increase or decrease the rank of hub genes based on their relative interconnectivity with other genes. Generating ethanol-responsive ceRNA networks from four prominent RNA subtypes, lncRNA, mRNA, circRNA, and miRNA, allowed for novel networks and hub genes to be identified in the present study. A list of top-ranked putative hub ethanol-responsive

lncRNAs was generated and genes were prioritized for functional interrogation *via* CRISPR/Cas9 mutagenesis.

The acquisition of transcriptome data has greatly outpaced our capacity to functionally study genes *in vivo* that are hypothesized to contribute to AUD (82). To circumvent this bottleneck, we recently developed an accelerated CRISPR/Cas9 approach to create a cohort of functional KnockOut (KO) animals in a single generation (83). Here we applied this CRISPR Turbo Accelerated KO (CRISPy TAKO) methodology to test the hypothesis that mutation of ethanol-responsive lncRNAs identified from hippocampal ceRNA network analyses impact ethanol drinking behavior. We tested the top four lncRNAs that were identified as potential hubs for ethanol-responsive networks *via* ceRNA analysis. We generated four CRISPy TAKO mouse lines targeting the top four lncRNA candidates identified: *Gm42575*, *4930413E15Rik*, *Gm15767*, and *Gm33447*, hereafter referred to as Pitt1, Pitt2, Pitt3, and Pitt4, respectively. All gene-targeted cohorts were tested for binge-like drinking behavior and intermittent ethanol consumption and preference.

Materials and methods

Animals

All experiments were approved by the Institutional Animal Care and Use Committee of the University of Pittsburgh and conducted in accordance with the National Institutes of Health Guidelines for the Care and Use of Laboratory Animals. C57BL/6J male and female mice used for chronic intermittent ethanol vapor (CIEV) exposure, generation of embryos for electroporation, and purchased control groups were procured from The Jackson Laboratory (Bar Harbor, ME). CD-1 recipient females and vasectomized males were procured from Charles River Laboratories, Inc. (Wilmington, MA). Mice were housed in individually ventilated caging under specific pathogen-free conditions with 12-h light/dark cycles (lights on at 7 AM) and had *ad libitum* access to food (irradiated 5P76 ProLab IsoProRMH3000; LabDiet, St. Louis, MO) and water.

Chronic intermittent ethanol vapor exposure

Male mice were exposed to a 16-h CIEV or room-air paradigm as previously reported (84) (n = 5–6/treatment). Briefly, mice were given a priming intraperitoneal injection of either 1.5 g/kg ethanol (Decon Labs, Inc., #2716GEA) and 68 mg/kg pyrazole (Sigma-Aldrich, P56607-5G) or saline and 68 mg/kg pyrazole, then immediately subjected to vaporized ethanol or room air (respectively) for 16 h/day, 4 days/week, for 7 weeks. Hippocampal tissue was harvested 24 h following the final vapor exposure.

Total RNA isolation and microarray profiling

Left hippocampi were homogenized in 1 ml TRIzol reagent (Invitrogen, #15596018) and sent to Arraystar Inc. (Rockville, MD) for transcriptome analysis. For circRNA analysis, Arraystar Inc. isolated total RNA, digested with RNase R (Epicentre, Inc.), fluorescently labeled (Arraystar Super RNA Labeling Kit), and subsequently hybridized to Arraystar Mouse circRNA Array V2 (8 × 15K). For lncRNA and mRNA analysis, Arraystar Inc. isolated rRNA depleted RNA (mRNA-ONLY™ Eukaryotic mRNA Isolation Kit, Epicentre) from total RNA. rRNA depleted RNA was amplified, fluorescently labeled (Arraystar Flash RNA Labeling Kit), and hybridized to Agilent Arrays (Mouse LncRNA Array v3.0, 8 × 60K). An Agilent Scanner G2505C was used to scan the arrays. The University of Pittsburgh Genomics Sequencing Core used Applied Biosystems GeneChip miRNA 4.0 Arrays to measure changes in abundance of miRNAs from the total RNA samples isolated from the hippocampal tissue. The median intensity expression values were $\log_2$ transformed and quantile normalized across samples. Differential expression were determined using linear models for microarray data (limma) (85) with nominal p-value less than or equal to 0.05 as statistically significant. Weighted gene co-expression network (WGCNA) was used to determine all pairwise correlation among RNAs (i.e., lncRNA, mRNA, circRNA, miRNA) across samples. An unsigned network was constructed using minimum module size of 100, a cut height of 0.99, and a power of 6 to approximate a scale-free topology. The expression of unassigned RNAs were labeled as gray. The total connectivity of individual probes was determined from the pairwise adjacency matrix for an unsigned network.

gRNA design

Guide RNAs (gRNAs) were generated using a commercially available two-piece system termed ALT-R™ CRISPR/Cas9 Genome Editing System (IDT DNA, Coralville, IA). This system combines a custom CRISPR RNA (crRNA) for genomic specificity with an invariant trans-activating RNA (tracrRNA) to produce gRNAs (86). crRNAs were designed using the computational program CCTop/CRISPRator (87, 88), which gauges candidate gRNAs for efficiency and specificity. Each crRNA was annealed separately with tracrRNA in a 1:2 M ratio then combined into a single solution for each gene.

Four gRNAs were used to target each of the ethanol-responsive lncRNA genes Pitt1, Pitt3, and Pitt4 and six gRNAs for Pitt2 (see Supplementary Table S1 for gRNA target

sequences). These specifically designed gRNAs bind within a 598, 796, 341, or 372 base pairs (bp) target region that includes the putative promoter and first exon of Pitt1-Pitt4, respectively. We followed the annotations available at the time on the Ensembl Genome Browser (GRCm38/mm10).

CRISPR/Cas9 mutagenesis

Female C57BL/6J mice were superovulated with 0.1 ml of CARD HyperOva (CosmoBio, #KYD-010) between 10 and 11 AM, followed by 100 IU of human chorionic gonadotropin (Sigma, #CG10) 46–48 h later. Donor females were caged overnight with C57BL/6J males starting 4–6 h post-gonadotropin injection and allowed to mate. Embryos were harvested from oviducts between 9 and 10 AM the following morning, cumulus cells were removed using hyaluronidase, and embryos were cultured under 5% CO_2 in KSOM medium (Cytospring, #K0101) for 1–2 h. Embryos were electroporated in 5 µL total volume of Opti-MEM medium (ThermoFisher, #31985088) containing 100 ng/µL of each gRNA cocktail and 200 ng/µL Alt-R® S.p. HiFi Cas9 Nuclease V3 protein (IDT, #1081060) with a Bio-Rad Gene-Pulser Xcell in a 1 mm-gap slide electrode (Protech International, #501P1-10) using square-wave pulses (five repeats of 3 msec 25V pulses with 100 msec interpulse intervals). Electroporated embryos were placed back into culture under 5% CO_2 in KSOM. For *in vitro* validation of Pitt1-Pitt4 gRNAs, embryos were cultured for 3 days until the morulea/blastocyst stage and subsequently analyzed for mutations. For *in vivo* cohort generation, one- or two-cell embryos were surgically implanted into the oviducts of plug-positive CD-1 recipients (20–40 embryos per recipient) that had been mated to vasectomized males the previous night.

Genotyping

DNA was amplified from individual Pitt1-Pitt4 gRNA-electroporated embryos using a Qiagen Repli-G kit (Qiagen, #150025). DNA was isolated from ear snips of Pitt1-Pitt4 TAKO offspring using Quick Extract (Lucigen, #QE09050). DNAs were genotyped by PCR under the following settings: 95°C for 5 min (1x); 95°C for 30 s, 60°C for 30 s, 72°C for 1 min (40x); 72°C for 10 min (1x). Primers for PCR amplification of Pitt1-Pitt4 are listed in Supplementary Table S1. PCR amplicons of Pitt1-Pitt4 [Wild-type (WT): 929, 963, 581 and 583 bp, respectively] were analyzed by agarose gel electrophoresis.

RNA preparation

Hippocampal brain tissue from Pitt1-Pitt4 mice was used for RT-PCR analysis. All mice were 16–20 weeks of age at time of euthanasia. Total RNA was isolated using TRIzol (Invitrogen, #15596018) according to the manufacturer's protocol, and DNA contamination was removed with a TURBO DNA-*free*™ Kit (Invitrogen, #AM1907). Total RNA was analyzed for purity and concentration using a Nanodrop Spectrophotometer (Thermo Scientific, Waltham, MA). One microgram of purified RNA was converted into cDNA using Superscript™ III First-Strand Synthesis System (Invitrogen, #18080051) with random hexamer primers. RT-PCR primers were used that span both the mutation site as well as the downstream probe-binding exonic region for Pitt1-Pitt4 (Supplementary Table S1). A reaction that lacked reverse transcriptase was used as a negative control for each sample tested.

Behavioral testing

All mice were moved into a reverse light-cycle housing/testing room (lights off at 10 AM) at 5 weeks of age and allowed to acclimate for 2–3 weeks before the start of experiments. Mice were weighed weekly during behavioral experimentation. Ethanol-drinking experiments were performed in the housing room. Mice were singly-housed for all behavioral studies. Mice were sequentially tested on DID and EOD-2BC, with a minimum of 7 days between assays.

Pitt1 and Pitt2 were studied together with a purchased control group (controlled for age, sex, and strain) previously shown to be comparable to mock-treatment controls (83). Similarly, Pitt3 and Pitt4 were studied together with a separate purchased control group.

One-bottle drinking in the dark

Mice were given access to ethanol (20% v/v) in 15 ml drinking bottles with 3.5-inch sipper tubes (Amuza, San Diego) 2 h into the dark-cycle for 2 consecutive days. Fresh ethanol solution was prepared daily. The first day's training session lasted for 2 h. The second day's experimental session lasted 4 h. The amount of ethanol consumed by each mouse was recorded. Empty cages with sipper bottles only were used to control for sipper tube leakage, and leakage amount was subtracted from amount of ethanol consumed by the mice. Immediately following the experimental session, blood samples were collected from tail nicks and the plasma isolated. An Analox analyzer was used to measure the blood ethanol concentrations (BECs) of each mouse (mg/dL; 5 µL).

The Pitt1/Pitt2/control cohorts were assayed based on genotype and not sex (i.e., the Pitt1 TAKOs were assayed separately from the Pitt2 TAKOs). The Pitt3/Pitt4/control cohorts were assayed based on sex and not genotype (i.e., the male Pitt3 and Pitt4 TAKOs were assayed separately from the female Pitt3 and Pitt4 TAKOs).

Every-other-day two-bottle choice drinking

Mice were given access to ethanol (v/v; ramping every-other-day from 3%, 6%, 9%, 12% until 15% was reached then maintained for a total of 12 days at 15%) and water for 24-h sessions every other day. If a 20% difference from controls in ethanol consumption was not observed at 15% ethanol, then the concentration was increased to 20% v/v and the experiment extended an additional 12 days. Water alone was offered on off days. The side placement of the ethanol bottles was switched with each drinking session to avoid side preference. Bottles were weighed before placement and after removal from the experimental cages. Empty cages with sipper bottles only were used to control for fluid leakage, and leakage amount was subtracted from the amount consumed by the mice. The quantity of ethanol consumed, and total fluid intake was calculated as g/kg body weight per 24 h. Preference was calculated as amount ethanol consumed divided by total fluid consumed per 24 h. Ethanol drinking results were transformed to reflect the percent change in ethanol consumption compared to control. Ethanol solutions were prepared fresh daily.

Preference for non-ethanol tastants

When a significant difference in ethanol consumption was observed between genotypes, mice were subsequently tested for saccharin (sweet tastant; Sigma-Aldrich, 240931) and quinine (bitter tastant; Sigma-Aldrich, 145912) preference using a 24-h Two-Bottle Choice (2BC) paradigm. One sipper bottle contained the tastant solution and the other contained water. Mice were offered two concentrations of saccharin (0.03% and 0.06%) and quinine (0.03 and 0.06 mM). For each tastant, the lower concentration was presented first followed by the higher concentration. Each concentration was presented for 2 days (4 days total) with at least 7 days of water-only between tastants. Empty cages with sipper bottles only were used to control for leakage, and leakage amount was subtracted from the amount consumed by the mice. Fresh tastant solution was prepared daily.

Statistical analysis

Statistical analysis was performed using GraphPad Prism (GraphPad Software, Inc., La Jolla, CA). Two-way ANOVA with multiple comparisons was used for Pitt1, Pitt2, and control DID and BEC data, and one-way ANOVA with multiple comparisons was used for Pitt3, Pitt4, and control DID and BEC data. Two-way mixed-effects ANOVA with multiple comparisons and repeated measures was used for Pitt1, Pitt2, and control weight over time, and two-way ANOVA with multiple comparisons and repeated measures was used for EOD-2BC data and Pitt3, Pitt4, and control weight over time. Significant main effects were subsequently analyzed with Benjamini, Krieger, and Yekutieli two-stage linear step up procedure post-hoc analysis (89). Technical failures were appropriately removed from analysis.

Because of well-known sex differences of C57BL/6J on ethanol consumption in the DID and EOD-2BC assays (90–93), male and female mice were tested on separate days (except for Pitt1/Pitt2/control DID and BEC), and each sex was analyzed separately. Statistical significance was defined as $p \leq 0.05$ and $q \leq 0.05$. All data are presented as mean ± S.E.M.

Results

Perturbation of the transcriptome following CIEV exposure

Hippocampi were dissected from male mice chronically exposed to ethanol vapor (CIEV) or room air control for 16 h/day, 4 days/week, for 7 weeks, 24 h after the final vapor exposure. The first 24 h of withdrawal from alcohol is a critical window of time associated with relapse, which can be highly detrimental to the long-term goal of reduced drinking (16). This hippocampal tissue originated from the sires previously described in (84) wherein males maintained BECs ranging from 100 to 250 mg/dl throughout the experiment. Total RNA was isolated from hippocampi for transcriptome analysis to identify biological systems affected by chronic ethanol exposure (Figure 1). We detected a total of 18,283 mRNA probes, 27,177 lncRNA probes, 14,182 circRNA probes, and 23,386 miRNA probes on the microarray. To identify RNAs differentially expressed due to CIEV, our analysis separately examined statistically significant changes ($p < 0.05$) in expression for mRNA, lncRNA, circRNA, and miRNA. Among these four classes of RNAs we found that lncRNAs showed the largest number of changes in expression due to chronic ethanol exposure (n = 1,923 up-regulated, n = 2,694 down-regulated). This was followed by mRNA (n = 1,948 up-regulated, n = 2,121 down-regulated), circRNA (n = 750 up-regulated, n = 729 down-regulated), and miRNA (n = 481 up-regulated, n = 723 down-regulated) (Figure 2). This data may suggest that a large number of different RNA within the hippocampus are susceptible to chronic ethanol exposure; however, each of these RNA biotypes do not exist in isolation and must work in concert for homeostatic function of cellular systems.

The expression of different RNA subtypes creates tightly coordinated ceRNA networks to mediate the biological function of molecular circuits (76–81) (Figure 1). We used WGCNA to determine the pairwise correlation of RNA expression across samples and assess the total connectivity of lncRNA, mRNA,

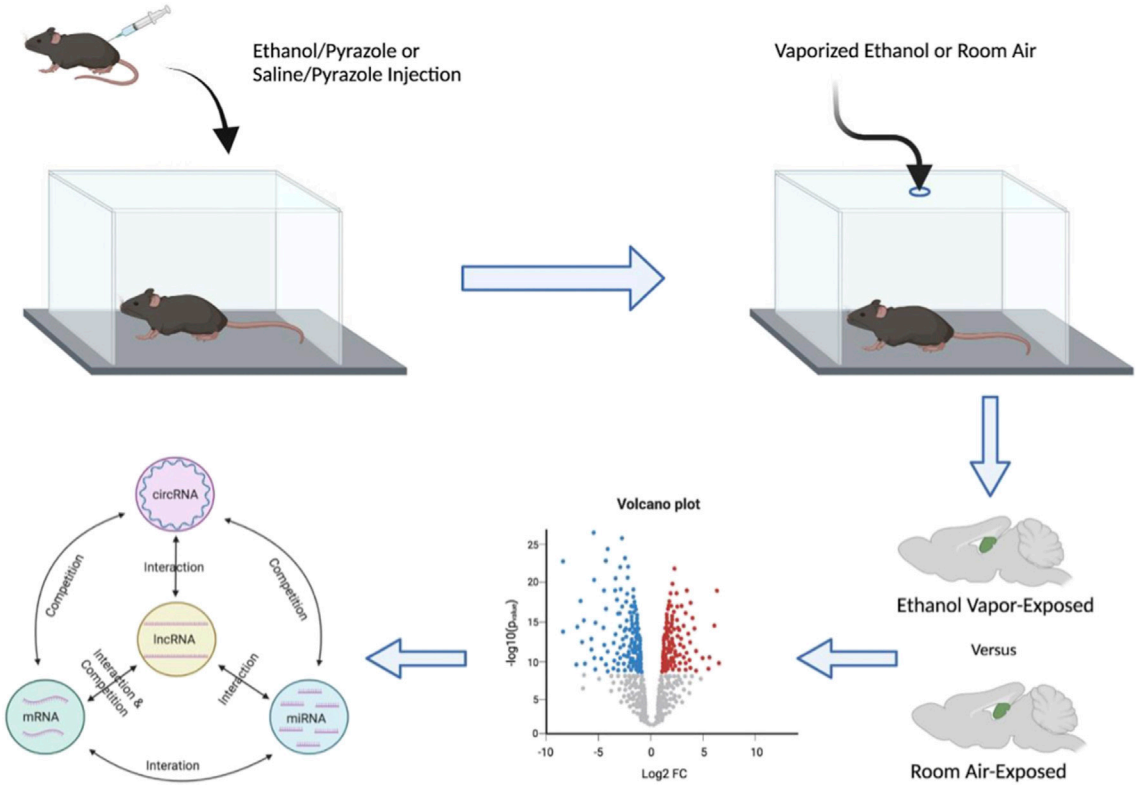

FIGURE 1
Schematic diagram detailing the experimental pipeline utilized to generate the list of top novel ethanol-responsive hub lncRNA candidates to target for ethanol-related functional interrogation. Male mice were given a priming injection of either ethanol and pyrazole or saline and pyrazole and placed in either an ethanol- or room-air vapor champers for 16 h/day, 4 days/week, for 7 weeks, respectively. Hippocampi were dissected 24 h after the final vapor exposure and then subject to mRNA, lncRNA, circRNA, and miRNA microarray analysis. These data sets were then used to generate ceRNA networks of ethanol-responsive RNA genes.

circRNA, and miRNA. Due to the known biological roles in the regulation of gene expression and their perturbation by chronic ethanol exposure, our analysis focused on identifying ethanol-responsive lncRNAs for *in vivo* characterization. Our unbiased transcriptome analysis determined that there were multiple ethanol-responsive lncRNAs that are present in the GRCm38/mm10 mouse genome assembly but have yet to be characterized for molecular or behavioral function. To determine suitable lncRNAs for follow-up *in vivo* studies, we used a summed rank of lncRNAs based on their statistical significance ($p < 0.05$), fold-change in up-regulation of expression, overall level of expression to focus on the most abundant lncRNAs, and lncRNAs with the highest total connectivity within the correlation networks to concentrate on hubs of coordinatedly regulated RNA expression. Additionally, lncRNAs were screened for the capacity to easily create CRISPy TAKO mice by identifying candidates within intergenic regions that did not overlap any other known genes or regulatory regions in the GRCm38/mm10 mouse genome. Based on this selection criteria the top 4 candidate lncRNA selected for testing were *Gm42575*, *4930413E15Rik*, *Gm15767*, and *Gm33447* (Table 1).

CRISPy TAKOs–Pitt1 and Pitt2

CRISPR/Cas9-mediated mutagenesis

To enhance CRISPR mutagenesis frequency as previously described (83), all lncRNA genes were targeted simultaneously with 4–6 gRNAs tiled 50–200 bp apart from each other, spanning the putative promoter and first exon of each gene. Four gRNAs were designed to span a 598 bp range within the Pitt1 gene (Figure 3A). Six gRNAs were designed to span a 796 bp range within the Pitt2 gene (Figure 3D).

Pitt1 and Pitt2 gRNAs were validated for efficient mutagenesis by analyzing *in vitro* cultured embryos following electroporation. Agarose gel electrophoresis of PCR amplicons that span the targeted locus of Pitt1 and Pitt2 indicated that 100% of embryos harbored indels of various sizes (Supplementary Figures S1A,B, respectively).

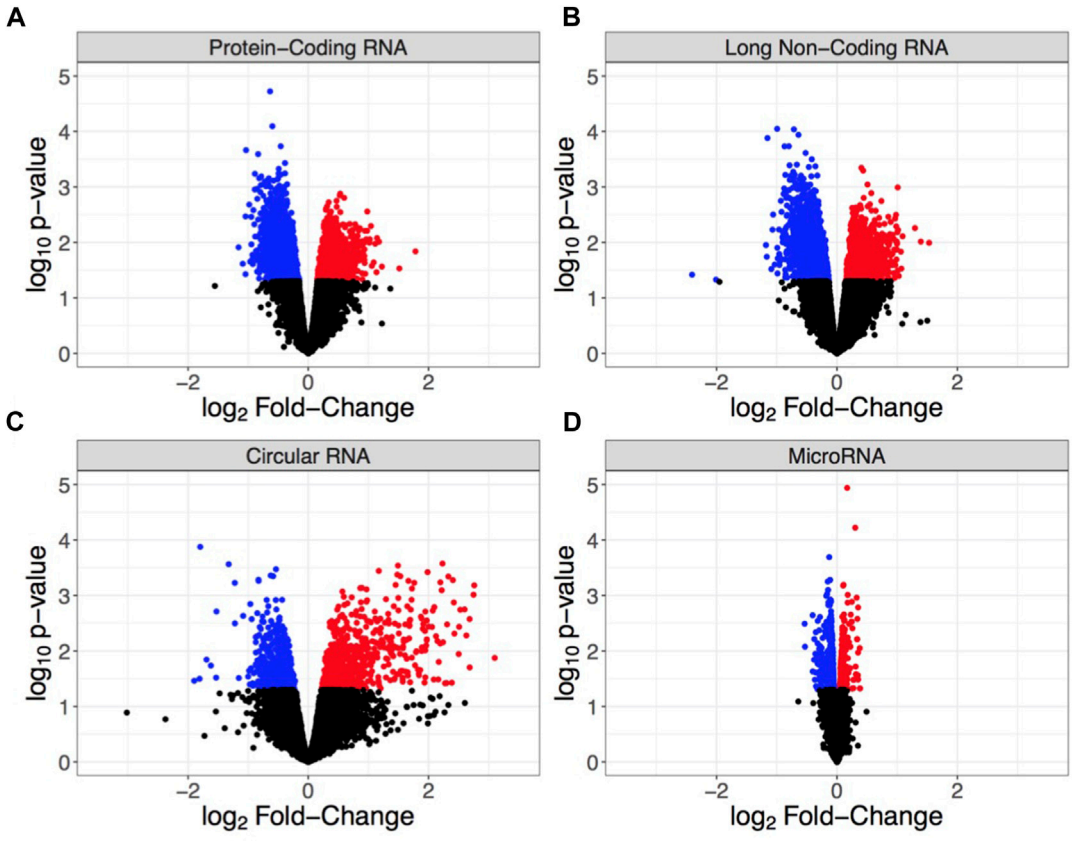

FIGURE 2
Volcano plots showing differential RNA expression based on $\log_2$ fold-change in expression (x-axis) and $\log_{10}$ p-value (y-axis) for **(A)** protein-coding RNA (mRNA), **(B)** long non-coding RNA (lncRNA), **(C)** circular RNA (circRNA), and **(D)** microRNA (miRNA). Each point indicates an individual non-duplicated probe on the microarray with blue = significantly down-regulated, red = significantly up-regulated, and black = non-significant. Significance is defined by $p < 0.05$.

TABLE 1 Bioinformatic data of the top-ranked lncRNA genes identified from the ceRNA networks in order.

Name	Probe	Gene symbol	Chromosome	Strand	Start	End	log fold-change	Mean expression	*p*-value
Pitt1	ASMM10P031898	*Gm42575*	chr5	+	74754373	74754432	0.35	9.71	0.03
Pitt2	ASMM10P032341	*4930413E15Rik*	chr5	+	118961191	118961250	0.28	8.82	0.02
Pitt3	ASMM10P034032	*Gm15767*	chr6	–	147242527	147242586	0.27	9.27	0.03
Pitt4	ASMM10P010493	*Gm33447*	chr13	+	97380367	97380426	0.35	8.25	0.02

Given name, probe, gene symbol, chromosome, strand, gene start, gene end, log fold-change, mean expression, and *p*-value are presented.

A cohort of 35 Pitt1 offspring and 42 Pitt2 offspring, all on the C57BL/6J genetic background, were generated using the CRISPy TAKO approach. All mice born from electroporated embryos were genotyped for gross indels using PCR. The Pitt1 929 bp WT PCR amplicon was readily apparent in control WT DNA but only 2 out of 35 Pitt1 animals (data not shown). The remaining 33 displayed gross indels encompassing the targeted region of interest. PCR bands from a random representative subset of Pitt1 mice selected for behavioral experimentation is shown in Figure 3B. The Pitt2 963 bp WT PCR amplicon was readily apparent in the WT control and 2 out of 42 Pitt2 animals (data not shown). The remaining 40 displayed gross indels encompassing the targeted region of interest. PCR bands from a random representative subset of Pitt2 mice selected for behavioral experimentation is shown in Figure 3E.

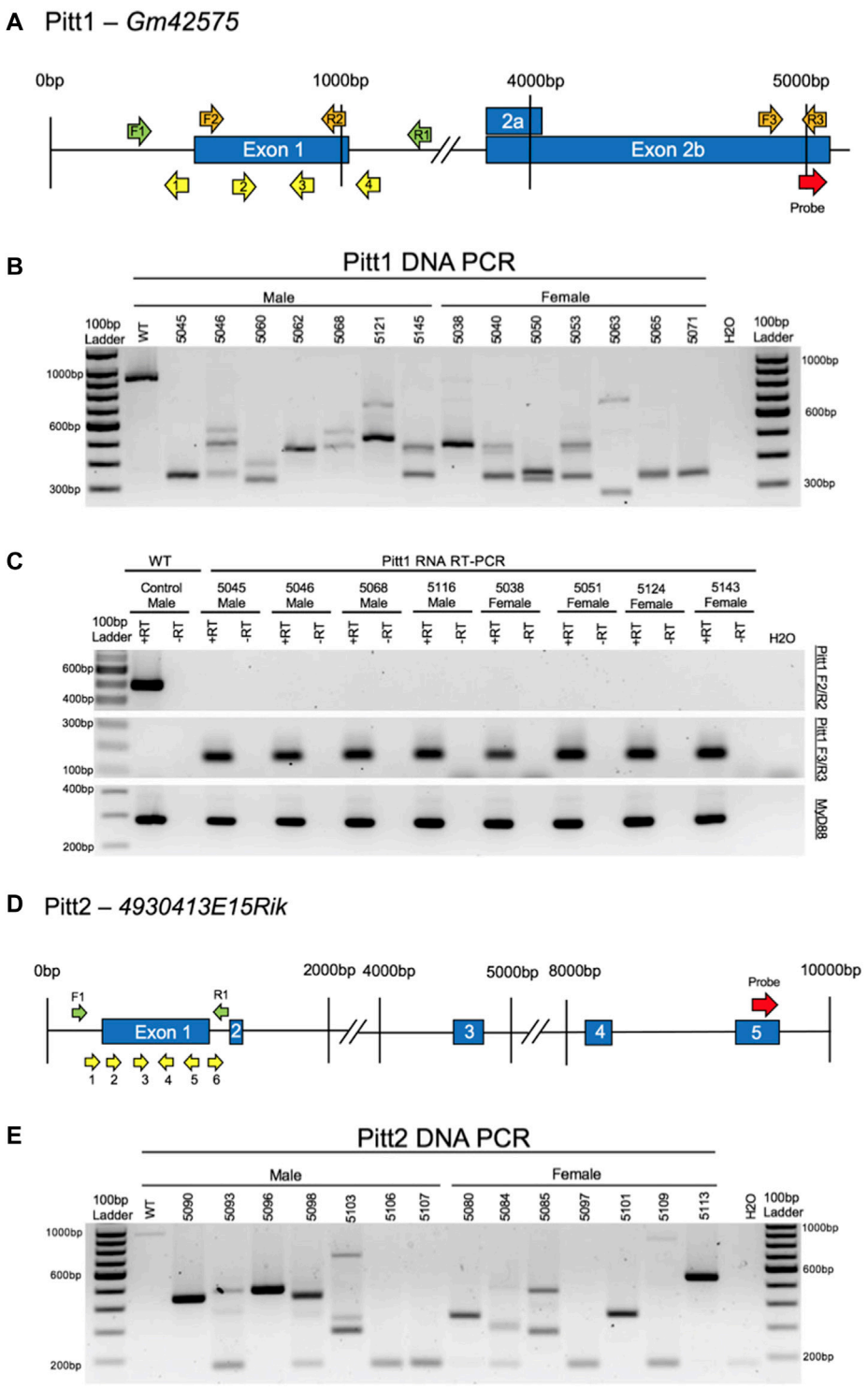

FIGURE 3
CRISPy TAKO schematics and genotypes for Pitt1 and Pitt2. **(A)** Pitt1 gene symbol and structure. The gRNAs, PCR primers, RT-PCR primers, and probe binding site are shown as yellow, green, orange, and red arrows, respectively. **(B)** Agarose gel electrophoresis of PCR amplicons of Pitt1 DNA in a random representative subset of Pitt1 TAKOs demonstrating abnormal amplicons in TAKO mice compared to WT control. Individual mouse numbers are presented above the gel. **(C)** Random representative subset RT-PCR results from Pitt1 hippocampal brain tissue showing abnormal RNA transcripts. (Top) RT-PCR of Pitt1 exon 1 amplicons using the F2/R2 primers demonstrating abnormal RNA transcripts in TAKO mice compared to WT control. (Middle) RT-PCR amplicons using the F3/R3 primers spanning downstream Pitt1 exons, demonstrating abnormal RNA products in Pitt1 mutant TAKOs that are not present in WT. (Bottom) RT-PCR of *MyD88* amplicons used as an internal control. **(D)** Pitt2 gene symbol and
(*Continued*)

FIGURE 3 (Continued)
structure. The gRNAs, PCR primers, and probe binding site are shown as yellow, green, and red arrows, respectively. **(E)** Agarose gel electrophoresis of PCR amplicons of Pitt2 DNA in a random representative subset of Pitt2 TAKOs demonstrating abnormal amplicons in TAKO mice compared to WT control. Individual mouse numbers are presented above the gel.

The indels varied from animal to animal and most appeared to be deletions, as evidenced by the PCR products being ~50–400 bp smaller than the 929 bp WT amplicons for Pitt1, and ~50–600 bp smaller than the 963 bp WT amplicons for Pitt2 (Figures 3B,E, respectively). Out of the 35 Pitt1 mice and 42 Pitt2 mice, only a subset (n = 11M/14F Pitt1; 16M/12F Pitt2) harboring a large mutation(s) spanning the putative promoter and exon 1 of Pitt1 or Pitt2 were selected for behavioral phenotyping. It should be noted that the mice used for phenotyping presented variable deletions mainly ranging in 230–730 bp (Figures 3B,E, respectively). Despite all Pitt1 and Pitt2 mice showing variability in mutation site and size, all mice within a genotype were expected to manifest the same effect on gene expression and behavioral phenotypes [as previously shown (83)].

We have previously demonstrated that control C57BL/6J mice purchased from Jackson Laboratories are not significantly different from in-house generated Mock-treatment control mice (83). Therefore, Pitt1 and Pitt2 TAKO mice were compared to age and sex-matched C57BL/6J controls. Mice were weighed once per week during behavioral experimentation. Both TAKO cohorts for both sexes had significantly increased weight compared to controls. Males and females had an effect of genotype [$F(1.715, 7.717) = 87.22$; $p < 0.0001$] and [$F(1.626, 9.758) = 89.44$; $p < 0.0001$], respectively (Supplementary Figure S2). Post-hoc analysis revealed an effect of genotype for both Pitt1 and Pitt2 males ($q < 0.001$), and Pitt1 and Pitt2 females ($q < 0.0001$). These results are consistent with previously observed differences in our laboratory in purchased versus in-house produced offspring (data not shown).

RNA analysis

Hippocampal RNA from a subset of mutant mice used for phenotyping was analyzed by RT-PCR to validate that the DNA mutations surrounding the putative promoter and first exon of Pitt1 and Pitt2 disrupted expression of the targeted genes. Two RT-PCR primer sets were used for each genotype to characterize the RNA transcript in TAKO versus WT hippocampal RNA. F2/R2 RT-PCR primers were used to validate KO of RNA at the mutation site. F3/R3 RT-PCR primers were used to characterize the downstream exon containing the microarray probe-binding site to investigate expression of downstream lncRNA sequences (Figures 3A,D, respectively).

Pitt1—The top panel of Figure 3C demonstrates that the targeted exon 1 region is not transcribed in Pitt1 TAKOs. The middle panel highlights that the mutation(s) modulate the downstream lncRNA transcript, resulting in expression of a novel transcript that is not observed in the WT control. The bottom panel targeting *MyD88* was used as an internal control.

Pitt2—Despite extensive efforts to produce reliable RT-PCR amplicons for the Pitt2 RNA transcript(s), it was not achievable. RT-PCR amplicons for both the mutation site and probe-binding site of the Pitt2 transcript were inconsistent and variable even in WT control samples (data not shown).

Drinking in the dark

Pitt1 and Pitt2 DID data were analyzed separately based on genotype (i.e., Pitt1 males and females were analyzed together with half of the controls, and Pitt2 males and females were analyzed together with the other half of the controls). No statistically significant difference was observed between Pitt1 versus control or Pitt2 versus control for either the 2-h training day (data not shown) or the 4-h experimental day (Figures 4A,B, respectively). Consistently, there was no significant difference between the BECs of Pitt1 and control or Pitt2 and control following the 4-h experimental day for both males and females (Figures 4C,D, respectively). We observed a significant main effect of sex for Pitt1 DID [$F(1, 39) = 8.300$; $p < 0.01$] where females consumed more ethanol than males. Interestingly, a significant main effect of sex was also observed in Pitt2 DID [$F(1, 37) = 5.545$; $p < 0.05$], however females unexpectedly consumed less ethanol than the males.

Every-other-day two-bottle choice drinking

Pitt1, Pitt2, and control mice were tested for ethanol drinking using an EOD-2BC ethanol consumption assay over a period of 20 days. Pitt1, Pitt2 and control male analysis of ethanol intake revealed a main effect of day [$F(5.103, 199.0) = 159.5$; $p < 0.0001$], but no effect of genotype or day x genotype (Figure 5A). Analysis of ethanol preference in males revealed a main effect of day [$F(4.715, 183.9) = 15.83$; $p < 0.0001$] and genotype [$F(2, 39) = 3.755$; $p < 0.05$], but no day x genotype significant differences (Figure 5C). Post-hoc analysis revealed that on day 14 Pitt1 males had significantly higher ethanol preference than control males ($q < 0.05$). Pitt1 male ethanol preference at 15% v/v ranged from 0% to 9% increase, while Pitt2 male ethanol preference ranged from an increase of 6% to a decrease of 17% (Supplementary Figure S3C). For total fluid intake, there was a main effect of day [$F(3.508, 136.8) = 4.612$; $p < 0.01$] but no

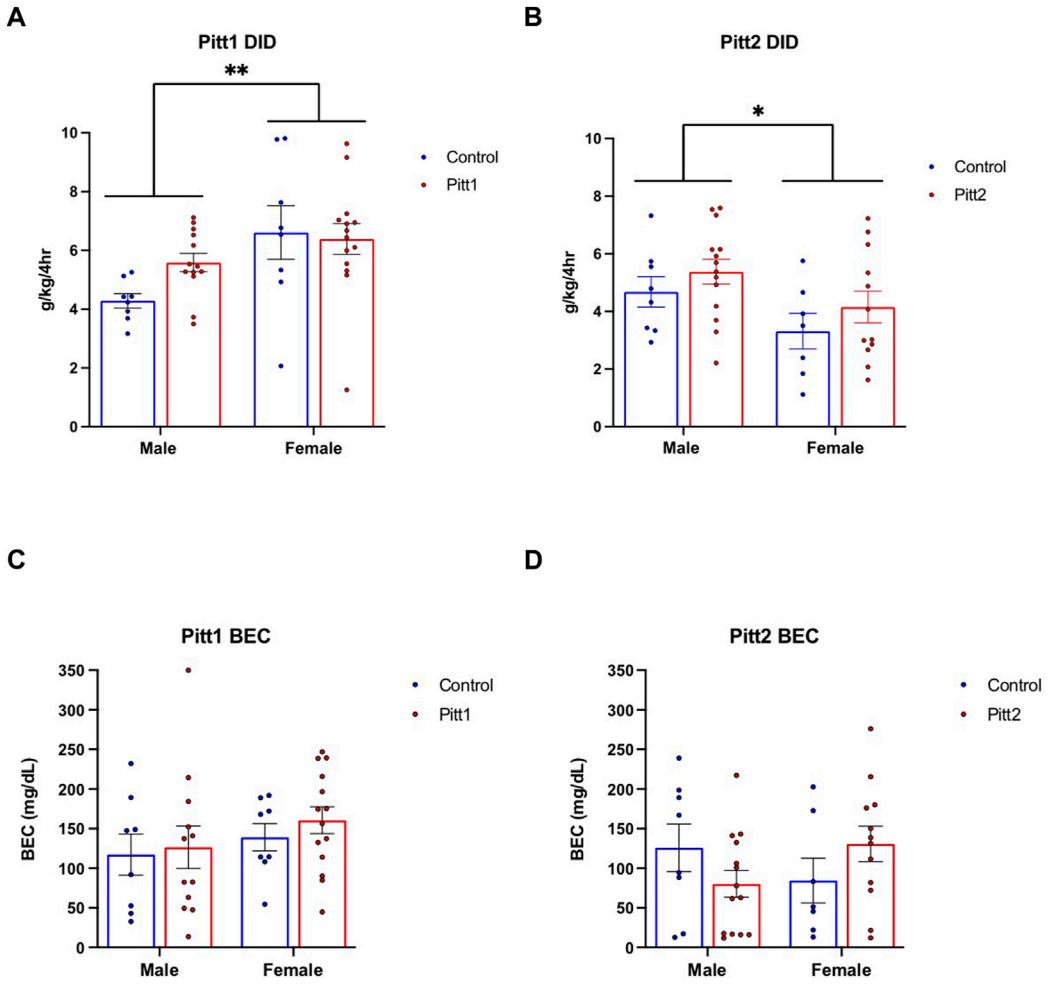

FIGURE 4
Effect of Pitt1 and Pitt2 mutation on ethanol consumption in the Drinking in the Dark assay. **(A)** Total ethanol consumption of Pitt1 and control mice over a 4-h experimental period (g/kg/4h). N = 13–14 Pitt1 TAKOs; *n* = 8 controls. **(B)** Total ethanol consumption of Pitt2 and control mice over a 4-h experimental period (g/kg/4h). N = 12–14 Pitt2 TAKOs; *n* = 7–8 controls. **(C)** Blood ethanol concentrations (mg/dL; 5 µL) from plasma collected from all Pitt1 mice immediately following removal of ethanol-filled bottles. N = 12–14 Pitt1 TAKOs; *n* = 8 controls. **(D)** Blood ethanol concentrations (mg/dL; 5 µL) from plasma collected from all Pitt2 mice immediately following removal of ethanol-filled bottles. N = 12–14 Pitt2 TAKOs; *n* = 7–8 controls.

effect of genotype or day × genotype interaction for the males (Figure 5E). Due to a record-keeping error, data from day 16, at 15% v/v ethanol, was lost.

Analysis of Pitt1, Pitt2, and control female cohorts on total ethanol intake revealed a day × genotype interaction [F (16, 304) = 2.679; $p < 0.001$] and main effect of day [F (4.409, 167.5) = 286.3; $p < 0.0001$], but no effect of genotype (Figure 5B). Post-hoc analysis revealed that on days 14, 16, and 20 Pitt1 females consumed significantly less ethanol than control ($q < 0.01$), and Pitt2 females consumed significantly more ethanol than control on day 4 ($q < 0.05$), and significantly less on day 14 ($q < 0.05$). Pitt1 females consistently consumed 10%–20% less ethanol at 15% v/v. Pitt2 females only consumed up to 10% less ethanol at 15% v/v (Supplementary Figure S3B). Analysis of ethanol preference in females revealed a main effect of day [F (3.743, 142.2) = 13.60; $p < 0.0001$], but no effect of genotype or day x genotype (Figure 5D). For total fluid intake, there was a day x genotype [F (16, 304) = 1.938; $p < 0.01$] and main effect of day [F (2.272, 86.32) = 31.91; $p < 0.0001$], but no effect of genotype (Figure 5F). Post-hoc analysis revealed that on days 14, 18, and 20 Pitt1 females consumed significantly less total fluid than control females ($q < 0.0001$, $q < 0.05$, and $q < 0.01$, respectively) and that on days 14 and 18 Pitt2 females consumed less total fluid than control females ($q < 0.0001$ and $q < 0.05$, respectively). The change in ethanol intake coincided with a reduction in total fluid for Pitt1 females at 15% v/v ethanol ranging from a reduction of 8.5%–20.5%, and Pitt2 females ranging from a reduction of 5%–

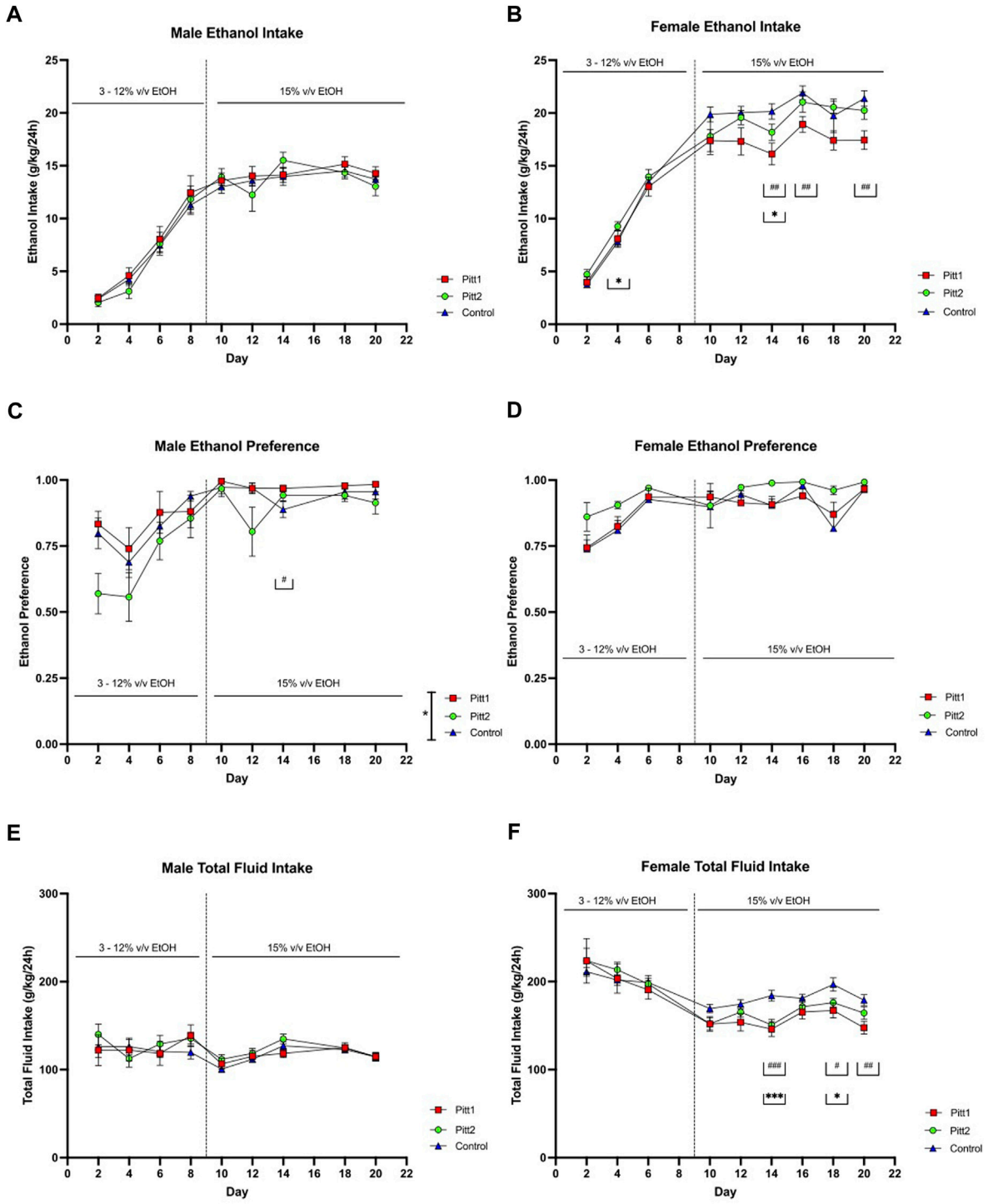

FIGURE 5
EOD-2BC drinking in Pitt1, Pitt2, and control mice. Left, males; right, females. **(A,D)** ethanol intake (g/kg/24 h), **(B,E)** ethanol preference, and **(C,F)** total fluid intake (g/kg/24 h) in Pitt1 mutant, Pitt2 mutant, and control mice across time and concentration. $^{\#}$ or $^{*}q < 0.05$, $^{\#\#}$ or $^{**}q < 0.01$, and $^{\#\#\#}$ or $^{***}q < 0.001$ between Pitt1 and control, and Pitt2 and control, respectively. N = 11–16/sex/genotype.

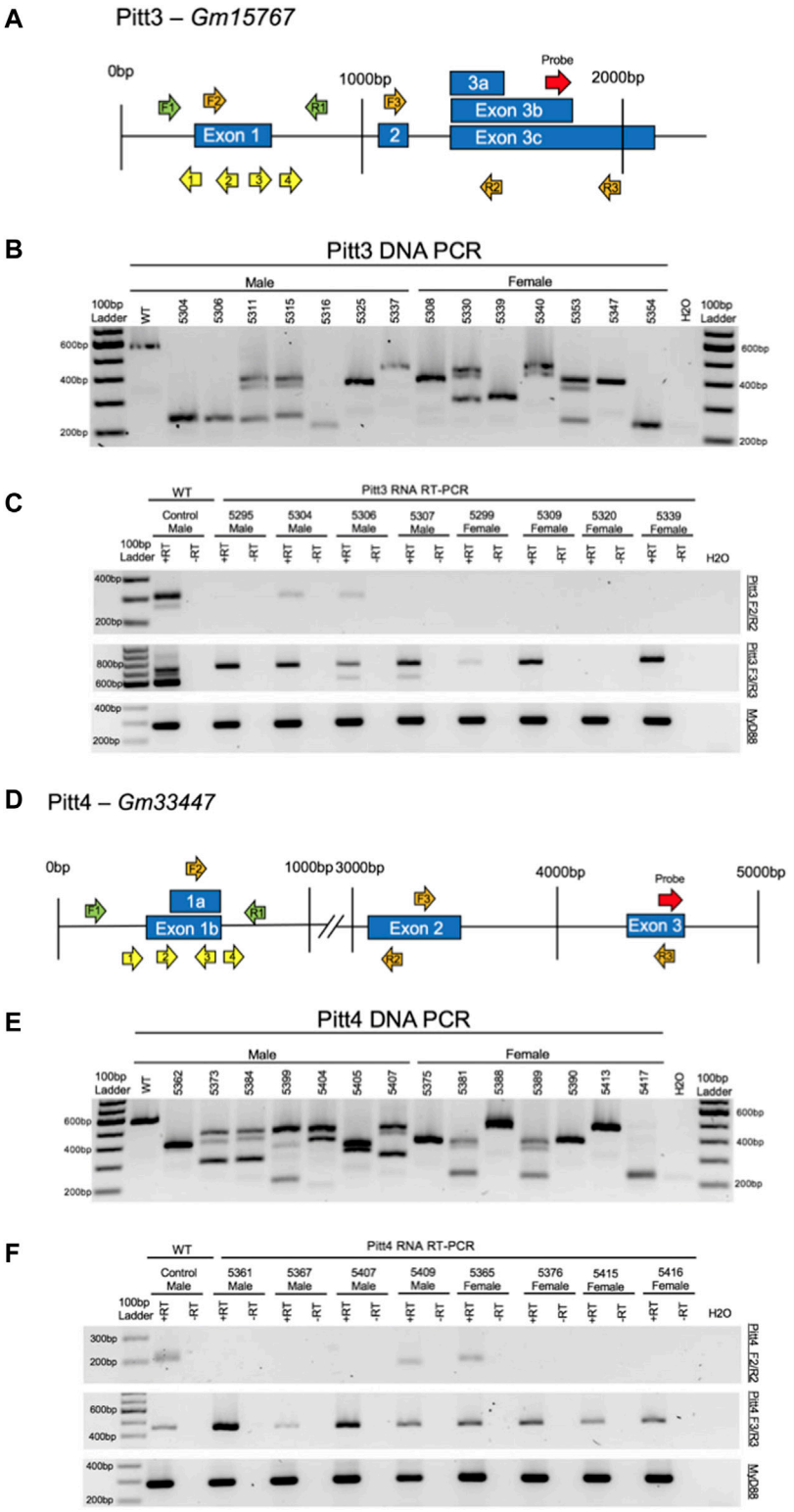

FIGURE 6
CRISPy TAKO schematics and genotypes for Pitt3 and Pitt4. **(A)** Pitt3 gene symbol and structure. The gRNAs, PCR primers, RT-PCR primers, and probe binding site are shown as yellow, green, orange, and red arrows, respectively. **(B)** Agarose gel electrophoresis of PCR amplicons of DNA from a random representative subset of Pitt3 TAKOs. Individual mouse numbers are presented above the gel. **(C)** Random representative subset of RT-PCR results from Pitt3 hippocampal brain tissue showing abnormal RNA transcripts in TAKO mice compared to WT control. (Top) RT-PCR of

(*Continued*)

FIGURE 6 (Continued)
Pitt3 exon 1 using the F2/R2 primers demonstrating the absence of the WT amplicon in most mice, although two animals (5304 and 5306) express a WT sized transcript at an apparently reduced level. (Middle) RT-PCR amplicons using F3/R3 primers spanning downstream Pitt3 exons demonstrating abnormal RNA products in Pitt3 mutant TAKOs compared to controls. (Bottom) RT-PCR of *MyD88* used as an internal control. **(D)** Pitt4 gene symbol and structure. The gRNAs, PCR primers, RT-PCR primers, and probe binding site are shown as yellow, green, orange, and red arrows, respectively. **(E)** Agarose gel electrophoresis of PCR amplicons of DNA from a random representative subset of Pitt4 TAKOs. Individual mouse numbers are presented above the gel. **(F)** Random representative subset of RT-PCR results from Pitt4 hippocampal brain tissue showing abnormal RNA transcripts. (Top) RT-PCR of Pitt4 exon 1 amplicons using the F2/R2 primers demonstrating that the mutations eliminate expression of the WT transcript in 7 of 8 Pitt4 TAKOs analyzed. (Middle) RT-PCR amplicons of downstream Pitt4 exons amplified with the F3/R3 primers demonstrating expression of normal sized transcripts in TAKOs compared to WT control. (Bottom) RT-PCR of *MyD88* amplicons used as an internal control.

18% (Supplementary Figure S3F). Due to a record-keeping error, data from day 8, at 12% v/v ethanol, was lost. Since the decrease in female ethanol intake could be linked to a reduction in overall fluid intake, and the male data was not highly compelling, the experiment was terminated following the completion of 15% v/v EOD-2BC.

Preference for non-ethanol tastants

Changes in taste perception can alter ethanol consumption in mice (94–96). Because female Pitt1 and Pitt2 displayed altered EOD-2BC ethanol consumption compared to controls, females were subjected to both sweet (i.e., saccharin) and bitter (i.e., quinine) tastants. A 24-h 2BC assay was used to determine whether an alteration in taste perception could account for the observed changes in ethanol consumption in the mutant lines tested. No significant difference was observed between genotypes for either saccharin (Supplementary Figure S4A) or quinine preference (Supplementary Figure S4B).

CRISPy TAKOs—Pitt3 and Pitt4

CRISPR/Cas9-mediated mutagenesis

A second cohort of mice targeting Pitt3 and Pitt4 (Figures 6A,D, respectively) were subsequently characterized and tested for behavior. Initial validation of gRNAs designed to target Pitt3 and Pitt4 occurred *in vitro* using electroporated embryos (Supplementary Figures S1C,D, respectively) and demonstrated that both genes were mutated at a high frequency.

A total of 70 offspring for Pitt3 and 62 offspring for Pitt4 were generated on the C57BL/6J background using the CRISPy TAKO approach. All mice born from electroporated embryos were genotyped for gross indels using PCR and agarose gel electrophoresis. The Pitt3 581 bp WT PCR amplicon was readily apparent in WT control and 9 out of 70 Pitt3 animals (data not shown). The remaining 61 mutants displayed gross indels encompassing the targeted region of interest. The indels from a random representative subset of Pitt3 TAKOs used for behavioral phenotyping varied from animal to animal and most appeared to be deletions, as evidenced by the PCR products being ~50–350 bp smaller than the 581 bp WT amplicons (Figure 6B). The Pitt4 583 bp WT PCR amplicon was readily apparent in WT control and 4 out of 62 Pitt4 animals (data not shown). The remaining 58 mutants displayed gross indels encompassing the targeted region of interest. The indels from a random representative subset of Pitt4 TAKOs used for behavioral phenotyping demonstrated deletions ranging from ~50–350 bp smaller than the 583 bp WT amplicon (Figure 6E). Of the Pitt3 and Pitt4 mutant mice produced, a subset (n = 15/sex/genotype) harboring large deletions spanning the putative promoter and first exon of Pitt3 or Pitt4 were selected for behavioral phenotyping.

As noted for Pitt1 and Pitt2 cohorts, Pitt3 and Pitt4 males and females consistently weighed significantly more than controls (Supplementary Figure S5). Analysis of male Pitt3, Pitt4, and control weight over time revealed a main effect of day [F (2.477, 104) = 412.1; $p < 0.0001$], a main effect of genotype [F (2, 42) = 19.48; $p < 0.0001$], and day x genotype [F (12, 252) = 3.599; $p < 0.0001$]. Post-hoc analysis for both males and females, for all weeks, had a significant increase in weight compared to control ($q < 0.0001$).

RNA analysis

Hippocampal RNA was isolated from a subset of mutant mice used for behavioral phenotyping and analyzed by RT-PCR to validate that the DNA mutations surrounding the putative promoter and first exon of Pitt3 and Pitt4 disrupted expression. Two RT-PCR primer sets were used for each genotype to characterize the RNA transcript in TAKO versus control hippocampal RNA. F2/R2 RT-PCR primers were used to examine RNA at the site of mutation, and F3/R3 RT-PCR primers were used to characterize expression of the downstream exon containing the microarray probe-binding site (Figures 6A,D, respectively).

Pitt3—The top panel of Figure 6C demonstrates that the exon 1 region in the control sample expressed both the expected 303 bp amplicon as well as an unexpected, slightly larger amplicon. These transcripts were not transcribed in 75% of the Pitt3 TAKOs tested. Two of eight mice (25%; 5304 and 5306) still expressed the slightly larger RNA transcript from exon 1, but at an apparently reduced level. The middle panel highlights variability in expression between animals. Some TAKO mice expressed two downstream transcripts (5306 and 5307), some only one transcript (5295, 5304, 5229, 5309, and 5339), and one had no downstream transcripts (5320). This is likely due to variability in

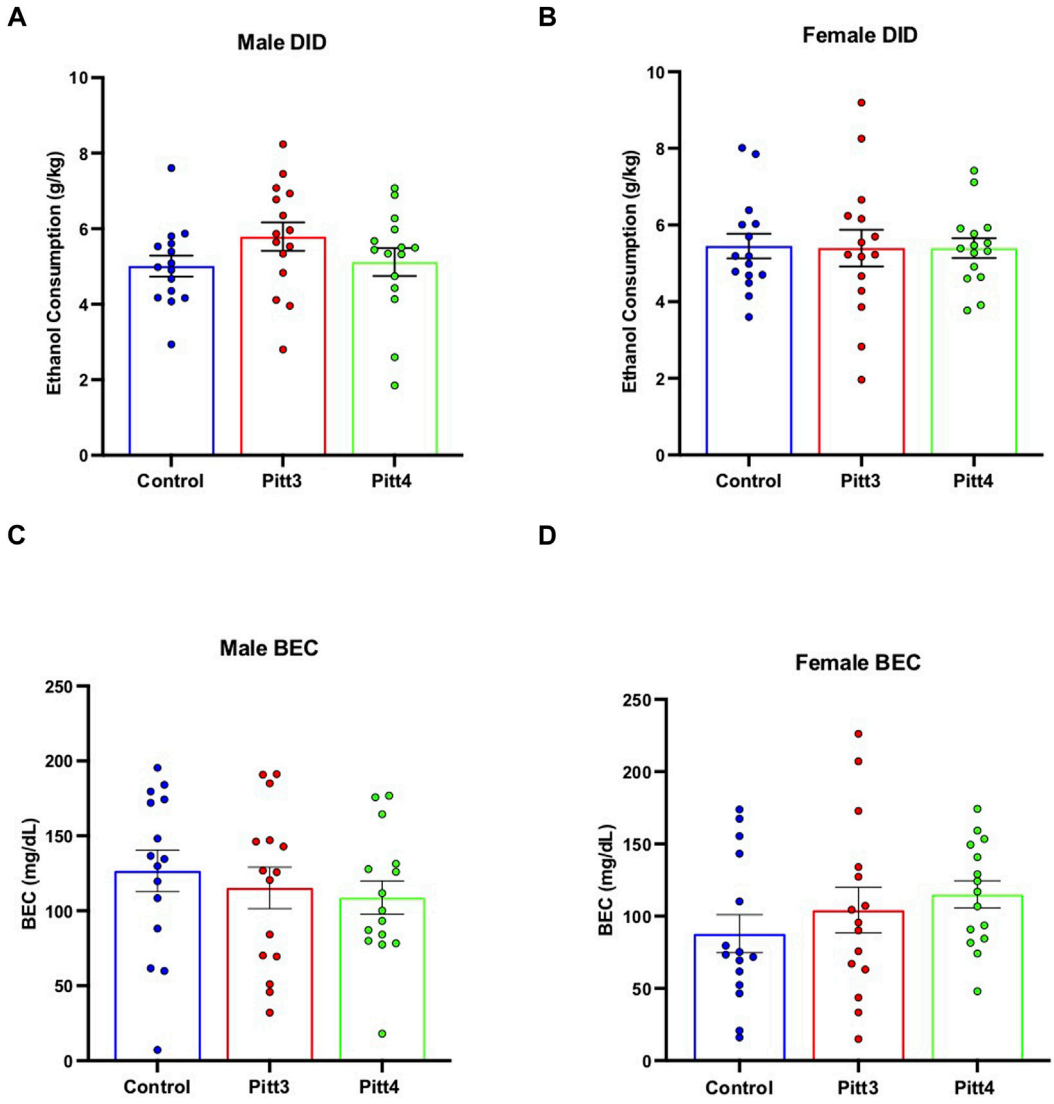

FIGURE 7
Effect of Pitt3 and Pitt4 mutation on ethanol consumption in the Drinking in the Dark assay. Total ethanol consumption of Pitt3, Pitt4, and control male **(A)** and female **(B)** mice over a 4-h experimental period (g/kg/4h). Blood ethanol concentrations (mg/dL; 5 μL) from plasma collected from all male **(C)** and female **(D)** mice immediately following the removal of ethanol-filled bottles.

deletions of poorly characterized regulatory sequences surrounding the mutation site. The bottom panel targeting *MyD88* was used as an internal control.

Pitt4—The top panel of Figure 6F demonstrates that the targeted exon 1 region was not transcribed in 75% of Pitt4 TAKOs tested. One sample, 5365, still expressed the control-sized transcript, and one sample, 5409, expressed a slightly smaller RNA transcript. This ~10–20 nt smaller RNA transcript likely reflects an internal mutation that was within the boundaries of the RT-PCR primers. The middle panel revealed that all Pitt4 TAKO mice still produced the downstream Pitt4 transcript, albeit at variable levels of expression. The bottom panel targeting *MyD88* was used as an internal control.

Drinking in the dark

Mice were tested for binge-like drinking behavior using the DID ethanol consumption paradigm. Cohorts were separated and analyzed based on sex. No significant difference was observed between Pitt3, Pitt4, and control males (Figure 7A) or females (Figure 7B) for either the 2-h training day (data not shown) or the 4-h experimental day. Consistently, there were also

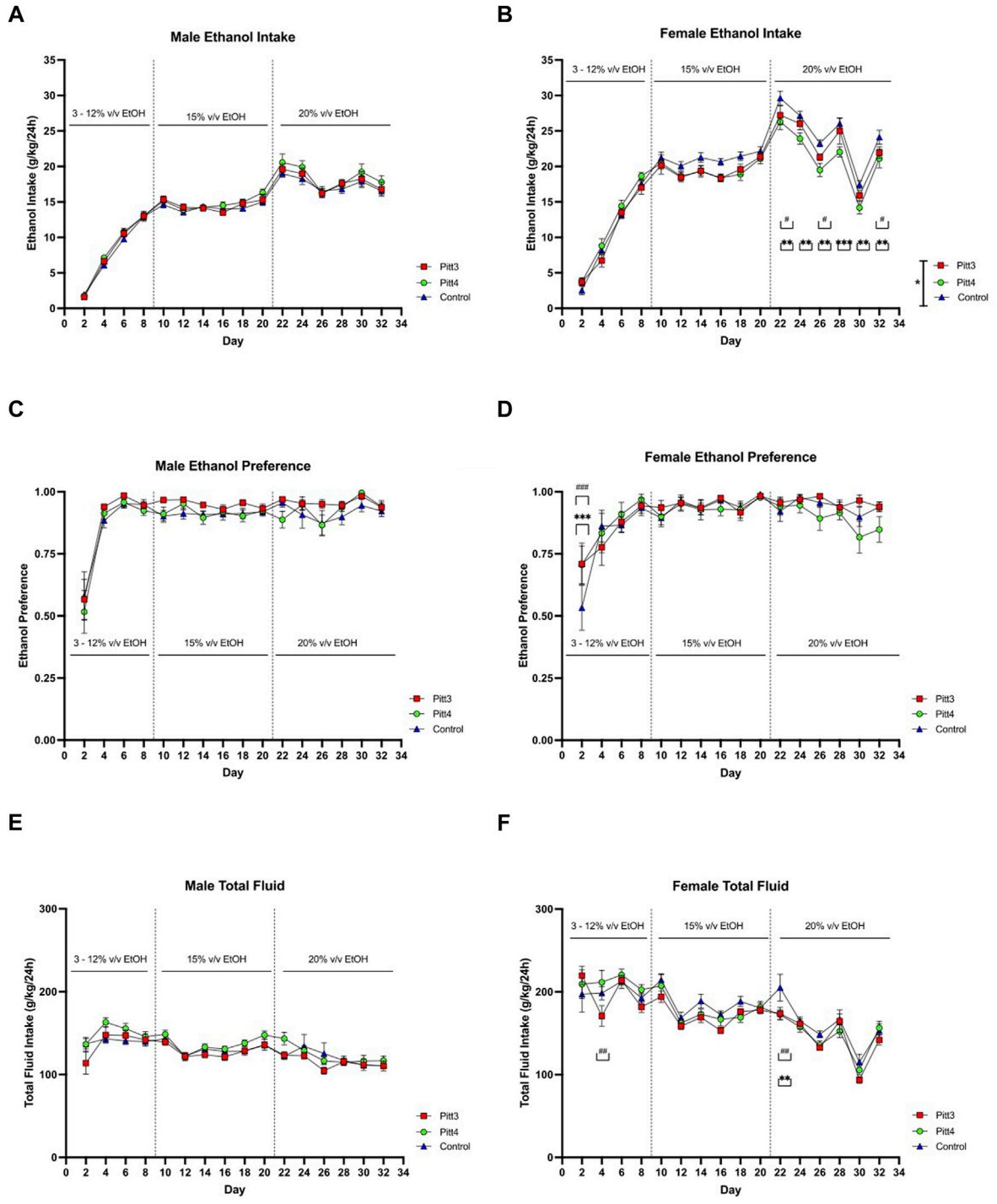

FIGURE 8
EOD-2BC drinking in Pitt3, Pitt4, and control mice. Left, males; right, females. **(A,D)** ethanol intake (g/kg/24 h), **(B,E)** ethanol preference, and **(C,F)** total fluid intake (g/kg/24 h) in Pitt3 mutant, Pitt4 mutant and control mice across time and concentration. Values represent Mean ± SEM. $^{\#}$ or $^{*}q < 0.05$, $^{\#\#}$ or $^{**}q < 0.01$, and $^{\#\#\#}$ or $^{***}q < 0.001$ between Pitt3 and control, and Pitt4 and control, respectively).

no significant differences between Pitt3, Pitt4, and control male (Figure 7C) or female (Figure 7D) BECs following the 4-h experimental day.

Every-other-day two-bottle choice drinking

Pitt3, Pitt4, and control mice were tested for ethanol drinking using an EOD-2BC ethanol consumption assay.

Because this set of TAKO animals did not present a significant difference in total fluid intake following 15% v/v ethanol, the experimental paradigm was expanded to include 20% v/v ethanol. Analysis of male Pitt3, Pitt4, and control ethanol intake revealed a main effect of day [F (15, 625) = 335.2; $p < 0.0001$], but no effect of genotype or day x genotype (Figure 8A). Analysis of male ethanol preference revealed a main effect of day [F (15, 624) = 39.54; $p < 0.0001$], but no effect of genotype or day x genotype (Figure 8C). Consistently, analysis of male total fluid revealed a significant main effect of day [F (15, 624) = 19.39; $p < 0.0001$], but no effect of genotype or day x genotype (Figure 8E).

Analysis of ethanol intake in Pitt3, Pitt4, and control females revealed significant main effects of genotype [F (2, 42) = 3.302; $p < 0.05$], day [F (15, 630) = 248.6; $p < 0.0001$], and a day x genotype [F (30, 630) = 2.201; $p < 0.001$] (Figure 8B). Post-hoc analysis revealed that on day 22, 26, and 32 Pitt3 females consumed significantly less ethanol than controls ($q < 0.05$). On days 22–32 Pitt4 females consumed significantly less than control females ($q < 0.01$, $q < 0.01$, $q < 0.01$, $q < 0.001$, $q < 0.01$, and $q < 0.01$, respectively). Pitt3 females at both 15% and 20% v/v ethanol consumed up to 10% less ethanol compared to control. Pitt4 females consumed up to 12% less at 15% v/v and reached a reduction of up to 18.5% at 20% v/v ethanol. Interestingly, both Pitt3 and Pitt4 females consumed ~50% more ethanol at 3% v/v (Supplementary Figure S6B). Analysis of female ethanol preference revealed a significant main effect of day [F (15, 630) = 19.28; $p < 0.0001$] and day x genotype [F (30, 630) = 1.596; $p < 0.05$], but no effect of genotype (Figure 8D). Post-hoc analysis revealed a significant increase in ethanol preference compared to control on day 2 for both Pitt3 and Pitt4 ($q < 0.001$). Both Pitt3 and Pitt4 females had a preference ranging from 0–10% difference from control at 15% and 20% v/v ethanol, with ~35% increase at 3% v/v (Supplementary Figure S6D). Considering total fluid intake in females, there was a significant main effect of day [F (15, 630) = 43.97; $p < 0.0001$] and day x genotype [F (30, 630) = 1.542; $p < 0.05$], but no effect of genotype (Figure 8F). Post-hoc analysis revealed that on day 4 Pitt3 females consumed significantly less total fluid than control females ($q < 0.01$) and on day 22 both Pitt3 and Pitt4 females consumed significantly less total fluid than control females ($q < 0.01$). Both Pitt3 and Pitt4 females had reductions in total fluid intake by up to 19% in Pitt3 and 16% in Pitt4 females at 20% v/v ethanol (Supplementary Figure S6F).

Preference for non-ethanol tastants

Since Pitt3 and Pitt4 females had altered EOD-2BC ethanol consumption when compared to controls, females were subject to both sweet (i.e., saccharin) and bitter (i.e., quinine) tastant preference analysis. No differences were observed between genotypes for saccharin preference (Supplementary Figure S7A). For quinine preference, there was a significant main effect of day [F (3, 126) = 3.444; $p < 0.05$], but no main effect of genotype or day x genotype (Supplementary Figure S7B).

Discussion

Identification of phenotypically relevant ethanol-responsive regulatory genes that control brain transcriptional networks offer valuable insight into the chronic effects of ethanol exposure and AUD. Microarray analysis of hippocampal RNA from male mice exposed to CIEV was used to discern ceRNA expression networks that included four prominent RNA subtypes: lncRNA, mRNA, circRNA, and miRNA (Figure 1). The top four ethanol-responsive hub lncRNAs were identified and selected for functional interrogation. These novel lncRNAs, named Pitt1-Pitt4, interact and compete with a myriad of transcripts to modulate specific ceRNA networks. We hypothesized that directly altering the expression of these lncRNAs would change downstream biological processes and change ethanol-related drinking behavior. Cohorts of Pitt1-Pitt4 gene KO mice were created using the CRISPy TAKO method (83) and subsequently screened for changes in ethanol drinking using the DID and EOD-2BC drinking assays. We observed female-specific reductions in ethanol consumption ranging from 10%–20% in the EOD-2BC paradigm compared to control in three of the tested Pitt mutant lines; Pitt1, Pitt3, and Pitt4. Some of the observed changes were associated with reductions in total fluid consumption but they were not influenced by a change in taste perception. No changes in binge-like drinking in the DID paradigm were observed in either the male or female mutants for any Pitt TAKO genotype (Table 2).

The CRISPy TAKO approach was utilized to rapidly generate a cohort of mutant animals in a single generation (83). This offers a quick approach to functionally screen novel lncRNAs of interest so the genes can be quickly tested for the ability to alter behavior, saving both time and resources. This is important when screening large numbers of genes with unknown function for ethanol-related behaviors and avoids the bottleneck of standard reverse-genetic approaches. Electroporating embryos with 4–6 gRNAs targeting a >1 kb region led to unique mutations from the various combinations of gRNAs in each animal produced (83). Those harboring desirable large mutations in their DNA were selected for behavioral experimentation, producing a cohort of uniquely mutated mice in one generation, all hypothesized to interfere with gene function (83).

RNA analysis

Hippocampal RNA was analyzed by RT-PCR to confirm that mutation of the putative promoter and first exon of each lncRNA

TABLE 2 Summary table of behavioral results.

Behavior	M	M	M	M	F	F	F	F
	Pitt1	Pitt2	Pitt3	Pitt4	Pitt1	Pitt2	Pitt3	Pitt4
DID and BEC	No	No	No	No	No	No	No	No
Ethanol Intake	No	No	No	No	Yes (−20%–6%)	Yes (−10%–26%)	Yes (−18%–49%)	Yes (−19%–48%)
Ethanol Preference	Yes (−6%–9%)	Yes (−28%–6%)	No	No	No	No	Yes (−10%–33%)	Yes (−10%–33%)
Total Fluid	No	No	No	No	Yes (−21%–6%)	Yes (−18%–6%)	Yes (−19%–11%)	Yes (−16%–6%)

Words in red represent unchanged behaviors, words in green represent changed behaviors.

gene disrupted gene expression from each targeted locus. Using primers that bind to the putative first exon (Pitt1 and Pitt3) or exon 1 and exon 2 (Pitt4) we established that the CRISPy TAKO mutagenesis approach successfully disrupted gene expression of the targeted loci. Nearly all animals failed to amplify with these primer sets. It should be noted that Pitt4 5365 was the only mouse to express transcripts that appeared like WT, but likely at a reduced level of expression (Figure 6F; top panel). The other Pitt4 mouse, 5409, expressed a slightly smaller transcript than WT, suggesting that an internal mutation within the boundaries of the RT-PCR primers may have been retained, or an alternate splice variant was expressed.

Each hippocampal RNA sample was also analyzed with RT-PCR using primers targeting the probe-binding exon used for the initial microarray analyses that identified these lncRNAs, downstream from the mutation site. This was conducted to determine if the full transcript had been knocked out, or if downstream sequences were still transcribed following mutagenesis of the putative promoter and first exonic region. Regions downstream of the Pitt1, Pitt3, and Pitt4 mutations were expressed in the majority of animals. Surprisingly, the Pitt1 downstream amplicon was not detectable in control samples but was consistently expressed in all Pitt1 TAKO mice (Figure 3C; middle panel). These results are likely due to mutation of the putative promoter activating a normally silent promoter, or by altering downstream splicing events. Pitt3 RT-PCR results revealed variable downstream RNA products; of the eight TAKOs used for RT-PCR, two TAKOs express two downstream transcripts (5306 and 5307), five TAKOs express only a single downstream transcript (5295, 5304, 5229, 5309, and 5339), and one TAKO does not express either downstream transcript (5320). Interestingly, none of the Pitt3 TAKOs had similar RT-PCR results compared to WT (Figure 6C; middle panel). As detailed previously, CRISPy TAKO mutants harbor variable mutations (83) and at some loci such as Pitt3, this can lead to expression of novel transcripts from the targeted locus. This could be the result of the mutations impacting the 5' splice site(s), or mutating splicer enhancer/repressor binding sites and therefore shifting splicing dynamics (97–101). Analysis of downstream sequences in Pitt4 mutants revealed that the downstream cDNA amplicon was readily detected in control and all TAKOs analyzed (Figure 6F; middle panel). The most parsimonious explanation for these results is that an alternate promoter is present that is driving this downstream transcript (102–104).

Unexpectedly, following extensive experimentation, the Pitt2 transcript at the mutation site and probe-binding site were unable to be reliably amplified from either control or Pitt2 TAKO cDNA. This could have occurred due to Pitt2 RNA being expressed at very low levels, or the Pitt2 gene structure could have been inaccurately annotated. These results highlight an important limitation of working with previously unstudied genes including the majority of lncRNAs. Current gene structure annotations may not accurately predict function and unexpected changes in gene expression may be observed when putative regulatory sequences are deleted form the genome.

The RT-PCR data provided a representative look into the potential transcriptome differences between the TAKO mice within a genotype, such as the three different variants of the downstream Pitt3 amplicon(s). Whereas all Pitt1 TAKOs tested produced identical amplicons for both the mutation site and downstream probe-binding region, it is possible that the Pitt3 TAKO mice could be further divided into sub-genotypes based on their retained RNA transcripts and their expression levels. The observed Pitt3 phenotype could be dampened by the variability of transcripts expressed in each TAKO. Variation in behaviors within a mutant line could be the result of small versus large mutations, novel transcripts being produced, altered expression levels of unmutated transcripts, altered or ablated lncRNA functionality, ethanol-responsive versus ethanol-unresponsive variations, or a combination of such molecular events. However, the spread of data points from all genotypes were similar to control and each other; they were well clustered together, suggesting that independent sub-genotypes did not differ in behavior significantly from each other. To discern these intricacies however, Sanger Sequencing, subcloning, and

rigorous molecular testing and statistical analysis of the individual animals would be required.

Behavioral results

Pitt1-Pitt4 female TAKO mice all demonstrated at least a 10% difference from control in ethanol drinking behavior when tested with the EOD-2BC paradigm (Table 2). This includes ~20% decrease in ethanol consumption in Pitt1 females at 15% v/v ethanol and in Pitt4 females at 20% v/v ethanol. However, the associated reduction in total fluid intake at their respective concentrations could suggest an alternate reason for the ethanol consumption reduction beyond genotype and sex alone. It should be noted, however, that there was no difference found in total fluid intake under the non-ethanol 2BC tastant paradigms for females of all genotypes (data not shown). Large changes in ethanol consumption and/or preference were also observed between mutant lines and controls during the initial ethanol ramping stage (Figures 5, 8). Pitt2, Pitt3, and Pitt4 female mutants all showed increased ethanol consumption ranging from ~25%–50% on ramping days with 3% and 6% v/v ethanol (Supplementary Figures S3, S6, respectively). While these results at lower ethanol concentrations are intriguing, our primary focus was the impact on the higher-level concentrations of 15% and 20% v/v ethanol. All four of the lncRNAs targeted are capable of modulating ethanol drinking behavior, with Pitt1, Pitt3, and Pitt4 influencing ethanol consumption in a sex-specific manner.

While differences in ethanol intake were readily apparent throughout the EOD-2BC paradigm in all mutant lines, no differences were observed in DID ethanol consumption or the BECs of the animals immediately following DID (Table 2). This could be due to the obvious differences between the short-term binge-like paradigm and the long-term escalation-of-drinking paradigm and suggestive of specific behavioral patterns being altered by mutation of these lncRNAs that only present in one manner of ethanol consumption. The impacted ceRNA networks may function alternatively from control dependent on the paradigm employed, leading to the deviation in drinking behavior over time.

Sexual dimorphism

Our data supports the identification and partial characterization of four novel ethanol-responsive lncRNAs that can alter ethanol drinking behavior, specifically in females. Sexually dimorphic behavioral responses to ethanol have been previously reported in the literature for alcohol (30, 105–109). LncRNA genes have shown sex-specific expression in reward pathways, cell signaling, structural plasticity, complex decision making, and behaviors (110–112). Sexually dimorphic biology is present in many stages of drug addiction, including acute reinforcement, the transition to compulsive drug use, withdrawal-associated states of negative affect, craving, and relapse (113). Further, there are known differences in neural systems related to addiction and reward behavior such as epigenetic organization, expression, and contingency that are sex-dependent (113). This suggests that lncRNAs may be important in sexually dimorphic biology and behaviors associated with substance misuse.

The female-specific behavioral changes observed in ethanol drinking were somewhat unexpected as the ethanol-regulated lncRNAs studied were identified from microarray data that originated from a male-only cohort. Male samples were used because of tissue availability [hippocampal tissue originated from the sires described in (84)]. The sex differences observed are likely either qualitative and/or based on underlying differences in mechanism(s) of action (113). For example, there may be differences between the sexes in baseline or ethanol-induced expression levels of Pitt1-Pitt4 lncRNAs. To investigate possible expression differences, analogous female tissue would need to be collected, analyzed, and compared to the male microarray data. This would shed light on not only potential differences in Pitt1-Pitt4 expression between sexes and insight into the observed behavior presented, but also would allow for the identification of sex-independent and additional sex-specific genes.

LncRNAs and conclusion

A handful of studies has already begun to research lncRNAs in relation to the neurobiology of AUD (4, 41, 42, 114–116). The biological functions of these novel ethanol-linked lncRNAs have been associated with altered gene networks and RNA co-expression (114), alternative splicing (4), and neural function (116). The lncRNA *brain-derived neurotrophic factor antisense* has previously been described as a regulator of epigenetic events in the amygdala of humans with AUD (41). Additionally, the lncRNA named *long non-coding RNA for alcohol preference* was identified as a hub gene whose mutation increased alcohol consumption and preference in Wistar rats compared to controls (42). While the field is growing, there are still over 100,000 lncRNA transcripts (45–49) that remain uncharacterized for their relevance to AUD and other human disorders but hold the potential to regulate multiple cellular mechanisms and behaviors.

Mutating these novel uncharacterized Pitt1-Pitt4 lncRNA genes may impact a number of molecular functions, such as subcellular localization, sequestration, scaffolding, and epigenetic regulation of gene expression (44, 50–53). Our study was specifically designed to test genes with no known molecular or behavioral functions related to models for AUD. We conducted

these studies with the hypothesis that several, if not all, of the top-ranked genes would have the ability to alter ethanol drinking and provide an ideal candidate gene for more in-depth molecular characterization. By removing a large exonic region of these genes, many different mechanisms of action could have been altered that manifest as a change in ethanol drinking behavior. Future studies should delve into further ethanol-related behaviors and the mechanism(s) of action of these ethanol-responsive lncRNAs.

Here, we demonstrated that mutating and screening top-ranked ethanol-responsive hub lncRNA genes from chronic ethanol exposed mouse hippocampus led to altered ethanol drinking behavior in all of the generated TAKO cohorts. Among the mutant lines tested, Pitt4 appears to be the ideal target to generate a true breeding line for further studies. This would permit studying additional ethanol-related behaviors as well as an in-depth molecular analysis to discern the potential function(s) and mechanism of action(s) for this novel lncRNA. The data presented here add to the growing body of literature supporting the hypothesis that expression of specific lncRNAs is important for mediating addiction-related behaviors relevant to human health (63, 69–71).

Data availability statement

The datasets presented in this study can be found in online repositories. The names of the repository/repositories and accession number(s) can be found in the article/ Supplementary Material.

Ethics statement

The animal study was reviewed and approved by the Institutional Animal Care and Use Committee of the University of Pittsburgh.

Author contributions

Project conception and gRNA design devised by GH and SP. Bioinformatics and ceRNA network generation completed by SF. *In vitro* analysis, *in vivo* project design, organization, and analysis conducted by SP. SP and VC managed the behavioral experimentation. All authors contributed to writing and editing of the manuscript.

Funding

This work was supported by the National Institutes of Health grants T32GM08424, F31AA030176, F31AA029942, AA10422, AA020889, and AA020926.

Acknowledgments

The authors would like to acknowledge Carolyn Ferguson for expert technical support and members of the INIA-Neuroimmune consortium for helpful discussions and constant encouragement.

Conflict of interest

The authors declare that the research was conducted in the absence of any commercial or financial relationships that could be construed as a potential conflict of interest.

Supplementary material

The Supplementary Material for this article can be found online at: https://www.frontierspartnerships.org/articles/10.3389/adar.2022.10831/full#supplementary-material

References

1. Jones C, Paulozzi L, Mack K, Centers for Disease Control and Prevention (CDC). Alcohol involvement in opioid pain reliever and benzodiazepine drug abuse-related emergency department visits and drug-related deaths-United States, 2010. *MMWR Morb Mortal Wkly Rep* (2014) 63:881–5.

2. Sacks JJ, Gonzales KR, Bouchery EE, Tomedi LE, Brewer RD. 2010 national and state costs of excessive alcohol consumption. *Am J Prev Med* (2015) 49:e73–e79. doi:10.1016/j.amepre.2015.05.031

3. Sullivan EV, Harris RA, Pfefferbaum A. Alcohol's effects on brain and behavior. *Alcohol Res Health* (2010) 33 (1–2):127–143.

4. Van Booven D, Li M, Sunil Rao J, Blokhin IO, Dayne Mayfield R, Barbier E, et al. Alcohol use disorder causes global changes in splicing in the human brain. *Transl Psychiatry* (2021) 11:2–9. doi:10.1038/s41398-020-01163-z

5. Pignataro L, Varodayan FP, Tannenholz LE, Harrison NL. The regulation of neuronal gene expression by alcohol. *Pharmacol Ther* (2009) 124:324–35. doi:10.1016/j.pharmthera.2009.09.002

6. Grantham EK, Farris SP. Bioinformatic and biological avenues for understanding alcohol use disorder. *Alcohol* (2019) 74:65–71. doi:10.1016/j.alcohol.2018.05.004

7. Mayfield RD. Emerging roles for ncRNAs in alcohol use disorders. *Alcohol* (2017) 60:31–9. doi:10.1016/j.alcohol.2017.01.004

8. Farris SP, Arasappan D, Hunicke-Smith S, Harris RA, Mayfield RD. Transcriptome organization for chronic alcohol abuse in human brain. *Mol Psychiatry* (2015) 20:1438–47. doi:10.1038/mp.2014.159

9. Mira RG, Lira M, Tapia-Rojas C, Rebolledo DL, Quintanilla RA, Cerpa W. Effect of alcohol on hippocampal-dependent plasticity and behavior: Role of glutamatergic synaptic transmission. *Front Behav Neurosci* (2020) 13:288. doi:10.3389/fnbeh.2019.00288

10. Sun W, Li X, Tang C, An L. Acute low alcohol disrupts hippocampus-striatum neural correlate of learning strategy by inhibition of PKA/CREB pathway in rats. *Front Pharmacol* (2018) 9:1439. doi:10.3389/fphar.2018.01439

11. White AM, Matthews DB, Best PJ. Ethanol, memory, and hippocampal function: A review of recent findings. *Hippocampus* (2000) 10:88–93. doi:10.1002/(SICI)1098-1063(2000)10:1<88:AID-HIPO10>3.0.CO;2-L

12. Montesinos J, Alfonso-Loeches S, Guerri C. Impact of the innate immune response in the actions of ethanol on the central nervous system. *Alcohol Clin Exp Res* (2016) 40:2260–70. doi:10.1111/acer.13208

13. Geil CR, Hayes DM, McClain JA, Liput DJ, Marshall SA, Chen KY, et al. Alcohol and adult hippocampal neurogenesis: Promiscuous drug, wanton effects. *Prog Neuropsychopharmacol Biol Psychiatry* (2014) 54:103–13. doi:10.1016/j.pnpbp.2014.05.003

14. Zahr NM, Mayer D, Rohlfing T, Hasak MP, Hsu O, Vinco S, et al. Brain injury and recovery following binge ethanol: Evidence from *in vivo* magnetic resonance spectroscopy. *Biol Psychiatry* (2010) 67:846–54. doi:10.1016/j.biopsych.2009.10.028

15. Grifasi IR, McIntosh SE, Thomas RD, Lysle DT, Thiele TE, Marshall SA. Characterization of the hippocampal neuroimmune response to binge-like ethanol consumption in the drinking in the dark model. *Neuroimmunomodulation* (2019) 26:19–32. doi:10.1159/000495210

16. Glover EJ, Starr EM, Chao Y, Jhou TC, Chandler LJ. Inhibition of the rostromedial tegmental nucleus reverses alcohol withdrawal-induced anxiety-like behavior. *Neuropsychopharmacology* (2019) 44:1896–905. doi:10.1038/s41386-019-0406-8

17. Macht V, Crews FT, Vetreno RP. Neuroimmune and epigenetic mechanisms underlying persistent loss of hippocampal neurogenesis following adolescent intermittent ethanol exposure. *Curr Opin Pharmacol* (2020) 50:9–16. doi:10.1016/j.coph.2019.10.007

18. Edenberg HJ, Strother WN, McClintick JN, Tian H, Stephens M., Jerome RE, et al. Gene expression in the hippocampus of inbred alcohol-preferring and -nonpreferring rats. *Genes Brain Behav* (2005) 4:20–30. doi:10.1111/j.1601-183X.2004.00091.x

19. Kutlu MG, Gould TJ. Effects of drugs of abuse on hippocampal plasticity and hippocampus-dependent learning and memory: Contributions to development and maintenance of addiction. *Learn Mem* (2016) 23:515–33. doi:10.1101/lm.042192.116

20. Taffe MA, Kotzebue RW, Crean RD, Crawford EF, Edwards S, Mandyam CD. Long-lasting reduction in hippocampal neurogenesis by alcohol consumption in adolescent nonhuman primates. *Proc Natl Acad Sci U S A* (2010) 107:11104–9. doi:10.1073/pnas.0912810107

21. Basu S, Suh H. Role of hippocampal neurogenesis in alcohol withdrawal seizures. *Brain Plast* (2020) 6:27–39. doi:10.3233/BPL-200114

22. Zhou Z, Yuan Q, Mash DC, Goldman D. Substance-specific and shared transcription and epigenetic changes in the human hippocampus chronically exposed to cocaine and alcohol. *Proc Natl Acad Sci U S A* (2011) 108:6626–31. doi:10.1073/pnas.1018514108

23. Han H, Dong Z, Jia Y, Mao R, Zhou Q, Yang Y, et al. Opioid addiction and withdrawal differentially drive long-term depression of inhibitory synaptic transmission in the hippocampus. *Sci Rep* (2015) 5:9666. doi:10.1038/srep09666

24. Zhang P, Wu W, Chen Q, Chen M. Non-coding RNAs and their integrated networks. *J Integr Bioinform* (2019) 16:20190027. doi:10.1515/jib-2019-0027

25. Saba L, Vanderlinden L, Homanics GE, Flink S, Hoffman PL, Tabakoff B. "Control of alcohol consumption by a long non-coding RNA," in *Alcoholism-Clinical and experimental research* (2016), 190A. Hoboken, NJ, USA: Wiley-Blackwell.

26. Kapoor M, Wang JC, Farris SP, Liu Y, McClintick J, Gupta I, et al. Analysis of whole genome-transcriptomic organization in brain to identify genes associated with alcoholism. *Transl Psychiatry* (2019) 9:89. doi:10.1038/s41398-019-0384-y

27. Osterndorff-Kahanek EA, Becker HC, Lopez MF, Farris SP, Tiwari GR, Nunez YO, et al. Chronic ethanol exposure produces time-and brain region-dependent changes in gene coexpression networks. *PloS one* (2015) 10:e0121522. doi:10.1371/journal.pone.0121522

28. Bach H, Arango V, Kassir SA, Tsaava T, Dwork AJ, Mann JJ, et al. Alcoholics have more tryptophan hydroxylase 2 mRNA and protein in the dorsal and median raphe nuclei. *Alcohol Clin Exp Res* (2014) 38:1894–901. doi:10.1111/acer.12414

29. Even-Chen O, Herburg L, Kefalakes E, Urshansky N, Grothe C, Barak S. FGF2 is an endogenous regulator of alcohol reward and consumption. *Addict Biol* (2022) 27:e13115. doi:10.1111/adb.13115

30. Blednov YA, Bergeson SE, Walker D, Ferreira VMM, Kuziel WA, Harris RA. Perturbation of chemokine networks by gene deletion alters the reinforcing actions of ethanol. *Behav Brain Res* (2005) 165:110–25. doi:10.1016/j.bbr.2005.06.026

31. Mayfield J, Arends MA, Harris RA, Blednov YA. Genes and alcohol consumption: Studies with mutant mice. *Int Rev Neurobiol* (2016) 126:293–355. doi:10.1016/bs.irn.2016.02.014

32. Mitsuyama H, Little KY, Sieghart W, Devaud LL, Morrow AL. GABA(A) receptor alpha1, alpha4, and beta3 subunit mRNA and protein expression in the frontal cortex of human alcoholics. *Alcohol Clin Exp Res* (1998) 22:815–22. doi:10.1097/00000374-199806000-00007

33. Bhandage AK, Jin Z, Bazov I, Kononenko O, Bakalkin G, Korpi ER, et al. GABA-A and NMDA receptor subunit mRNA expression is altered in the caudate but not the putamen of the postmortem brains of alcoholics. *Front Cel Neurosci.* (2014) 8:415. doi:10.3389/fncel.2014.00415

34. Jin Z, Bhandage AK, Bazov I, Kononenko O, Bakalkin G, Korpi ER, et al. Selective increases of AMPA, NMDA, and kainate receptor subunit mRNAs in the hippocampus and orbitofrontal cortex but not in prefrontal cortex of human alcoholics. *Front Cel Neurosci.* (2014) 8:11. doi:10.3389/fncel.2014.00011

35. Osterndorff-Kahanek EA, Tiwari GR, Lopez MF, Becker HC, Harris RA, Mayfield RD. Long-term ethanol exposure: Temporal pattern of microRNA expression and associated mRNA gene networks in mouse brain. *PloS One* (2018) 13:e0190841. doi:10.1371/journal.pone.0190841

36. Kyzar EJ, Bohnsack JP, Zhang H, Pandey SC. MicroRNA-137 drives epigenetic reprogramming in the adult amygdala and behavioral changes after adolescent alcohol exposure. *Eneuro* (2019) 6:ENEURO.0401-19.2019. doi:10.1523/ENEURO.0401-19.2019

37. Ignacio C, Hicks SD, Burke P, Lewis L, Szombathyne-Meszaros Z, Middleton FA. Alterations in serum microRNA in humans with alcohol use disorders impact cell proliferation and cell death pathways and predict structural and functional changes in brain. *BMC Neurosci* (2015) 16:55. doi:10.1186/s12868-015-0195-x

38. Lim Y, Beane-Ebel JE, Tanaka Y, Ning B, Husted CR, Henderson DC, et al. Exploration of alcohol use disorder-associated brain miRNA–mRNA regulatory networks. *Transl Psychiatry* (2021) 11:504–10. doi:10.1038/s41398-021-01635-w

39. Wyczechowska D, Lin HY, LaPlante A, Jeansonne D, Lassak A, Parsons CH, et al. A miRNA signature for cognitive deficits and alcohol use disorder in persons living with HIV/AIDS. *Front Mol Neurosci* (2017) 10:385. doi:10.3389/fnmol.2017.00385

40. Vornholt E, Drake J, Mamdani M, McMichael G, Taylor ZN, Bacanu SA, et al. Identifying a novel biological mechanism for alcohol addiction associated with circRNA networks acting as potential miRNA sponges. *Addict Biol* (2021) 26:e13071. doi:10.1111/adb.13071

41. Bohnsack JP, Teppen T, Kyzar EJ, Dzitoyeva S, Pandey SC. The lncRNA BDNF-AS is an epigenetic regulator in the human amygdala in early onset alcohol use disorders. *Transl Psychiatry* (2019) 9:34. doi:10.1038/s41398-019-0367-z

42. Saba LM, Hoffman PL, Homanics GE, Mahaffey S, Daulatabad SV, Janga SC, et al. A long non-coding RNA (Lrap) modulates brain gene expression and levels of alcohol consumption in rats. *Genes Brain Behav* (2021) 20:e12698. doi:10.1111/gbb.12698

43. Kryger R, Fan L, Wilce PA, Jaquet V. MALAT-1, a non protein-coding RNA is upregulated in the cerebellum, hippocampus and brain stem of human alcoholics. *Alcohol* (2012) 46:629–34. doi:10.1016/j.alcohol.2012.04.002

44. Quinn JJ, Chang HY. Unique features of long non-coding RNA biogenesis and function. *Nat Rev Genet* (2016) 17:47–62. doi:10.1038/nrg.2015.10

45. Benetatos L, Benetatou A, Vartholomatos G. Long non-coding RNAs and MYC association in hematological malignancies. *Ann Hematol* (2020) 99:2231–42. doi:10.1007/s00277-020-04166-4

46. Salviano-Silva A, Lobo-Alves SC, Almeida RCd, Malheiros D, Petzl-Erler ML. Besides pathology: Long non-coding RNA in cell and tissue homeostasis. *Noncoding RNA* (2018) 4:3. doi:10.3390/ncrna4010003

47. Spurlock CF, Shaginurova G, Tossberg JT, Hester JD, Chapman N, Guo Y, et al. Profiles of long noncoding RNAs in human naive and memory T cells. *J Immunol* (2017) 199:547–58. doi:10.4049/jimmunol.1700232

48. Marchese FP, Huarte M. Long non-coding RNAs and chromatin modifiers: Their place in the epigenetic code. *Epigenetics* (2014) 9:21–6. doi:10.4161/epi.27472

49. Volders P-J, Anckaert J, Verheggen K, Nuytens J, Martens L, Mestdagh P, et al. LNCipedia 5: Towards a reference set of human long non-coding RNAs. *Nucleic Acids Res* (2019) 47:D135–D139. doi:10.1093/nar/gky1031

50. Mercer TR, Dinger ME, Sunkin SM, Mehler MF, Mattick JS. Specific expression of long noncoding RNAs in the mouse brain. *Proc Natl Acad Sci U S A* (2008) 105:716–21. doi:10.1073/pnas.0706729105

51. Jarroux J, Morillon A, Pinskaya M. History, discovery, and classification of lncRNAs. *Adv Exp Med Biol* (2017) 1008:1–46. doi:10.1007/978-981-10-5203-3_1

52. Kopp F, Mendell JT. Functional classification and experimental dissection of long noncoding RNAs. *Cell* (2018) 172:393–407. doi:10.1016/j.cell.2018.01.011

53. Beermann J, Piccoli MT, Viereck J, Thum T. Non-coding RNAs in development and disease: Background, mechanisms, and therapeutic approaches. *Physiol Rev* (2016) 96:1297–325. doi:10.1152/physrev.00041.2015

54. Statello L, Guo C-J, Chen L-L, Huarte M. Gene regulation by long non-coding RNAs and its biological functions. *Nat Rev Mol Cel Biol.* (2021) 22:96–118. doi:10.1038/s41580-020-00315-9

55. Guttman M, Rinn JL. Modular regulatory principles of large non-coding RNAs. *Nature* (2012) 482:339–46. doi:10.1038/nature10887

56. Khalil AM, Guttman M, Huarte M, Garber M, Raj A, Rivea Morales D, et al. Many human large intergenic noncoding RNAs associate with chromatin-modifying complexes and affect gene expression. *Proc Natl Acad Sci U S A* (2009) 106:11667–72. doi:10.1073/pnas.0904715106

57. Sarropoulos I, Marin R, Cardoso-Moreira M, Kaessmann H. Developmental dynamics of lncRNAs across mammalian organs and species. *Nature* (2019) 571: 510–4. doi:10.1038/s41586-019-1341-x

58. Chen L-L. Linking long noncoding RNA localization and function. *Trends Biochem Sci* (2016) 41:761–72. doi:10.1016/j.tibs.2016.07.003

59. Raveendra BL, Swarnkar S, Avchalumov Y, Liu XA, Grinman E, Badal K, et al. Long noncoding RNA GM12371 acts as a transcriptional regulator of synapse function. *Proc Natl Acad Sci U S A* (2018) 115:E10197–E10205. doi:10.1073/pnas.1722587115

60. Liu J, Zhang KS, Hu B, Li SG, Li Q, Luo YP, et al. Systematic analysis of RNA regulatory network in rat brain after ischemic stroke. *Biomed Res Int* (2018) 2018: 8354350. doi:10.1155/2018/8354350

61. Elkouris M, Kouroupi G, Vourvoukelis A, Papagiannakis N, Kaltezioti V, Matsas R, et al. Long non-coding rnas associated with neurodegeneration-linked genes are reduced in Parkinson's disease patients. *Front Cel Neurosci.* (2019) 13:58. doi:10.3389/fncel.2019.00058

62. Huo X, Han S, Wu G, Latchoumanin O, Zhou G, Hebbard L, et al. Dysregulated long noncoding RNAs (lncRNAs) in hepatocellular carcinoma: Implications for tumorigenesis, disease progression, and liver cancer stem cells. *Mol Cancer* (2017) 16:165. doi:10.1186/s12943-017-0734-4

63. Sartor GC, St Laurent G, 3rd, Wahlestedt C. The emerging role of non-coding RNAs in drug addiction. *Front Genet* (2012) 3:106. doi:10.3389/fgene.2012.00106

64. Yu V, Singh P, Rahimy E, Zheng H, Kuo SZ, Kim E, et al. RNA-seq analysis identifies key long non-coding RNAs connected to the pathogenesis of alcohol-associated head and neck squamous cell carcinoma. *Oncol Lett* (2016) 12:2846–53. doi:10.3892/ol.2016.4972

65. Liu Y, Chang X, Hahn CG, Gur RE, Sleiman PAM, Hakonarson H. Non-coding RNA dysregulation in the amygdala region of schizophrenia patients contributes to the pathogenesis of the disease. *Transl Psychiatry* (2018) 8:44. doi:10.1038/s41398-017-0030-5

66. Dallner OS, Marinis JM, Lu YH, Birsoy K, Werner E, Fayzikhodjaeva G, et al. Dysregulation of a long noncoding RNA reduces leptin leading to a leptin-responsive form of obesity. *Nat Med* (2019) 25:507–16. doi:10.1038/s41591-019-0370-1

67. Plasil SL, Blednov Y, Harris RA, Messing R, Aziz HC, Lambeth PS, et al. Long noncoding RNA and AUD; molecular pharmacology, behavior, and electrophysiology of TX2 knockout mice. *Alcohol Clin Exp Res* (2020) 44. doi:10.1111/acer.14358

68. Carrizales DG, Aziz HC, Borghese CM, Osterndorff-Kahanek EA, Homanics GE, Farris SP, et al. Deletion of an alcohol-responsive long non-coding RNA, "TX1", has sexually divergent effects on NMDA receptor-mediated transmission in hippocampal area CA1 of mice. *Alcoholism-Clinical Exp Res* (2019) 43:93A. doi:10.1111/acer.14058

69. Zhu L, Zhu J, Liu Y, Chen Y, Li Y, Huang L, et al. Methamphetamine induces alterations in the long non-coding RNAs expression profile in the nucleus accumbens of the mouse. *BMC Neurosci* (2015) 16:18–3. doi:10.1186/s12868-015-0157-3

70. Bannon MJ, Savonen CL, Jia H, Dachet F, Halter SD, Schmidt CJ, et al. Identification of long noncoding RNA s dysregulated in the midbrain of human cocaine abusers. *J Neurochem* (2015) 135:50–9. doi:10.1111/jnc.13255

71. Xu H, Brown AN, Waddell NJ, Liu X, Kaplan GJ, Chitaman JM, et al. Role of long noncoding RNA Gas5 in cocaine action. *Biol Psychiatry* (2020) 88:758–66. doi:10.1016/j.biopsych.2020.05.004

72. Rusconi F, Battaglioli E, Venturin M. Psychiatric disorders and lncRNAs: A synaptic match. *Int J Mol Sci* (2020) 21:3030. doi:10.3390/ijms21093030

73. Zhou Y, Lutz P-E, Wang YC, Ragoussis J, Turecki G. Global long non-coding RNA expression in the rostral anterior cingulate cortex of depressed suicides. *Transl Psychiatry* (2018) 8:224–13. doi:10.1038/s41398-018-0267-7

74. Valadkhan S, Valencia-Hipólito A. Long non-coding RNAs. In: *Human disease*. Springer (2015). p. 203–36.

75. Pirogov SA, Gvozdev VA, Klenov MS. Long noncoding RNAs and stress response in the nucleolus. *Cells* (2019) 8:668. doi:10.3390/cells8070668

76. Kartha RV, Subramanian S. Competing endogenous RNAs (ceRNAs): New entrants to the intricacies of gene regulation. *Front Genet* (2014) 5:8. doi:10.3389/fgene.2014.00008

77. Ala U. Competing endogenous RNAs, non-coding RNAs and diseases: An intertwined story. *Cells* (2020) 9:1574. doi:10.3390/cells9071574

78. Moreno-García L, Lopez-Royo T, Calvo AC, Toivonen JM, de la Torre M, Moreno-Martinez L, et al. Competing endogenous RNA networks as biomarkers in neurodegenerative diseases. *Int J Mol Sci* (2020) 21:9582. doi:10.3390/ijms21249582

79. Lan C, Peng H, Hutvagner G, Li J. Construction of competing endogenous RNA networks from paired RNA-seq data sets by pointwise mutual information. *BMC genomics* (2019) 20:943–10. doi:10.1186/s12864-019-6321-x

80. Ala U, Karreth FA, Bosia C, Pagnani A, Taulli R, Leopold V, et al. Integrated transcriptional and competitive endogenous RNA networks are cross-regulated in permissive molecular environments. *Proc Natl Acad Sci U S A* (2013) 110:7154–9. doi:10.1073/pnas.1222509110

81. Mitra A, Pfeifer K, Park K-S. Circular RNAs and competing endogenous RNA (ceRNA) networks. *Transl Cancer Res* (2018) 7:S624–S628. doi:10.21037/tcr.2018.05.12

82. Pandey AK, Lu L, Wang X, Homayouni R, Williams RW. Functionally enigmatic genes: A case study of the brain ignorome. *PloS one* (2014) 9:e88889. doi:10.1371/journal.pone.0088889

83. Plasil SL, Seth A, Homanics GE. CRISPR Turbo Accelerated KnockOut (CRISPy TAKO) for rapid *in vivo* screening of gene function. *Front Genome Ed* (2020) 2:598522. doi:10.3389/fgeed.2020.598522

84. Rathod RS, Ferguson C, Seth A, Baratta AM, Plasil SL, Homanics GE. Effects of paternal preconception vapor alcohol exposure paradigms on behavioral responses in offspring. *Brain Sci* (2020) 10:E658. doi:10.3390/brainsci10090658

85. Ritchie ME, Phipson B, Wu D, Hu Y, Law CW, Shi W, et al. Limma powers differential expression analyses for RNA-sequencing and microarray studies. *Nucleic Acids Res* (2015) 43:e47. doi:10.1093/nar/gkv007

86. Homanics GE. Gene-edited CRISPy Critters for alcohol research. *Alcohol* (2019) 74:11–9. doi:10.1016/j.alcohol.2018.03.001

87. Stemmer M, Thumberger T, del Sol Keyer M, Wittbrodt J, Mateo JL. CCTop: An intuitive, flexible and reliable CRISPR/Cas9 target prediction tool. *PloS one* (2015) 10:e0124633. doi:10.1371/journal.pone.0124633

88. Labuhn M, Adams FF, Ng M, Knoess S, Schambach A, Charpentier EM, et al. Refined sgRNA efficacy prediction improves large-and small-scale CRISPR–Cas9 applications. *Nucleic Acids Res* (2018) 46:1375–85. doi:10.1093/nar/gkx1268

89. Benjamini Y, Krieger A, Yekutieli D. Adaptive linear step-up procedures that control the false discovery rate. *Biometrika* (2006) 93:491–507. doi:10.1093/biomet/93.3.491

90. Sneddon EA, White RD, Radke AK. Sex differences in binge-like and aversion-resistant alcohol drinking in C57BL/6J mice. *Alcohol Clin Exp Res* (2019) 43:243–9. doi:10.1111/acer.13923

91. Becker JB, Koob GF. Sex differences in animal models: Focus on addiction. *Pharmacol Rev* (2016) 68:242–63. doi:10.1124/pr.115.011163

92. Finn DA, Hashimoto JG, Cozzoli DK, Helms ML, Nipper MA, Kaufman MN, et al. Binge ethanol drinking produces sexually divergent and distinct changes in nucleus accumbens signaling cascades and pathways in adult C57BL/6J mice. *Front Genet* (2018) 9:325. doi:10.3389/fgene.2018.00325

93. Gelineau RR, Arruda NL, Hicks JA, Monteiro De Pina I, Hatzidis A, Seggio JA. The behavioral and physiological effects of high-fat diet and alcohol consumption: Sex differences in C57BL/6J mice. *Brain Behav* (2017) 7:e00708. doi:10.1002/brb3.708

94. Belknap JK, Crabbe JC, Young E. Voluntary consumption of ethanol in 15 inbred mouse strains. *Psychopharmacology* (1993) 112:503–10. doi:10.1007/BF02244901

95. Blednov Y, Walker D, Martinez M., Levine M., Damak S, Margolskee RF. Perception of sweet taste is important for voluntary alcohol consumption in mice. *Genes Brain Behav* (2008) 7:1–13. doi:10.1111/j.1601-183X.2007.00309.x

96. Blednov Y, Ozburn AR, Walker D, Ahmed S, Belknap JK, Harris RA. Hybrid mice as genetic models of high alcohol consumption. *Behav Genet* (2010) 40: 93–110. doi:10.1007/s10519-009-9298-4

97. Koren E, Lev-Maor G, Ast G. The emergence of alternative 3′ and 5′ splice site exons from constitutive exons. *Plos Comput Biol* (2007) 3:e95. doi:10.1371/journal.pcbi.0030095

98. Nolte C, Staiger D. RNA around the clock–regulation at the RNA level in biological timing. *Front Plant Sci* (2015) 6:311. doi:10.3389/fpls.2015.00311

99. Roca X, Krainer AR, Eperon IC. Pick one, but be quick: 5′ splice sites and the problems of too many choices. *Genes Dev* (2013) 27:129–44. doi:10.1101/gad.209759.112

100. Anna A, Monika G. Splicing mutations in human genetic disorders: Examples, detection, and confirmation. *J Appl Genet* (2018) 59:253–68. doi:10.1007/s13353-018-0444-7

101. Fredericks AM, Cygan KJ, Brown BA, Fairbrother WG. RNA-Binding proteins: Splicing factors and disease. *Biomolecules* (2015) 5:893–909. doi:10.3390/biom5020893

102. Landry J-R, Mager DL, Wilhelm BT. Complex controls: The role of alternative promoters in mammalian genomes. *Trends Genet* (2003) 19:640–8. doi:10.1016/j.tig.2003.09.014

103. Wang J, Zhang S, Lu H, Xu H. Differential regulation of alternative promoters emerges from unified kinetics of enhancer-promoter interaction. *Nat Commun* (2022) 13:2714–4. doi:10.1038/s41467-022-30315-6

104. Singer GA, Wu J, Yan P, Plass C, Huang THM, Davuluri RV. Genome-wide analysis of alternative promoters of human genes using a custom promoter tiling array. *BMC genomics* (2008) 9:349–15. doi:10.1186/1471-2164-9-349

105. Finn DA, Snelling C, Fretwell AM, Tanchuck MA, Underwood L, Cole M, et al. Increased drinking during withdrawal from intermittent ethanol exposure is blocked by the CRF receptor antagonist D-Phe-CRF (12–41). *Alcohol Clin Exp Res* (2007) 31:939–49. doi:10.1111/j.1530-0277.2007.00379.x

106. Souza TP, Franscescon F, Stefanello FV, Muller TE, Santos LW, Rosemberg DB. Acute effects of ethanol on behavioral responses of male and female zebrafish in the open field test with the influence of a non-familiar object. *Behav Process.* (2021) 191:104474. doi:10.1016/j.beproc.2021.104474

107. Jury NJ, DiBerto JF, Kash TL, Holmes A. Sex differences in the behavioral sequelae of chronic ethanol exposure. *Alcohol* (2017) 58:53–60. doi:10.1016/j.alcohol.2016.07.007

108. Barker JM, Bryant KG, Osborne JI, Chandler L. Age and sex interact to mediate the effects of intermittent, high-dose ethanol exposure on behavioral flexibility. *Front Pharmacol* (2017) 8:450. doi:10.3389/fphar.2017.00450

109. Darnieder L, Melon LC, Do T, Walton NL, Miczek KA, Maguire JL. Female-specific decreases in alcohol binge-like drinking resulting from GABAA receptor delta-subunit knockdown in the VTA. *Sci Rep* (2019) 9:8102–11. doi:10.1038/s41598-019-44286-0

110. Shansky RM, Murphy AZ. Considering sex as a biological variable will require a global shift in science culture. *Nat Neurosci* (2021) 24:457–64. doi:10.1038/s41593-021-00806-8

111. Shansky RM. Estrogen, stress and the brain: Progress toward unraveling gender discrepancies in major depressive disorder. *Expert Rev Neurother* (2009) 9:967–73. doi:10.1586/ern.09.46

112. Farrell MR, Gruene TM, Shansky RM. The influence of stress and gonadal hormones on neuronal structure and function. *Horm Behav* (2015) 76:118–24. doi:10.1016/j.yhbeh.2015.03.003

113. Becker JB, Chartoff E. Sex differences in neural mechanisms mediating reward and addiction. *Neuropsychopharmacology* (2019) 44:166–83. doi:10.1038/s41386-018-0125-6

114. Drake J, McMichael GO, Vornholt ES, Cresswell K, Williamson V, Chatzinakos C, et al. Assessing the role of long noncoding RNA in nucleus accumbens in subjects with alcohol dependence. *Alcohol Clin Exp Res* (2020) 44:2468–80. doi:10.1111/acer.14479

115. Zheng H, Li P, Kwok JG, Korrapati A, Li WT, Qu Y, et al. Alcohol and hepatitis virus-dysregulated lncRNAs as potential biomarkers for hepatocellular carcinoma. *Oncotarget* (2018) 9:224–35. doi:10.18632/oncotarget.22921

116. Zhou A, Wang Y, Liu Y, Feng W, Edenberg HJ. In: 2016 IEEE International Conference on Bioinformatics and Biomedicine (BIBM), Shenzhen, China, December 15–18, 2016. (2016) IEEE. p. 167–73.

ADAR | Publishing Partnerships

TYPE Original Research
PUBLISHED 06 June 2023
DOI 10.3389/adar.2023.11323

OPEN ACCESS

EDITED BY
Emmanuel Onaivi,
William Paterson University,
United States

REVIEWED BY
Jim Tiao,
Pathwest Laboratory Medicine, Australia
David Turner,
University of Michigan, United States

*CORRESPONDENCE
Andrzej Zbigniew Pietrzykowski,
andre.z.piet@gmail.com

†PRESENT ADDRESS
Edward Andrew Mead,
Department of Genetics and Genomic Sciences, Icahn School of Medicine at Mount Sinai, New York, NY, United States;
Yongping Wang,
Holmdel Township School, Holmdel, NJ, United States;
Austin P. Thekkumthala,
Bristol-Myers Squibb, New Brunswick, NJ, United States;
Rebecca Kepich,
Syneos Health, Morrisville, NC, United States;
Elizabeth Benn-Hirsch,
Ross University School of Medicine, Portsmith, Dominica;
Victoria Lee,
JP Morgan Chase, Jersey City, NJ, United States;
Azra Basaly,
Fresenius Medical Care, Waltham, MA, United States;
Hava T. Siegelmann,
Biologically Inspired Neural & Dynamical Systems Laboratory, The Manning College of Information and Computer Sciences, University of Massachusetts, Amherst, MA, United States;
Andrzej Zbigniew Pietrzykowski,
Weight & Life MD, LLC, Hamilton, NJ, United States;
Biologically Inspired Neural & Dynamical Systems Laboratory, The Manning College of Information and Computer Sciences, University of Massachusetts, Amherst, MA, United States

RECEIVED 01 March 2023
ACCEPTED 16 May 2023
PUBLISHED 06 June 2023

miR-9 utilizes precursor pathways in adaptation to alcohol in mouse striatal neurons

Edward Andrew Mead[1†], Yongping Wang[1†], Sunali Patel[2], Austin P. Thekkumthala[1†], Rebecca Kepich[1†], Elizabeth Benn-Hirsch[1†], Victoria Lee[1†], Azra Basaly[1†], Susan Bergeson[3], Hava T. Siegelmann[4,5†] and Andrzej Zbigniew Pietrzykowski[1*†]

[1]Laboratory of Adaptation, Reward and Addiction, Department of Animal Sciences, Rutgers, The State University of New Jersey, New Brunswick, NJ, United States, [2]Thermo Fisher Scientific Inc., Austin, TX, United States, [3]Department of Cell Biology and Biochemistry, School of Medicine, Texas Tech University Health Sciences Center, Lubbock, TX, United States, [4]Department of Machine Learning, Mohamed bin Zayed University of Artificial Intelligence, Abu Dhabi, United Arab Emirates, [5]Biologically Inspired Neural & Dynamical Systems Laboratory, The Manning College of Information and Computer Sciences, University of Massachusetts, Amherst, MA, United States

microRNA-9 (miR-9) is one of the most abundant microRNAs in the mammalian brain, essential for its development and normal function. In neurons, it regulates the expression of several key molecules, ranging from ion channels to enzymes, to transcription factors broadly affecting the expression of many genes. The neuronal effects of alcohol, one of the most abused drugs in the world, seem to be at least partially dependent on regulating the expression of miR-9. We previously observed that molecular mechanisms of the development of alcohol tolerance are miR-9 dependent. Since a critical feature of alcohol action is temporal exposure to the drug, we decided to better understand the time dependence of alcohol regulation of miR-9 biogenesis and expression. We measured the effect of intoxicating concentration of alcohol (20 mM ethanol) on the expression of all major elements of miR-9 biogenesis: three pri-precursors (pri-mir-9-1, pri-mir-9-2, pri-mir-9-3), three pre-precursors (pre-mir-9-1, pre-mir-9-2, pre-mir-9-3), and two mature microRNAs: miR-9-5p and miR-9-3p, using digital PCR and RT-qPCR, and murine primary medium spiny neurons (MSN) cultures. We subjected the neurons to alcohol based on an exposure/withdrawal matrix of different exposure times (from 15 min to 24 h) followed by different withdrawal times (from 0 h to 24 h). We observed that a short exposure increased mature miR-9-5p expression, which was followed by a gradual decrease and subsequent increase of the expression, returning to pre-exposure levels within 24 h. Temporal changes of miR-9-3p expression were complementing miR-9-5p changes. Interestingly, an extended, continuous presence of the drug caused a similar pattern. These results suggest the presence of the adaptive mechanisms of miR-9 expression in the presence and absence of alcohol. Measurement of miR-9 pre- and pri-precursors showed further that the primary effect of alcohol on miR-9 is through the mir-9-2 precursor pathway with a smaller contribution of mir-9-1 and mir-9-3 precursors. Our results provide new insight into the adaptive mechanisms of neurons to alcohol exposure. It would be of interest to determine next which microRNA-based mechanisms are involved in a transition from the acute, intoxicating effects of alcohol to the chronic, addictive effects of the drug.

KEYWORDS
addiction, digital PCR, alcohol adaptation, microRNA miR-9, medium spiny neurons

Introduction

Alcohol Use Disorder (AUD) is a chronic, incurable disease affecting people worldwide regardless of their social or economic status. AUD leads to an estimated 132.6 million disability-adjusted life years (DALYs), and an estimated 3 million deaths per year [1]. In the United States AUD is one of the largest drug problems, and alcohol abuse costs the country hundreds of billions of dollars each year in lost revenue, treatments, and mortality [2, 3]. Development of alcohol addiction takes place over time through the complex actions of alcohol on the brain's reward system. Temporal characteristics of alcohol actions are critical yet poorly understood.

In recent years, many studies have focused on the epigenetic underpinnings of addiction to better understand the development of AUD [4]. MicroRNAs (miRNAs), small (~21 nt long) endogenous RNA molecules are powerful epigenetic modulators regulating gene expression on a genome-wide scale [5]. It has been estimated that microRNAs modify the expression of approximately 60% of the transcripts in humans [6] and play a fundamental role in the development and maintenance of neurons in the brain [7]. microRNAs are also key elements of the development of drug [8–10] and alcohol addiction [11–13].

One particular microRNA involved in brain development [14], function [15], and malfunction [16] is miR-9 (specifically miR-9-5p). Dysregulation of miR-9-5p by alcohol has a broad impact on the brain, and several downstream targets of miR-9-5p have been well-established ([17], reviewed in depth in [18]). However, effects of upstream changes in miR-9 biogenesis on mature miR-9 are less studied. Understanding alcohol regulation of miR-9 biogenesis could help to uncover new mechanisms of alcohol action, and ultimately may lead to discovery of novel therapeutic options in addiction.

miR-9 is an ancient microRNA found from invertebrates to mammals [19, 20] and has a complex biogenesis. In many species there are three distinct miR-9 genes located on three different chromosomes. In humans, miR-9 genes are located on chromosomes 1, 5, and 15, while their equivalents in mice are on chromosomes 3, 7, and 13, respectively [21]. In both species, each gene gives rise to a separate, long, primary precursor, pri-mir-9-1, pri-mir-9-2, and pri-mir-9-3 (Figure 1). Each pri-precursor is subsequently trimmed to a shorter pre-precursor of a characteristic hairpin loop structure (Figure 1). The next step produces an even shorter, small, double-stranded duplex consisting mostly of two complementarily bound miRNA strands. Ultimate processing of the duplex separates the strands yielding two short, single-stranded, distinct mature microRNAs: miR-9-5p and miR-9-3p. Importantly, in the case of miR-9, all final mature miR-9-5p products of the 3 biogenesis pathways are identical [22]. Similarly, all mature miR-9-3p end products are indistinguishable (Figure 1). Both mature miR-9 strands execute biological action by interacting through complementarity with multiple targets (RNA transcripts), which usually leads to suppression of expression of the targets.

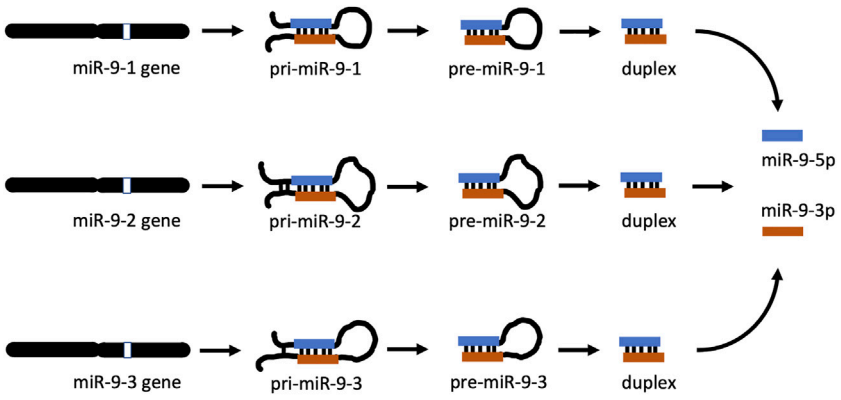

FIGURE 1
miR-9 biogenesis pathways. In apes (including humans) and rodents (including mice), there are 3 mir-9 genes (mir-9-1, mir-9-2, and mir-9-3) located on different chromosomes. Each gene produces its own primary RNA precursor (pri-mir-9-1, pri-mir-9-2, and pri-mir-9-3), which is cleaved to a pre-precursor (pre-mir-9-1, pre-mir-9-2, and pre-mir-9-3). Each precursor is further processed to yield a duplex containing both miR-9-5p and miR-9-3p. Separation of each duplex into single-stranded RNA sequences generates two final forms of miR-9, which are physiologically active: miR-9-5p and miR-9-3p. All miR-9-5p produced via 3 separate biogenesis pathways are identical. Similarly, all final miR-9-3p are indistinguishable.

miR-9-3p has been shown to be biologically active and play an important role in carcinogenesis [23] such as in Burkitt's lymphoma [24] and breast cancer [23, 25] as well as brain pathologies. Decreased expression of miR-9-3p has been linked to neurological disorders including Alzheimer's and Huntington's diseases [26].

Thus, understanding temporal regulation of the expression of various miR-9 precursors as well as both forms of mature miR-9 by alcohol is critical in enhancing our understanding of the mechanisms involved in the development of alcohol addiction and adaptation to alcohol exposure.

Materials and methods

Striatal culture

C57BL6/J mice (Jackson Laboratory, Bar Harbor, ME) were maintained under 12h:12h light:dark cycles at standard temperature and humidity with food and water provided *ad libitum* at the Bartlett Animal Facility (Rutgers-New Brunswick). Mice were monitored daily, and cages were routinely changed. Mice were bred for litters to use in generating cultures. All animal experiments were approved by the Rutgers Institutional Animal Care and Use Committee (IACUC Protocol # 10-024).

Cultures of Medium Spiny Neurons (MSN) at ~95% purity [27, 28], were prepared following well-established protocols [29–31]. At day 5 after birth (P5), pups were decapitated, and brains were immediately removed and placed into a 60 mm plate containing ice-cold CMF-HBSS (100 mL of final solution made with 10 mL 10x HBSS (Life Technologies), 0.7 mL 5% $NaHCO_3$ (Sigma), final pH 7.1, brought to final volume with ultrapure water, then filter sterilized and stored at room temperature). The Nucleus Accumbens (NAc) was removed using a mouse brain atlas for visual reference [32]. Equal numbers of male and female pups were used for each preparation to limit the bias of using a single gender. Striatal tissue was diced into smaller fragments, ~1 mm in diameter in 3.15 mL cold CMF-HBSS, and trypsinized with the addition of 0.35 mL of 2.5% trypsin at 37°C. After 10 min, 8 mL DMEM-FBS medium (178 mL DMEM (high glucose, no sodium pyruvate, no glutamine (Irvine Scientist), with 20 mL FBS, 0.5 mL 10,000 u Pen/Strep and 2 mL 200 mM glutamine (Life Technologies), stored at 4°C in the dark) was added, and the solution was centrifuged at 300 x g for 5 min to pellet the cells. The medium was aspirated from the tube, and 5 mL of Growth Medium (100 mL DMEM/F12 (with Glutamax; Life Technologies), with 2 mL FBS (1.9% v/v), 2 mL B-27 (1.9% v/v; Life Technologies), and 1 mL penicillin/streptomycin (0.95% v/v), stored at 4°C in the dark) was added. Trituration to further break apart aggregates was conducted using a fire-polished Pasteur pipet, and the tube was spun again as above. Excess media was removed, and the cells were resuspended in 10 mL of Growth Medium. Preparations were conducted under a sterile hood to help maintain sterility, except for centrifugation. The concentration of live cells/mL was estimated by hemocytometer counts of live:dead cells using trypan blue, and the cell stock solution was diluted to a final concentration of 0.5×10^6 cells/mL. Plates of striatal cells were prepared by seeding 2 mL of the cell stock solution onto 35 mm cell culture plates that had been coated with ornithine (Sigma-Aldrich, St. Louis, MO) and laminin (Life Technologies, Carlsbad, CA) for cell adherence and enrichment for neurons. Preparations were rapidly conducted as speed was critical for cell viability. Twenty-four hours post-seeding, after allowing cells to adhere, the media was replaced with a 2 mL Neurobasal Medium (NB)/plate (100 mL Neurobasal A Medium supplemented to 2.0 mM glutamine final concentration; Life Technologies), with 2 mL FBS (1.9% v/v), 2 mL B-27 (1.9% v/v; Life Technologies), and 1 mL penicillin/streptomycin (0.95% v/v) stored at 4°C in the dark). Cultures were maintained at 37°C/5% CO2 in a cell culture incubator with saturated humidity for another week before starting exposures, and as a result, the neurons were nearly 2 weeks old since birth (5 days *in vivo* + 8 days *in vitro* = 13 days total) at the start of the experiments. Sometimes in microRNA studies alpha-amanitin is added to cultured cells to inhibit RNA polymerases II and III, which process microRNA. Since alpha-amanitin can also cause widespread transcriptional stress and apoptosis [33, 34] we did not add it to our cultures.

Ethanol exposure

We chose 20 mM ethanol for alcohol exposures as it represents a physiologically relevant dose of alcohol while maintaining cell viability. 20 mM ethanol corresponds to a 0.092% Blood Alcohol Content (BAC), which can be achieved in humans by a quick (30–60 min) consumption of 3–4 standard drinks of alcohol by a 150-pound individual [35] causing disinhibition, impaired thinking, and potential DWI/DUI in the US [35]. Previously we have shown that 20 mM ethanol can upregulate the expression of miR-9-5p within 15 min after exposure of the rat brain organotypic cultures containing supraoptic nucleus (SON) neurons leading to alcohol tolerance [17]. Importantly, 20 mM causes minimal neuronal cell death in culture as shown by us [12] and others [36].

Seven days after seeding neurons the cells were subjected to the alcohol exposure and withdrawal with the following collection time points: Control = 0 min exposure +0 h withdrawal, 15 min 20 mM ethanol exposure +0 h withdrawal, 15 min 20 mM ethanol exposure +1 h withdrawal, 15 min 20 mM ethanol exposure +6 h withdrawal, 15 min 20 mM ethanol exposure +12 h withdrawal, 15 min 20 mM ethanol exposure +24 h withdrawal, 6 h 20 mM ethanol exposure +0 h withdrawal, 6 h 20 mM ethanol exposure +6 h withdrawal, 6 h 20 mM ethanol exposure +24 h withdrawal. Collection at each time point was conducted in triplicate. For each control, 5–7 plates were prepared. Cells were treated by aspirating off media and replacing with either a neurobasal medium ("media only" control) or a neurobasal medium with alcohol (NBE with

20 mM final ethanol concentration). Ethanol evaporation was minimized by maintaining NBE plates in a semi-sealed container in the incubator with saturated humidity and additional plates of medium containing the same concentration of ethanol, based upon the methods of Pietrzykowski [12, 17].

After a defined length of exposure, NB or NBE media were removed. For plates without a withdrawal period, cells were collected immediately. For cells with a withdrawal period, the NB medium replaced the NBE medium for a defined length of time after which cells were collected.

Cell collection was carried out by quickly rinsing plates with 2 mL ice-cold PBS followed by scraping cells from the plate with a cell scraper in 200 uL PBS. Cells were immediately flash-frozen in liquid nitrogen and stored at −80°C until processed for total RNA isolation as described previously [16].

Alcohol concentration verification

Media samples were gathered at each collection point in the experimental process (before and after ethanol addition, during exposure and withdrawal) to verify alcohol concentration. Alcohol measurements were conducted using an AMI Analyzer according to the manufacturer's instructions (Analox Instruments Ltd., Lunenburg, MA). 10, 20, and 50 mM ethanol standards in media were used to calibrate the instrument prior to reads to ensure accuracy. Alcohol measurements confirmed that ethanol loss was minimized using our methodology as previously described in more detail [12, 17].

RNA isolation

Total RNA or Small RNA (for precursor assays) was isolated by miRVana kit according to the manufacturer's instructions (Life Technologies). Concentration and purity were analyzed by a Nanodrop 1000 Spectrophotometer (Thermo Fisher Scientific Inc., Wilmington, DE), and aliquots of each sample were used to prepare 10ng/ul dilutions in nuclease-free water for RT-qPCR. All samples were kept at −80°C.

RT-qPCR

miRNA

We conducted RT and qPCR steps to assess mature miR-9-5p and miR-9-3p based upon the manufacturer's protocols for TaqMan Small RNA Assays (Applied Biosystems, Inc., Foster City, CA). Using the TaqMan MicroRNA Reverse Transcription kit (Applied Biosystems, Inc., Foster City, CA), mature miRNA was converted into cDNA using a Veriti Thermal Cycler (Applied Biosystems, Inc., Foster City, CA). A working stock of 10 ng/ul of total RNA was prepared and used for RT with each experimental sample in a total volume of 15 µL. RT consisted of 16°C 30 min, 42°C 30 min, 85°C 5 min, and hold at 4°C. The two-step process of RT followed by qPCR permitted finer control/greater accuracy for the final RT-qPCR reaction by allowing us to equalize the quantities of cDNA. cDNAs were amplified with the Taqman Small RNA Assay kit (Applied Biosystems, Inc., Foster City, CA) using an ABI Step One Plus Thermocycler (Applied Biosystems, Inc., Foster City, CA). 1.33 µL of RT sample was used for Taqman qPCR in a total volume of 20 µL. TaqMan reactions were carried out using Universal Master Mix II, no UNG from Applied Biosystems, and 1 µL of TaqMan MicroRNA assay primers. Triplicates of each sample were used in the 96-well plate (except for controls, where $n = 5$, or $n = 7$) to ensure greater accuracy. The average was taken as the value for each. For normalization and quality assessment we followed absolute quantification methods which can provide better accuracy without the need of a separate housekeeping gene, as described by Iguchi [37], Arabkari [38], and Wang [39]. We used 7-log dilution range (10 fmol–10^{-4} fmol) of synthetic miR-9-5p and miR-9-3p oligos (amplification efficiency, R^2 = 0.9993). The cycling protocol consisted of 95°C for 10 min, followed by 40 cycles of (95°C for 15 s and 60°C for 1 min), in an ABI Step One Plus Thermocycler (Applied Biosystems, Inc., Foster City, CA). Data collection occurred at the 60°C step.

Pre- and Pri-miRNA precursors

We used the Ambion miRVana kit following the manufacturer's instructions, to separate small RNA molecules including pre-precursor miRNAs (~100 nt in length) from the much larger (over 1,000 nt in length) pri-precursors for subsequent studies.

Pre- precursors

RT was conducted using a miScript II RT kit (Qiagen). miR-9 precursors (pre-mir-9-1, pre-mir-9-2, pre-mir-9-3) were pre-amplified using stock primers for RT-qPCR from Qiagen. After this, a 1:20 dilution of the pre-amp product was used for normal qPCR. Standard curves were prepared from 100 fmol using stocks of 9-1, 9-2, and 9-3 oligos. Pre-amplification was carried out using Qiagen miScript Precursor assay kits for pre-mir-9-1, -9-2, and -9-3 respectively, along with a miScript PreAMP PCR Kit (Qiagen).

Pri-precursors

Cell cultures were obtained as indicated above. RT was carried out with SuperScript VILO Master Mix (Invitrogen) using the manufacturer's recommendations. cDNA samples were sent to Life Technologies for subsequent digital PCR.

Digital PCR

30 ng/µL of each alcohol exposure sample was tested with three TaqMan Pri-miRNA assays (Mm04227702 pri-mmu-mir-9-1, Mm03306269 pri-mmu-mir-9-2, and Mm03307250 pri-mmu-mir-9-3) (Thermo Fisher Scientific Inc.). 1µL of each sample was added to 10 µL QuantStudio 3D Digital PCR Master Mix, 1 µL of TaqMan Assay (20X), and 8 µL of nuclease-free water for 20 µL of

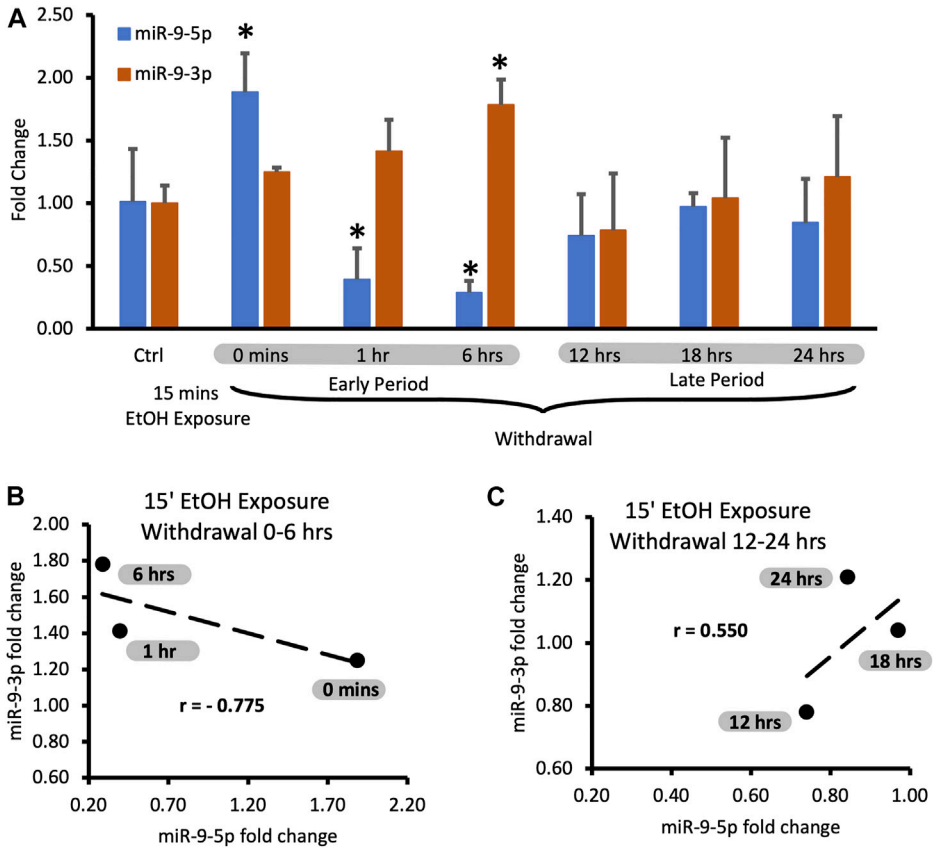

FIGURE 2
Expression levels of miR-9-5p and -3p during 24-hr long withdrawal after 15 min exposure to 20 mM ethanol. **(A)** Temporal expression profile of miR-9-5p (left bars) and miR-9-3p (right bars) measured by Taqman-based RT-qPCR. Data expressed as mean fold change ± SD. $n = 3$, except $n = 7$ in miR-9-5p control group, $n = 5$ in miR-9-3p control group). Asterisks indicate statistically significant differences comparing to the control, $p < 0.05$. **(B)** Strong, negative correlation of miR-9-5p and miR-9-3p expression levels during the first 6 h of alcohol withdrawal. Correlation coefficient r = −0.775. **(C)** Moderate, positive correlation of miR-9-5p and miR-93p expression levels during 12–24 h of alcohol withdrawal. The correlation coefficient r = 0.550.

the reaction mix. 14.5 µL of reaction mix was loaded on each QuantStudio 3D Digital PCR 20K Chip (Thermo Fisher Scientific Inc.) using QuantStudio 3D Digital PCR Chip Loader (Thermo Fisher Scientific Inc.) according to manufacturer's instruction. The digital PCR was performed on Proflex 2x Flat PCR System (Thermo Fisher Scientific Inc.) with thermal cycling of 10 min at 96°C, followed by 39 cycles at 60°C for 2 min and 98°C for 30 s, followed by holding at 60°C for 2 min and 10°C for long term. Each chip fluorescence intensity was read using QuantStudio 3D Digital PCR instrument (Thermo Fisher Scientific Inc.) and analyzed copies/µL based on Poisson distribution using QuantStudio 3D Analysis Suite Cloud Software (Thermo Fisher Scientific Inc.).

Statistical analysis

Expression data for statistical analysis were obtained using oligos in a standard curve method for mature miR-9-5p and miR-9-3p, $2^{-\Delta\Delta CT}$ method for pre-precursors, and Poisson distribution for pri-precursors. The data were analyzed using unpaired, two-tailed t-tests. Data were expressed as fold-change to visualize the relationship between exposure condition and molecule expression. p-value below 0.05 ($p < 0.05$) was set as statistically significant.

Results

Regulation of miR-9-5p and miR-9-3p expression by short exposure to alcohol

miR-9-5p is a prominent brain microRNA regulated by alcohol. Some reports describe the stimulatory effect of alcohol on miR-9-5p expression [17, 40], while others report the opposite effects [41]. To better understand the intricacies of miR-9-5p regulation by alcohol, we first exposed murine primary neuronal cultures to physiologically relevant 20 mM ethanol for

15 min (the short exposure) and measured its expression at various times after alcohol withdrawal up to 24 h post-exposure (Figure 2A).

We observed that after the short exposure expression levels of miR-9-5p increased almost two-fold (Figure 2A, left bars), in accordance with previously published findings [17]. Alcohol withdrawal caused a fast decrease of the elevated levels of miR-9-5p even below the pre-exposure, normal levels within 1 h after the start of the exposure (Figure 2A, left bars). In the alcohol-free environment, miR-9-5p levels decreased even further with time, reaching the lowest levels of around 40% of the pre-exposure levels at the 6 h post-exposure mark. Somewhere between 6 h and 12 h of the withdrawal miR-9-5p levels started to rebound from their nadir point and went back to the pre-exposure levels (Figure 2A, left bars). They reached the pre-exposure levels 12 h after the exposure and maintained normal levels up to 24 h after the exposure (Figure 2A, left bars).

Although miR-9-5p is the most recognized final product of miR-9 biogenesis, miR-9-3p also plays an important role in neural development [42] and neuronal differentiation [43] with more predicted targets then miR-9-5p (Supplementary Table S1, miR-9-5p: 1242 targets; Supplementary Table S2, miR-9-3p: 4334 targets). Interestingly, there is a quite large overlap of targets between these two microRNAs: over 34% of miR-9-5p targets are also targeted by miR-9-3p (425 targets, Supplementary Table S3).

We observed that short alcohol exposure also regulates the expression of miR-9-3p. The short exposure increased expression of miR-9-3p (Figure 2A, right bars) similar to its effect on the miR-9-5p expression. In contrast to miR-9-5p however, after the removal of alcohol, miR-9-3p levels continue to rise, reaching significantly higher levels 6 h post-exposure (Figure 2A, right bars).

After reaching the peak of expression, miR-9-3p levels return down to pre-exposure levels at the 12 h post-exposure timepoint and maintain that normal level up to the 24 h post-exposure, mimicking temporal dynamics of miR-9-5p expression changes within 12–24 h post-exposure time interval (Figure 2A, right bars).

It seems that, based on changes in the expression of both microRNAs, two withdrawal periods triggered by short alcohol exposure could be distinguished: the early period starting immediately after alcohol withdrawal and lasting around 6 h, and the late period following the early one and lasting up to the 24-hour post-exposure timepoint (Figure 2A).

During both time periods, the expression of miR-9-5p and miR-9-3p seems to be tightly associated with each other as determined by correlation analysis. During the early withdrawal period changes in miR-9-3p and miR-9-5p expression are strongly and negatively correlated (Figure 2B; Table 1, correlation coefficient r = −0.775). During the late withdrawal period, changes in the expression of miR-9-3p and miR-9-5p are moderately and positively correlated (Figure 2C; Table 2, correlation coefficient r = 0.55).

Regulation of miR-9-5p and miR-9-3p expression by continuous exposure to alcohol

We compared the short exposure results with the expression of miR-9-5p under the continuous presence of the drug for up to 24 h (continuous exposure).

We assumed that the continuous presence of the drug would maintain the elevated plateau of miR-9-5p since exposure to alcohol increased miR-9-5p levels in the first place. However, it was not the case. We observed that despite alcohol presence, after

TABLE 1 Correlation between expression fold change of miR-9-5p and miR-9-3p during the early period of alcohol withdrawal.

EtOH WD time [hrs]	miR-9-5p fold change	miR-9-3p fold change	r
0	1.89	1.25	- 0.775
1	0.39	1.41	
6	0.29	1.78	

EtOH WD—ethanol withdrawal, r—correlation coefficient.

TABLE 2 Correlation between expression fold change of miR-9-5p and miR-9-3p during the late period of alcohol withdrawal.

EtOH WD time [hrs]	miR-9-5p fold change	miR-9-3p fold change	r
12	0.74	0.78	0.550
18	0.97	1.04	
24	0.84	1.21	

EtOH WD—ethanol withdrawal, r—correlation coefficient.

the initial increase, miR-9-5p levels dropped within 6 h post-exposure (Figure 2B, left bars) and then increased (Figure 2B, left bars) with a similar temporal dynamic seen with the short exposure. Interestingly, in the continuing presence of alcohol beyond 6 h the miR-9-5p expression pattern shifted upwards above the pre-exposure levels presumably trying to set a new, higher equilibrium (Figure 2B, left bars).

During the continuous exposure to alcohol, the miR-9-3p expression did not change sufficiently to achieve standard statistical significance ($p < 0.05$) except for the last timepoint (Figure 3A, 24 h exposure). However, the changes of the miR-9-3p expression tightly followed the changes of the miR-9-5p expression, showing a strong and positive correlation at each timepoint studied (Figure 3A). We think that two periods with similar time frames can be distinguished here as well based on changes in the expression pattern: the early exposure period starting soon after alcohol addition and lasting about 6 h (Figure 3A) with a correlation coefficient r = 0.720 (Figure 3B; Table 3), and the late exposure period following the first one up to the 24-hour of alcohol exposure (Figure 3C; Table 4) with the correlation coefficient r = 0.853.

Regulation of expression of miR-9 precursors by short alcohol exposure

Both miR-9-5p and miR-9-3p are final products of miR-9 biogenesis (Figure 1, and ref 19). Three separate biogenesis pathways of the miR-9-5p/miR-9-3p pair start with each miR-9 gene generating its own pri-mir-9 precursor, and subsequently pre-mir-9 precursor, which ultimately contributes to the mature miR-9-5p and the mature miR-9-3p pools (Figure 1).

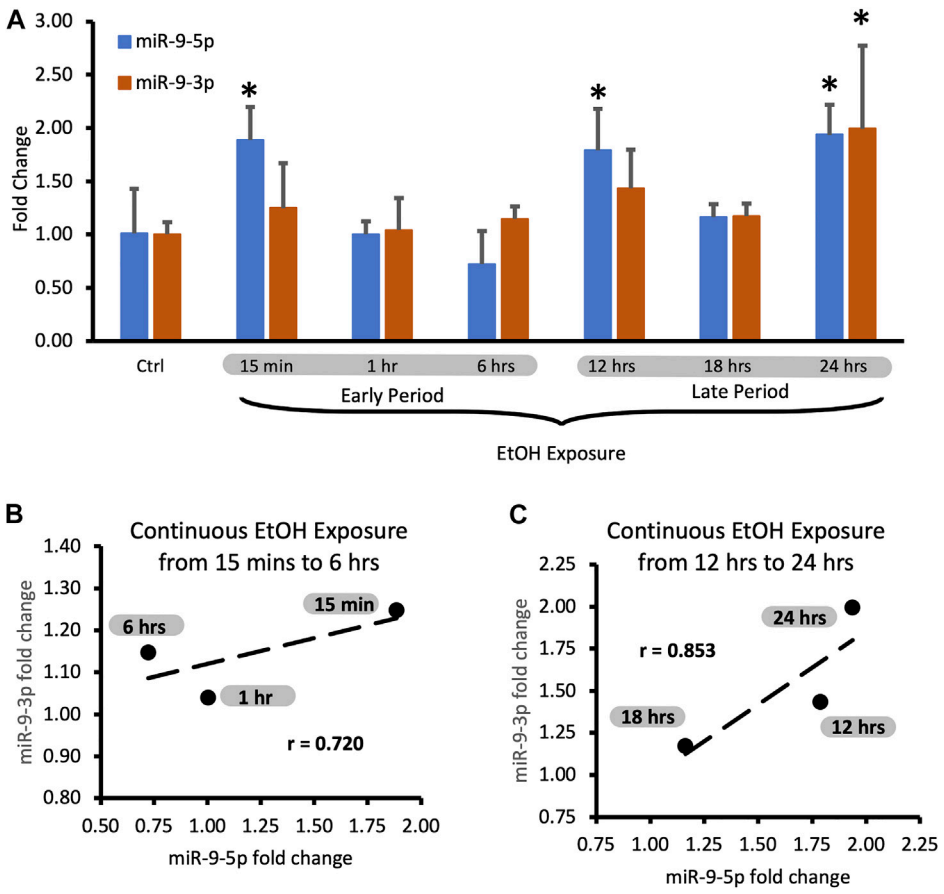

FIGURE 3
Expression levels of miR-9-5p and -3p during continuous, 24-hr long exposure to 20 mM ethanol. **(A)** Temporal expression profile of miR-9-5p (left bars) and miR-9-3p (right bars) measured by Taqman RT-qPCR. Data expressed as mean fold change ± SD. $n = 3$, except $n = 7$ in miR-9-5p control group, $n = 5$ in miR-9-5p control group). Asterisks indicate statistically significant differences comparing to the control, $p < 0.05$. **(B)** Strong, positive correlation of miR-9-5p and miR-9-3p expression levels during the first 6 h of alcohol exposure. The correlation coefficient $r = 0.720$. **(C)** Strong, positive correlation of miR-9-5p and miR-93p expression levels during 12–24 h of alcohol exposure. The correlation coefficient r = 0.853.

TABLE 3 Correlation between expression fold change of miR-9-5p and miR-9-3p during the early period of continuous alcohol exposure.

EtOH ex time [hrs]	miR-9-5p fold change	miR-9-3p fold change	r
0.25	1.89	1.25	0.720
1	1.00	1.04	
6	0.72	1.15	

EtOH ex—ethanol exposure, r—correlation coefficient.

We decided to determine the effects of both, the short and the continuous alcohol exposure, on the expression of all of these precursors.

We observed that the short alcohol exposure (15 min) had no effect on the expression of all three pre-mir-9 precursors (Figure 4A). Expression levels of none of the precursors changed immediately after the alcohol exposure. Since they remained consistently at the same, unchanged level for 6 h following the alcohol withdrawal (Figure 4A) we did not explore further time points.

In contrast, within the same timeframe of the early period of withdrawal, we observed a robust, over 2-fold upregulation of pri-mir-9-2 precursor expression by short alcohol exposure immediately following the exposure (Figure 4B). The pri-mir-9-2 precursor expression upregulation was sustained for at least 6 h after the alcohol withdrawal (Figure 4B). This effect was not observable for the other two pri-precursors: pri-mir-9-1 and the pri-mir-9-3 (Figure 4B).

Overall, it seems that a short, 15 min alcohol exposure elicited changes in the expression of pri-miR-9-2 precursor only and that these changes were quick, robust, and unceasing in alcohol absence.

Regulation of expression of miR-9 precursors by long alcohol exposure

The long (6 h) alcohol exposure affected the expression of both, pre- and pri-mir-9 precursors.

Both, pre-mir-9-1, and pre-mir-9-2 were significantly downregulated after 6 h of alcohol exposure, with pre-mir-9-3 following this trend but not reaching a statistical significance at $p < 0.05$ yet (Figure 5A). Withdrawal of alcohol for 6 h after the 6 hr-long exposure to the drug did not restore expression levels of any of the pre-mir-9 precursors with all of them being decreased. The decreased expressions of all three pre-miR-9 precursors continued in the absence of alcohol for up to 24 h after alcohol withdrawal (Figure 5A).

The effects of the long (6 h) alcohol exposure on the expression levels of pri-miR-9 precursors also affected all of these precursors but each in a different way (Figure 5B). The expression of the pri-mir-9-1 precursor was consistently downregulated to about 50% of its pre-exposure levels, and this downregulation persisted in the absence of alcohol for up to 24 h after alcohol withdrawal (Figure 5B). In contrast, the expression of the remaining two pri-precursors (pri-mir-9-2, pri-mir-9-3) was significantly upregulated by the long (6 h) alcohol exposure to about 1.5-fold above their pre-exposure levels. After alcohol withdrawal, the upregulated levels of both pri-precursors were sustained (Figure 5B). The pri-miR-9-3 precursor maintained its 1.5-fold upregulation at both, 6 h and 24 h after alcohol withdrawal (Figure 5B), while the pri-miR-9-2 precursor expression levels 6 h after alcohol withdrawal went even further up, reaching above 2-fold upregulation, and maintaining their higher expression levels 24 h post-exposure (Figure 5B).

Overall, it seems that longer alcohol exposure elicited wider changes in the expression of miR-9 precursors, affecting the expression of all precursors. Nevertheless, it seems that the miR-9-2 biogenesis pathway responded in the most striking way.

Discussion

Alcohol Use Disorder (AUD) is a very complex disease involving an array of biomolecules, multiple biological

TABLE 4 Correlation between expression fold change of miR-9-5p and miR-9-3p during the late period of continuous alcohol exposure.

EtOH ex time [hrs]	miR-9-5p fold change	miR-9-3p fold change	r
12	1.79	1.43	0.853
18	1.16	1.17	
24	1.94	1.99	

EtOH ex—ethanol exposure, r—correlation coefficient.

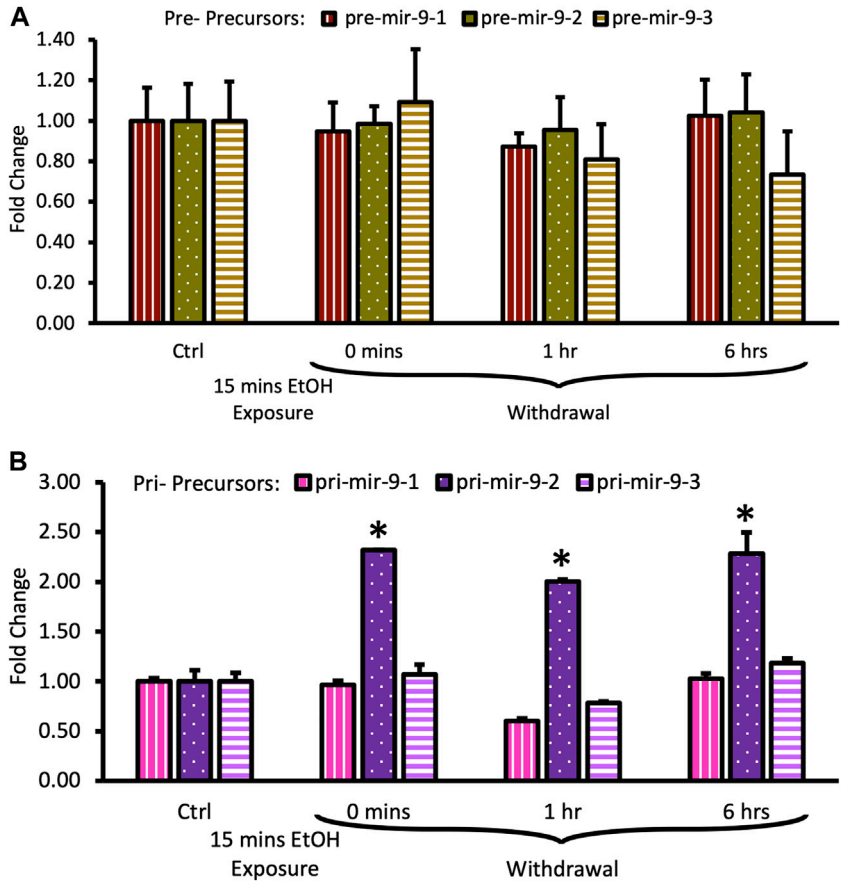

FIGURE 4
Expression levels of pre- and pri-precursors during the first 6 hours of withdrawal after 15 min exposure to 20 mM ethanol. **(A)** Temporal expression profile of pre-mir-9-1 (left bars), pre-mir-9-2 (middle bars), and pre-mir-9-3 (right bars) measured by miScript RT-PCR. **(B)** Temporal expression profile of pri-mir-9-1 (left bars), pri-mir-9-2 (middle bars), and pri-mir-9-3 (right bars) measured by QuantStudio 3D Digital RT-PCR. Data expressed as mean fold change ± SD. $n = 3$ (pre-precursors), $n = 2$ (pri-precursors). Asterisks indicate statistically significant differences comparing to the control, $p < 0.05$.

pathways, and several organismal systems. Time is a fundamental factor of alcohol-triggered changes in the brain's function as the development of AUD is happening progressively over time. We have attempted to shed some light on the temporal regulation of the biogenesis of miR-9, one of the key master regulators of gene expression in the brain [19], which is affected by alcohol in both, brain development [44, 45] and mature brain function [17, 46] and exists in two biologically active forms: miR-9-5p and miR-9-3p. We measured changes of both mature miR-9 forms in murine, primary cell culture consisting of Medium Spiny Neurons (MSN) derived from the Nucleus Accumbens (NAc), which is a part of the brain reward system integrating information from the cortex and subcortical regions [47–49] and highjacked by alcohol in AUD [50]. Alcohol affects the activity of MSN [51], disrupts information integration, and causes behavioral effects [52].

Although during intoxication, neurons in the brain can be exposed to a wide range of alcohol concentrations from around 10 mM to over 100 mM, 20 mM ethanol concentration has a low apoptotic effect [17, 36] yet significant effects on the CNS neurobiology (e.g., ion channel conductivity, neuronal excitability, neuronal network activity), morphology (e.g., synaptic shape and mitochondrial density [53], and behavior (e.g., sedation, motor incoordination, inability to operate motor vehicles, consistent with intoxication) [54]. We reported previously that exposure of the rat neurohypophysial brain explant to 20 mM alcohol for a short time (15 min) caused an upregulation of miR-9-5p expression and observable changes in expression of some of miR-9-5p targets, including the rearrangement of BK channel splice variants consistent with neuroadaptation [17]. Here, we extended our

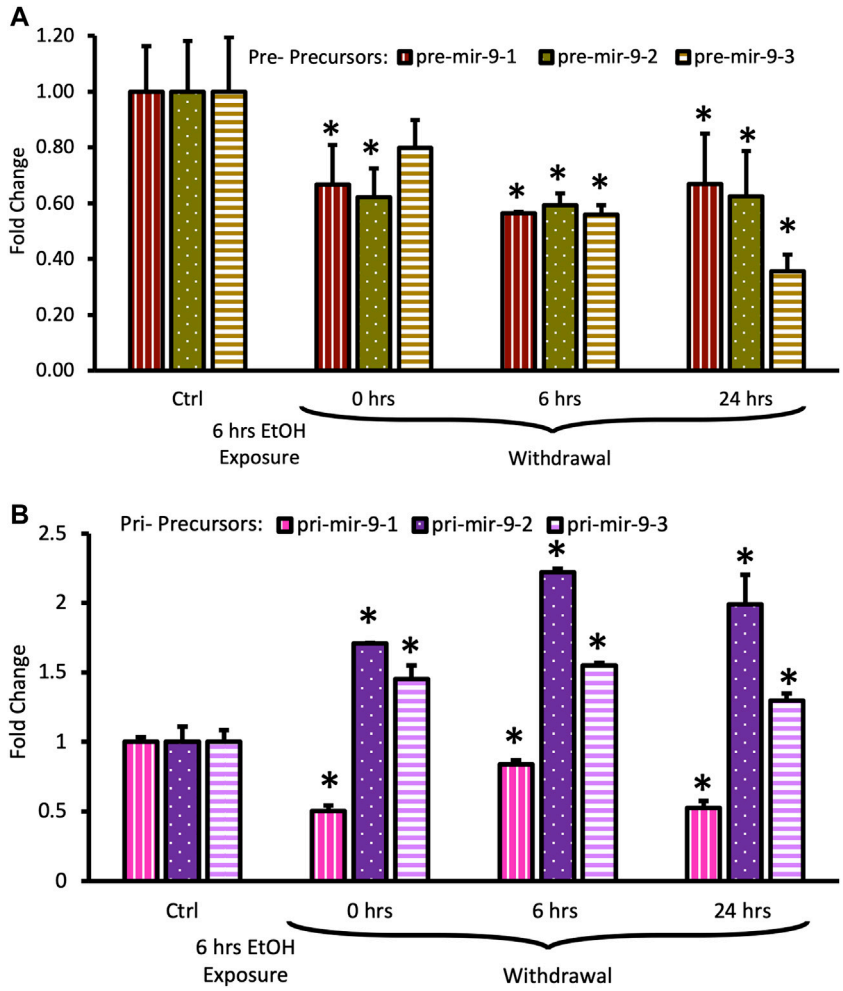

FIGURE 5
Expression levels of pre- and pri-precursors during 24 h withdrawal after 6 h of exposure to 20 mM ethanol. **(A)** Temporal expression profile of pre-mir-9-1 (left bars), pre-mir-9-2 (middle bars), and pre-mir-9-3 (right bars) measured by miScript RT-PCR. **(B)** Temporal expression profile of pri-mir-9-1 (left bars), pri-mir-9-2 (middle bars), and pri-mir-9-3 (right bars) measured by QuantStudio 3D Digital RT-PCR. Data expressed as mean fold change ± SD. $n = 3$ (pre-precursors), $n = 2$ (pri-precursors). Asterisks indicate statistically significant differences comparing to the control, $p < 0.05$.

studies to determine temporal characteristics of miR-9 adaptation to alcohol using murine primary neuronal cultures of medium spiny neurons harvested from the striatum, allowing precise control over alcohol exposure and withdrawal of the pivotal element of the brain reward system.

miR-9-5p homeostatic response to short alcohol exposure and withdrawal

After observing previously the biological effects of a short exposure to 20 mM alcohol [17], we questioned whether the upregulated miR-9-5p levels persist after alcohol withdrawal and for how long. We determined here that the short alcohol exposure triggered changes in miR-9-5p expression observable during withdrawal. These changes could be divided into two, subsequent phases: 1/downregulation below the pre-exposure level, and 2/upregulation to the pre-exposure level. These phases seem to follow a pattern of homeostatic regulation, during which miR-9-5p levels thrown off of the steady state equilibrium by alcohol exposure would undergo changes after alcohol withdrawal to return eventually to the pre-exposure *status quo*. Based on our collection time points we observed that MSN neurons need roughly around 6–12 h of the drug withdrawal to return miR-9-5p levels to normal (i.e., the pre-exposure steady-state equilibrium). It would be of interest, in the next studies, to further narrow down the time window of this homeostatic adaptation.

miR-9-3p upregulation attenuates the effects of the miR-9-5p downregulation

Recently, miR-9-3p, the passenger strand derived from the same duplex as miR-9-5p, gained recognition as biologically active on its own [43, 55]. Martinez et al. [56] showed that chronic ethanol exposure over the course of 55 days elevated miR-9-3p in the serum of rats. Balaraman proposed that the ratio between these two mature microRNAs is important in the regulation of neuronal differentiation and in the development of cancer [57]. Both microRNAs impact the differentiation of neural stem cells through the co-regulation of a transcription factor, REST (RE1 silencing transcription factor/neuron-restrictive silencer factor). miR-9-5p targets REST directly, while miR-9-3p regulates the expression of coREST, a cofactor of REST [42, 57]. Therefore, miR-9-5p and miR-9-3p working in tandem can create various combinations of REST:coREST, thus influencing neuronal differentiation [58, 59].

Our results postulate an even tighter, joint effect of miR-9-5p and miR-9-3p on gene expression. Simultaneous downregulation of miR-9-5p and upregulation of miR-9-3p observed at some points, and their convergence on a large number of targets (425 transcripts, over 34% of miR-9-5p targets) could be a neuronal attempt to attenuate, at least some acute alcohol effects on miR-9-5p targets, consistent with a homeostatic response and preservation of pre-exposure equilibrium. We also would like to propose that any future studies focused on the regulation of miR-9-5p and its targets by alcohol or other factors should include miR-9-3p and its targets as well.

Coordinated miR-9-5p/-3p allostatic response to continuous alcohol exposure

We expected that in the continuous presence of alcohol, upregulated levels of miR-9-5p and miR-9-3p would be maintained. However, that was not the case. We observed that despite the continuous presence of alcohol, both miR-9-5p and miR-9-3p levels followed a response pattern, similar to one observed in a short exposure/withdrawal experiment, which could be also divided into two phases: 1/initial downregulation, 2/subsequent upregulation, with a demarcation line between these two phases happening after 6–12 h of alcohol exposure. Interestingly, the final outcome after 24 h of alcohol exposure was a significant upregulation of both miR-9-5p and miR-9-3p. One could interpret these results as a neuronal adaptation at the molecular level to the continuous presence of alcohol by attempting to set up a new, overcorrected set-point of miR-9-5p and miR-9-3p expression despite the continued presence of the drug. This is consistent with achieving new stability through change—a tenet of allostasis [60, 61] and the allostatic model of addiction [62].

Regulation of miR-9 precursors and biogenesis pathways by alcohol

Since we observed the presence of the initial phase triggered by a short or continuous exposure lasting about 6 h, we decided to determine whether alcohol differently affects upstream elements of the miR-9 biogenesis pathway (precursors) during that window using two scenarios. First, we used this window as a withdrawal window preceded by the short exposure, second, we used it as an exposure window followed by a 24-hour withdrawal period. As we observed no measurable effect on all three miR-9 pre-precursors' expression levels during the first scenario, we concluded that the likelihood of alcohol affecting the steps of microRNA biogenesis responsible for the production of pre-precursors from pri-precursors is rather low. However, in scenario 2, alcohol downregulated all three miR-9 pre-precursors suggesting a possibility that alcohol could interfere with one or some of the steps producing pre-precursors from pri-precursors. Production of microRNA pre-precursors starts with pri-precursors cleavage by the Microprocessor machinery, followed by export from the nucleus to the cytoplasm by the exportin5 complex, and capture by Dicer for further processing by the RISC complex [63]. There are many proteins involved in microRNA biogenesis as each microRNA processing complex consists of several proteins. The microprocessor contains Drosha, DGCR8, RIIa and RIIb proteins, and Exportin-5, a mediator of nuclear export that needs a cofactor RanGTP protein [63], while Dicer works with auxiliary proteins TRBP and members of the Argonaute protein family (AGO) to form the RISC complex [63]. It is possible that some of the regulation of precursors by alcohol reported here is due to an alcohol effect on some of these proteins. Indeed, Mulligan [64] showed an association between Drosha and Dicer expression and response to alcohol, while Prins [65] determined that, in the rat hippocampus, alcohol alters Drosha and Dicer expression (also see 18). Moreover, Gedik [66] reported a genetic association of DGCR8, AGO1, and AGO2 alleles with alcohol dependence risk. It would be of great interest to gain a full picture of alcohol regulation of activity of the key elements of the microRNA biogenesis complexes which process precursors.

In order to better understand the temporal regulation of miR-9 expression by alcohol we should also focus our future efforts on the initial steps of the biogenesis, namely, the production of the miR-9 pri-precursors from their respective genes. Our results revealed that even the short alcohol exposure triggered upregulation of pri-mir-9-2, while longer exposure affected the expression of all three miR-9 pri-precursors. At this point we cannot rule out any mechanisms regulating miR-9 gene expression; however, we suspect epigenetic control of the mir-9-2 gene expression by alcohol. Pappalardo-Carter et al. [67] showed that alcohol increases CpG dinucleotide methylation of the mir-9-2 gene promoter. We believe that

further, comprehensive studies of the epigenetic regulation of all miR-9 genes by alcohol are fully warranted.

Further studies should also shed some light on the differential regulation of miR-9 expression not only by the temporal aspect of alcohol exposure but also by alcohol concentration. Pappalardo-Carter [67] reported that a high alcohol concentration (130 mM) suppressed miR-9 expression, while Tapocik [68] showed that an alcohol concentration of 70 mM inhibited the expression of miR-9, creating a lower steady-state level in alcohol-dependent rats.

AUD is known to have a genetic component [69, 70]. Because human miR-9-1 and miR-9-3 genes are located near or within the AUD susceptibility loci [8], we believe that exploring the differential effects of alcohol on each miR-9 biogenesis pathway is also of great importance in understanding the genetic predisposition to AUD. We would hypothesize that the first response to alcohol exposure is mostly through the mir-9-2 biogenesis pathway. However, with continuous exposure (longer than 6 h) or possibly multiple exposures (mimicking frequent drinking characteristic of the AUD) the mir-9-2 gene may be eventually substantially turned down, with the remaining contribution shifting to mir-9-1 and mir-9-3 genes. As these two genes combined produce less miR-9 than mir-9-2, this hypothesis would explain lower levels of miR-9 observed in chronic alcohol exposure experiments [67, 68]. This hypothesis would also rationalize the presence of miR-9-1 and miR-9-3 genes in the AUD susceptibility loci.

It is worth mentioning that a deeper understanding of alcohol regulation of miR-9 biogenesis would also benefit research focused on cancer and neurodegenerative diseases. Aberrant levels of miR-9 (either miR-9-5p, miR-9-3p, or both) have been reported in many types of cancer [71]: breast cancer [25, 72, 73], Burkitt's Lymphoma [24], hepatocarcinoma [74], prostate cancer [75], gastric cancer [76], colorectal cancer [77], as well as Alzheimer's and Huntington's diseases [78]. Chronic heavy alcohol consumption increases the risk of all of these cancers and neurodegenerative diseases [79–86].

Summary

AUD is a progressive brain disease. Understanding the temporal effects of alcohol on gene expression in neurons is of great importance. Using murine primary cultures of medium spiny neurons, we attempted to deepen our understanding of temporal regulation by alcohol of expression and biogenesis of miR-9-5p and miR-9-3p, key regulators of gene expression. Based on miR-9-5p and miR-9-3p responses to short alcohol exposure, we concluded that changes in expression of these two microRNAs seem to be consistent with the homeostatic model of addiction, while longer, continuous alcohol exposure evoked possibly allostatic changes. Finally, our results point out that the sensitivity of mir-9 genes to alcohol varies among genes and is also time-dependent. The mir-9-2 gene produces pri-mir-9-2 precursor almost immediately after alcohol exposure, while mir-9-1 and mir-9-3 genes need longer exposure to alcohol. Our studies may help us to understand better mechanisms of addiction, carcinogenesis, and neurodegenerative disorders.

Limitations and future directions

There are several limitations to consider when interpreting the results. We used the primary neuronal culture of the medium spiny neurons harvested from young mice pups' striatum. One needs to remember that neurons harvested in such a way are taken away from their natural environment of the whole brain "connected" to the whole animal. To preserve more "natural" conditions we could use brain striatal slices, however, their viability over 24 h is poor; we could also consider using whole animals, however, in this model, it is impossible to precisely control alcohol exposure and withdrawal. Thus, with its inherited limitations, this model provides us with precise control over alcohol exposure and withdrawal, as well as direct access to neurons derived from the striatum - a pivotal element of the reward system, which plays a fundamental role in the development of addiction.

Another limiting factor is that neurons harvested from newborn pups are not mature yet and for about 2 weeks correspond to the final *in utero* period of human development. However, we waited 5 days to harvest the neurons from the striata of P5 pups and then cultivated them on a dish for 8 days before starting alcohol exposure, thus likely passing the period corresponding to the *in utero* human development.

Another factor to remember is that neurons during a few days after plating undergo proliferation on the culture dish. It has been shown in another model that in the proliferating neurons of the retina miR-9 levels (presumably miR-9-5p) oscillate with a rhythmicity of 3 h [87] meaning the expression of miR-9 follows a sinusoid with the same levels observed every 3 hours. This rhythmicity is transient and stabilizes once the neurons mature. Cultivating neurons on a dish for about a week yields mostly mature neurons. However, it is possible that there are some proliferating neurons still present. Since most of our collection time points were multiplications of three, they were in sync with miR-9 oscillations, thus any miR-9 rhythmicity should have a minimal effect. Therefore, by harvesting MSN from the P5 pups and allowing them for a few days to mature before starting alcohol exposure, we think that we were able to circumnavigate at least some of the shortcomings of this model. Future collections with time intervals shorter than 3 h (or not in sync with 3 h) will require though additional controls.

We measured the expression of miR-9 precursors which are products of mir-9 genes and biogenesis machinery but did not directly study the regulation of gene expression or the

machinery activity. Future studies could focus on a systematic approach of determining the alcohol sensitivity of individual elements of microRNA biogenesis (e.g., using antisense oligonucleotides targeting each precursor individually) including temporal characteristics of epigenetic regulation of gene expression by alcohol.

Lastly, we used a single, low-dose alcohol concentration to minimize cellular death. Since higher alcohol concentrations have been shown to also regulate miR-9 expression [67, 68] determination of their effects on miR-9 biogenesis would be of interest.

Data availability statement

The raw data supporting the conclusion of this article will be made available by the authors, without undue reservation.

Ethics statement

The animal study was reviewed and approved the Rutgers Institutional Animal Care and Use Committee (IACUC Protocol # 10-024).

Author contributions

EM, YW, and AZP conceived the idea and planned the experiments; EM, APT, RK, EB-H, VL, and AB performed sample preparations, carried out all experiments except digital PCR experiments, and contributed to the interpretation of the results; EM and YW supervised experiments; SP performed and interpreted digital PCR experiments; EM and AZP interpreted the results and wrote the manuscript; SB and HTS provided critical feedback and contributed to the final version of the manuscript; AZP supervised the project and received grant support. All authors contributed to the article and approved the submitted version.

Funding

This study received funding from NIH-NIAAA grant #AA017920 to AZP.

Acknowledgments

We would like to thank Giles Martin at U. Mass Medical School and Troy Roepke at Rutgers-New Brunswick for assistance with neuron culture protocol development. We would like to thank Jennifer Keefer, Jessica Beck, and Anshul Patel for their assistance with the experiments. We would like to thank Patricia Hegerich for supervising digital PCR experiments during her tenure at Thermo Fisher Scientific Inc. We thank Rutgers Bartlett Hall Animal Care facilities staff for mouse colony maintenance.

Conflict of interest

Author SP was employed by company Thermo Fisher Scientific Inc.

Digital PCR runs (QuantStudio 3D; for research use only, not for use in diagnostic procedures) were conducted by Life Technologies, currently a subsidiary of Thermo Fisher Scientific Inc., as part of an Innovation Grant in the Digital PCR Applications Grant Program awarded to AZP.

Supplementary material

The Supplementary Material for this article can be found online at: https://www.frontierspartnerships.org/articles/10.3389/adar.2023.11323/full#supplementary-material

References

1. World Health Organization (WHO). *Global status report on alcohol and Health* (2018). Available at: https://www.who.int/publications/i/item/9789241565639 (Accessed March 4, 2023).

2. Centers for Disease Control and Prevention (CDC). *Alcohol use and Health* (2012). Available at: http://www.cdc.gov/alcohol/fact-sheets/alcohol-use.htm (Accessed March 3, 2023).

3. National Institutes of Health (NIH), National Institute on Alcohol Abuse and Alcoholism (NIH-NIAAA). *Alcohol facts and statistics* (2021). Available at: https://www.niaaa.nih.gov/publications/brochures-and-fact-sheets/alcohol-facts-andstatistics (Accessed March 4, 2023).

4. Berkel TD, Pandey SC. Emerging role of epigenetic mechanisms in alcohol addiction. *Alcohol Clin Exp Res* (2017) 41(4):666–80. doi:10.1111/acer.13338

5. Farh KK, Grimson A, Jan C, Lewis BP, Johnston WK, Lim LP, et al. The widespread impact of mammalian microRNAs on mRNA repression and evolution. *Science* (2005) 310(5755):1817–21. doi:10.1126/science.1121158

6. Shu J, Silva BVRE, Gao T, Xu Z, Cui J. Dynamic and modularized MicroRNA regulation and its implication in human cancers. *Sci Rep* (2017) 7(1):13356. doi:10.1038/s41598-017-13470-5

7. Wang H, Taguchi YH, Liu X. Editorial: miRNAs and neurological diseases. *Front Neurol* (2021) 12:662373. doi:10.3389/fneur.2021.662373

8. Pietrzykowski AZ. The role of microRNAs in drug addiction: A big lesson from tiny molecules. *Int Rev Neurobiol* (2010) 91:1–24. doi:10.1016/S0074-7742(10)91001-5

9. Smith ACW, Kenny PJ. MicroRNAs regulate synaptic plasticity underlying drug addiction. *Genes Brain Behav* (2018) 17(3):e12424. doi:10.1111/gbb.12424

10. Zhao Y, Qin F, Han S, Li S, Zhao Y, Wang H, et al. MicroRNAs in drug addiction: Current status and future perspectives. *Pharmacol Ther* (2022) 236:108215. doi:10.1016/j.pharmthera.2022.108215

11. Most D, Workman E, Harris RA. Synaptic adaptations by alcohol and drugs of abuse: Changes in microRNA expression and mRNA regulation. *Front Mol Neurosci* (2014) 7:85. doi:10.3389/fnmol.2014.00085

12. Pietrzykowski AZ, Martin GE, Puig SI, Knott TK, Lemos JR, Treistman SN. Alcohol tolerance in large-conductance, calcium-activated potassium channels of CNS terminals is intrinsic and includes two components: Decreased ethanol potentiation and decreased channel density. *J Neurosci* (2004) 24(38):8322–32. doi:10.1523/JNEUROSCI.1536-04.2004

13. Santos-Bezerra DP, Cavaleiro AM, Santos AS, Suemoto CK, Pasqualucci CA, Jacob-Filho W, et al. Alcohol use disorder is associated with upregulation of MicroRNA-34a and MicroRNA-34c in hippocampal postmortem tissue. *Alcohol Clin Exp Res* (2021) 45(1):64–8. doi:10.1111/acer.14505

14. Tsujimura K, Shiohama T, Takahashi E. microRNA biology on brain development and neuroimaging approach. *Brain Sci* (2022) 12(10):1366. doi:10.3390/brainsci12101366

15. Prochnik SE, Rokhsar DS, Aboobaker AA. Evidence for a microRNA expansion in the bilaterian ancestor. *Dev Genes Evol* (2007) 217(1):73–7. doi:10.1007/s00427-006-0116-1

16. Mead EA, Boulghassoul-Pietrzykowska N, Wang Y, Anees O, Kinstlinger NS, Lee M, et al. Non-invasive microRNA profiling in saliva can serve as a biomarker of alcohol exposure and its effects in humans. *Front Genet* (2022) 12:804222. doi:10.3389/fgene.2021.804222

17. Pietrzykowski AZ, Friesen RM, Martin GE, Puig SI, Nowak CL, Wynne PM, et al. Posttranscriptional regulation of BK channel splice variant stability by miR-9 underlies neuroadaptation to alcohol. *Neuron* (2008) 59(2):274–87. doi:10.1016/j.neuron.2008.05.032

18. Miranda RC. MicroRNAs and ethanol toxicity. *Int Rev Neurobiol* (2014) 115:245–84. doi:10.1016/B978-0-12-801311-3.00007-X

19. Coolen M, Katz S, Bally-Cuif L. miR-9: a versatile regulator of neurogenesis. *Front Cel Neurosci* (2013) 7:220. doi:10.3389/fncel.2013.00220

20. Bartel DP. Metazoan MicroRNAs. *Cell* (2018) 173(1):20–51. doi:10.1016/j.cell.2018.03.006

21. Chen X, Zhu L, Ma Z, Sun G, Luo X, Li M, et al. Oncogenic miR-9 is a target of erlotinib in NSCLCs. *Sci Rep* (2015) 5:17031. doi:10.1038/srep17031

22. Ramachandran D, Roy U, Garg S, Ghosh S, Pathak S, Kolthur-Seetharam U. Sirt1 and mir-9 expression is regulated during glucose-stimulated insulin secretion in pancreatic β-islets. *FEBS J* (2011) 278(7):1167–74. doi:10.1111/j.1742-4658.2011.08042.x

23. Wang Y, Dong L, Wan F, Chen F, Liu D, Chen D, et al. MiR-9-3p regulates the biological functions and drug resistance of gemcitabine-treated breast cancer cells and affects tumor growth through targeting MTDH. *Cell Death Dis* (2021) 12(10):861. doi:10.1038/s41419-021-04145-1

24. Onnis A, De Falco G, Antonicelli G, Onorati M, Bellan C, Sherman O, et al. Alteration of microRNAs regulated by c-Myc in Burkitt lymphoma. *PLoS One* (2010) 5(9):e12960. doi:10.1371/journal.pone.0012960

25. Zawistowski JS, Nakamura K, Parker JS, Granger DA, Golitz BT, Johnson GL. MicroRNA 9-3p targets β1 integrin to sensitize claudin-low breast cancer cells to MEK inhibition. *Mol Cel Biol* (2013) 33(11):2260–74. doi:10.1128/MCB.00269-13

26. Sim SE, Lim CS, Kim JI, Seo D, Chun H, Yu NK, et al. The brain-enriched MicroRNA miR-9-3p regulates synaptic plasticity and memory. *J Neurosci* (2016) 36(33):8641–52. doi:10.1523/JNEUROSCI.0630-16.2016

27. Tepper JM, Bolam JP. Functional diversity and specificity of neostriatal interneurons. *Curr Opin Neurobiol* (2004) 14(6):685–92. doi:10.1016/j.conb.2004.10.003

28. García-González D, Dumitru I, Zuccotti A, Yen TY, Herranz-Pérez V, Tan LL, et al. Neurogenesis of medium spiny neurons in the nucleus accumbens continues into adulthood and is enhanced by pathological pain. *Mol Psychiatry* (2021) 26(9):4616–32. doi:10.1038/s41380-020-0823-4

29. Ventimiglia R, Lindsay RM. Rat striatal neurons in low-density, serum-free culture. In: Goslin GBAK, editor. *Culturing nerve cells*. Cambridge, MA: MIT Press (1998). p. 371–93.

30. Misonou H, Trimmer JS. Determinants of voltage-gated potassium channel surface expression and localization in Mammalian neurons. *Crit Rev Biochem Mol Biol* (2004) 39(3):125–45. doi:10.1080/10409230490475417

31. Leveque JC, Macias W, Rajadhyaksha A, Carlson RR, Barczak A, Kang S, et al. Intracellular modulation of NMDA receptor function by antipsychotic drugs. *J Neurosci* (2000) 20(11):4011–20. doi:10.1523/JNEUROSCI.20-11-04011.2000

32. Franklin KBJ, Paxinos G. *The mouse brain in stereotaxic coordinates*, 3rd ed. San Diego: Academic Press (2008). p. 351.

33. Ljungman M. The transcription stress response. *Cell Cycle* (2007) 6(18):2252–7. doi:10.4161/cc.6.18.4751

34. Mao Y, Tamura T, Yuki Y, Abe D, Tamada Y, Imoto S, et al. The hnRNP-Htt axis regulates necrotic cell death induced by transcriptional repression through impaired RNA splicing. *Cel Death Dis* (2016) 7(4):e2207. doi:10.1038/cddis.2016.101

35. Calculator.net. *Blood alcohol concentration (BAC) calculator* (2023). Available at: https://www.calculator.net/bac-calculator.html (Accesed January 15, 2023).

36. Aydin Sinirlioğlu Z, Akbaş F. Differential expression of BDNF, MiR-206, and MiR-9 under the chronic ethanol exposure and its withdrawal. *Sigma J Eng Nat Sci* (2016) 34(2):191–6.

37. Iguchi T, Niino N, Tamai S, Sakurai K, Mori K. Absolute quantification of plasma microRNA levels in cynomolgus monkeys, using quantitative real-time Reverse transcription PCR. *J Vis Exp* (2018) 132:56850. doi:10.3791/56850

38. Arabkari V, Clancy E, Dwyer RM, Kerin MJ, Kalinina O, Holian E, et al. Relative and absolute expression analysis of microRNAs associated with luminal A breast cancer – a comparison. *Pathol Oncol Res* (2020) 26:833–44. doi:10.1007/s12253-019-00627-y

39. Wang J, Jiang D, Rao H, Zhao J, Wang Y, Wei L. Absolute quantification of serum microRNA-122 and its correlation with liver inflammation grade and serum alanine aminotransferase in chronic hepatitis C patients. *Int J Infect Dis* (2015) 30:52–6. doi:10.1016/j.ijid.2014.09.020

40. Wang LL, Zhang Z, Li Q, Yang R, Pei X, Xu Y, et al. Ethanol exposure induces differential microRNA and target gene expression and teratogenic effects which can be suppressed by folic acid supplementation. *Hum Reprod* (2009) 24(3):562–79. doi:10.1093/humrep/den439

41. Burrowes SG, Salem NA, Tseng AM, Balaraman S, Pinson MR, Garcia C, et al. The BAF (BRG1/BRM-Associated Factor) chromatin-remodeling complex exhibits ethanol sensitivity in fetal neural progenitor cells and regulates transcription at the miR-9-2 encoding gene locus. *Alcohol* (2017) 60:149–58. doi:10.1016/j.alcohol.2017.01.003

42. Packer AN, Xing Y, Harper SQ, Jones L, Davidson BL. The bifunctional microRNA miR-9/miR-9* regulates REST and CoREST and is downregulated in Huntington's disease. *J Neurosci* (2008) 28(53):14341–6. doi:10.1523/JNEUROSCI.2390-08.2008

43. Roese-Koerner B, Stappert L, Berger T, Braun NC, Veltel M, Jungverdorben J, et al. Reciprocal regulation between bifunctional miR-9/9(*) and its transcriptional modulator notch in human neural stem cell self-renewal and differentiation. *Stem Cel Rep* (2016) 7(2):207–19. doi:10.1016/j.stemcr.2016.06.008

44. Miranda RC, Pietrzykowski AZ, Tang Y, Sathyan P, Mayfield D, Keshavarzian A, et al. MicroRNAs: Master regulators of ethanol abuse and toxicity? *Alcohol Clin Exp Res* (2010) 34(4):575–87. doi:10.1111/j.1530-0277.2009.01126.x

45. Radhakrishnan B, Alwin Prem Anand A. Role of miRNA-9 in brain development. *J Exp Neurosci* (2016) 10:101–20. doi:10.4137/JEN.S32843

46. Kim CK, Asimes A, Zhang M, Son BT, Kirk JA, Pak TR. Differential stability of miR-9-5p and miR-9-3p in the brain is determined by their unique cis- and trans-acting elements. *eNeuro* (2020) 7(3):ENEURO0094-20. doi:10.1523/ENEURO.0094-20.2020

47. Humphries MD, Prescott TJ. The ventral basal ganglia, a selection mechanism at the crossroads of space, strategy, and reward. *Prog Neurobiol* (2010) 90:385–417. doi:10.1016/j.pneurobio.2009.11.003

48. Wassum KM, Izquierdo A. The basolateral amygdala in reward learning and addiction. *Neurosci Biobehav Rev* (2015) 57:271–83. doi:10.1016/j.neubiorev.2015.08.017

49. Klenowski PM. Emerging role for the medial prefrontal cortex in alcohol-seeking behaviors. *Addict Behav* (2018) 77:102–6. doi:10.1016/j.addbeh.2017.09.024

50. Fritz M, Klawonn AM, Zahr NM. Neuroimaging in alcohol use disorder: From mouse to man. *J Neuro Res* (2022) 100:1140–58. doi:10.1002/jnr.24423

51. Marty VN, Spigelman I. Effects of alcohol on the membrane excitability and synaptic transmission of medium spiny neurons in the nucleus accumbens. *Alcohol* (2012) 46(4):317–27. doi:10.1016/j.alcohol.2011.12.002

52. Kolpakova J, van der Vinne V, Giménez-Gómez P, Le T, You IJ, Zhao-Shea R, et al. Binge alcohol drinking alters synaptic processing of executive and emotional information in core nucleus accumbens medium spiny neurons. *Front Cel Neuro* (2021) 15:742207. doi:10.3389/fncel.2021.742207

53. Knabbe J, Protzmann J, Schneider N, Berger M, Dannehl D, Wei S, et al. Single-dose ethanol intoxication causes acute and lasting neuronal changes in the brain. *Proc Natl Acad Sci U S A* (2022) 119(25):e2122477119. doi:10.1073/pnas.2122477119

54. Harrison NL, Skelly MJ, Grosserode EK, Lowes DC, Zeric T, Phister S, et al. Effects of acute alcohol on excitability in the CNS. *Neuropharm* (2017) 122:36–45. doi:10.1016/j.neuropharm.2017.04.007

55. Xue Q, Yu C, Wang Y, Liu L, Zhang K, Fang C, et al. miR-9 and miR-124 synergistically affect regulation of dendritic branching via the AKT/GSK3β pathway by targeting Rap2a. *Sci Rep* (2016) 6:26781. doi:10.1038/srep26781

56. Martinez M, Rossetto IMU, Arantes RMS, Lizarte FSN, Tirapelli LF, Tirapelli DPC, et al. Serum miRNAs are differentially altered by ethanol and caffeine consumption in rats. *Toxicol Res (Camb)* (2019) 8(6):842–9. doi:10.1039/c9tx00069k

57. Balaraman S, Tingling JD, Tsai PC, Miranda RC. Dysregulation of microRNA expression and function contributes to the etiology of fetal alcohol spectrum disorders. *Alcohol Res* (2013) 35(1):18–24.

58. Abrajano JJ, Qureshi IA, Gokhan S, Zheng D, Bergman A, Mehler MF. REST and CoREST modulate neuronal subtype specification, maturation and maintenance. *PLoS One* (2009) 4(12):e7936. doi:10.1371/journal.pone.0007936

59. Abrajano JJ, Qureshi IA, Gokhan S, Molero AE, Zheng D, Bergman A, et al. Corepressor for element-1-silencing transcription factor preferentially mediates gene networks underlying neural stem cell fate decisions. *Proc Natl Acad Sci U S A* (2010) 107(38):16685–90. doi:10.1073/pnas.0906917107

60. Sterling P, Eyer J. Allostasis: A new paradigm to explain arousal pathology. In: Fisher S, Reason J, editors. *Handbook of life stress, cognition and health*. New York: John Wiley & Sons (1988). p. 629–49.

61. Ramsay DS, Woods SC. Clarifying the roles of homeostasis and allostasis in physiological regulation. *Psychol Rev* (2014) 121(2):225–47. doi:10.1037/a0035942

62. Koob GF, Moal ML. Drug addiction and allostasis. In: Schulkin J, editor. *Allostasis, homeostasis, and the costs of physiological adaptation*. Cambridge: Cambridge University Press (2004). p. 150–63.

63. Bushati N, Cohen SM. microRNA functions. *Annu Rev Cel Dev Biol* (2007) 23:175–205. doi:10.1146/annurev.cellbio.23.090506.123406

64. Mulligan MK, Dubose C, Yue J, Miles MF, Lu L, Hamre KM. Expression, covariation, and genetic regulation of miRNA Biogenesis genes in brain supports their role in addiction, psychiatric disorders, and disease. *Front Genet* (2013) 4:126. doi:10.3389/fgene.2013.00126

65. Prins SA, Przybycien-Szymanska MM, Rao YS, Pak TR. Long-term effects of peripubertal binge EtOH exposure on hippocampal microRNA expression in the rat. *PLoS One* (2014) 9(1):e83166. doi:10.1371/journal.pone.0083166

66. Gedik H, Erdal ME, Yilmaz SG, Sengul C, Sengul CB, Herken H. Association of microRNA biogenesis pathway gene variants and alcohol dependence risk. *DNA Cel Biol* (2015) 34(3):220–6. doi:10.1089/dna.2014.2549

67. Pappalardo-Carter DL, Balaraman S, Sathyan P, Carter ES, Chen WJ, Miranda RC. Suppression and epigenetic regulation of MiR-9 contributes to ethanol teratology: Evidence from zebrafish and murine fetal neural stem cell models. *Alcohol Clin Exp Res* (2013) 37(10):1657–67. doi:10.1111/acer.12139

68. Tapocik JD, Solomon M, Flanigan M, Meinhardt M, Barbier E, Schank JR, et al. Coordinated dysregulation of mRNAs and microRNAs in the rat medial prefrontal cortex following a history of alcohol dependence. *Pharmacogenomics J* (2013) 13(3):286–96. doi:10.1038/tpj.2012.17

69. Chen J, Hutchison KE, Bryan AD, Filbey FM, Calhoun VD, Claus ED, et al. Opposite epigenetic associations with alcohol use and exercise intervention. *Front Psychiatry* (2018) 9:594. doi:10.3389/fpsyt.2018.00594

70. Luo A, Jung J, Longley M, Rosoff DB, Charlet K, Muench C, et al. Epigenetic aging is accelerated in alcohol use disorder and regulated by genetic variation in APOL2. *Neuropsychopharm* (2020) 45(2):327–36. doi:10.1038/s41386-019-0500-y

71. Khafaei M, Rezaie E, Mohammadi A, Shahnazi Gerdehsang P, Ghavidel S, Kadkhoda S, et al. miR-9: From function to therapeutic potential in cancer. *J Cel Physiol* (2019) 234(9):14651–65. doi:10.1002/jcp.28210

72. Ma L, Young J, Prabhala H, Pan E, Mestdagh P, Muth D, et al. miR-9, a MYC/MYCN activated microRNA, regulates E-cadherin and cancer metastasis. *Nat Cel Biol* (2010) 12(3):247–56. doi:10.1038/ncb2024

73. Khew-Goodall Y, Goodall GJ. Myc-modulated miR-9 makes more metastases. *Nat Cel Biol* (2010) 12(3):209–11. doi:10.1038/ncb0310-209

74. Zhang Y, Wei C, Guo CC, Bi RX, Xie J, Guan DH, et al. Prognostic value of microRNAs in hepatocellular carcinoma: A meta-analysis. *Oncotarget* (2017) 8(63):107237–57. doi:10.18632/oncotarget.20883

75. Sang Z, Jiang X, Guo L, Yin G. MicroRNA-9 suppresses human prostate cancer cell viability, invasion and migration via modulation of mitogen-activated protein kinase kinase kinase 3 expression. *Mol Med Rep* (2019) 19(5):4407–18. doi:10.3892/mmr.2019.10065

76. Hang C, Yan HS, Gong C, Gao H, Mao QH, Zhu JX. MicroRNA-9 inhibits gastric cancer cell proliferation and migration by targeting neuropilin-1. *Exp Ther Med* (2019) 18(4):2524–30. doi:10.3892/etm.2019.7841

77. Bahrami A, Jafari A, Ferns GA. The dual role of microRNA-9 in gastrointestinal cancers: oncomiR or tumor suppressor? *Biomed Pharmacother* (2022) 145:112394. doi:10.1016/j.biopha.2021.112394

78. Wang S, Jiang G, Wang S. Neuroprotective role of MiRNA-9 in neurological diseases: A mini review. *Curr Mol Med* (2022) 23. doi:10.2174/1566524023666221025123132

79. Wong AW, Paulson QX, Hong J, Stubbins RE, Poh K, Schrader E, et al. Alcohol promotes breast cancer cell invasion by regulating the Nm23-ITGA5 pathway. *J Exp Clin Cancer Res* (2011) 30(1):75. doi:10.1186/1756-9966-30-75

80. Morch LS, Johansen D, Thygesen LC, Tjonneland A, Lokkegaard E, Stahlberg C, et al. Alcohol drinking, consumption patterns and breast cancer among Danish nurses: A cohort study. *Eur J Pub Health* (2007) 17(6):624–9. doi:10.1093/eurpub/ckm036

81. Testino G, Leone S, Borro P. Alcohol and hepatocellular carcinoma: A review and a point of view. *World J Gastroenterol* (2014) 20(43):15943–54. doi:10.3748/wjg.v20.i43.15943

82. Macke AJ, Petrosyan A. Alcohol and prostate cancer: Time to draw conclusions. *Biomolecules* (2022) 12(3):375. doi:10.3390/biom12030375

83. Li BY, Li HY, Zhou DD, Huang SY, Luo M, Gan RY, et al. Effects of different green tea extracts on chronic alcohol induced-fatty liver disease by ameliorating oxidative stress and inflammation in mice. *Oxid Med Cel Longev* (2021) 2021:5188205. doi:10.1155/2021/5188205

84. Dashti SG, Win AK, Hardikar SS, Glombicki SE, Mallenahalli S, Thirumurthi S, et al. Physical activity and the risk of colorectal cancer in Lynch syndrome. *Int J Cancer* (2018) 143(9):2250–60. doi:10.1002/ijc.31611

85. Peng B, Yang Q, B Joshi R, Liu Y, Akbar M, Song BJ, et al. Role of alcohol drinking in alzheimer's disease, Parkinson's disease, and amyotrophic lateral sclerosis. *Int J Mol Sci* (2020) 21(7):2316. doi:10.3390/ijms21072316

86. Byars JA, Beglinger LJ, Moser DJ, Gonzalez-Alegre P, Nopoulos P. Substance abuse may be a risk factor for earlier onset of Huntington disease. *J Neurol* (2012) 259(9):1824–31. doi:10.1007/s00415-012-6415-8

87. Fishman ES, Han JS, La Torre A. Oscillatory behaviors of microRNA networks: Emerging roles in retinal development. *Front Cel Dev Biol* (2022) 10:831750. doi:10.3389/fcell.2022.831750

Citation: Mead EA, Wang Y, Patel S, Thekkumthala AP, Kepich R, Benn-Hirsch E, Lee V, Basaly A, Bergeson S, Siegelmann HT and Pietrzykowski AZ (2023) miR-9 utilizes precursor pathways in adaptation to alcohol in mouse striatal neurons. Adv. Drug Alcohol Res. 3:11323. doi: 10.3389/adar.2023.11323

ADAR | Publishing Partnerships

TYPE Brief Research Report
PUBLISHED 14 August 2023
DOI 10.3389/adar.2023.11668

OPEN ACCESS

EDITED BY
Emmanuel Onaivi,
William Paterson University,
United States

REVIEWED BY
Pierre-Eric Lutz,
Centre National de la Recherche Scientifique (CNRS), France
Gregory C. Sartor,
University of Connecticut, United States

*CORRESPONDENCE
Stephanie E. Sillivan,
stephanie.sillivan@temple.edu

RECEIVED 09 June 2023
ACCEPTED 28 July 2023
PUBLISHED 14 August 2023

CITATION
Zanda MT, Saikali L, Morris P and Sillivan SE (2023), MicroRNA-mediated translational pathways are regulated in the orbitofrontal cortex and peripheral blood samples during acute abstinence from heroin self-administration. *Adv. Drug Alcohol Res.* 3:11668. doi: 10.3389/adar.2023.11668

MicroRNA-mediated translational pathways are regulated in the orbitofrontal cortex and peripheral blood samples during acute abstinence from heroin self-administration

Mary Tresa Zanda[1,2], Leila Saikali[1,3], Paige Morris[1,2] and Stephanie E. Sillivan[1,2]*

[1]Center for Substance Abuse Research, Temple University, Philadelphia, PA, United States, [2]Department of Neural Sciences, Temple University, Philadelphia, PA, United States, [3]College of Liberal Arts, Temple University, Philadelphia, PA, United States

Opioid misuse in the United States contributes to >70% of annual overdose deaths. To develop additional therapeutics that may prevent opioid misuse, further studies on the neurobiological consequences of opioid exposure are needed. Here we sought to characterize molecular neuroadaptations involving microRNA (miRNA) pathways in the brain and blood of adult male rats that self-administered the opioid heroin. miRNAs are ~18–24 nucleotide RNAs that regulate protein expression by preventing mRNA translation into proteins. Manipulation of miRNAs and their downstream pathways can critically regulate drug seeking behavior. We performed small-RNA sequencing of miRNAs and proteomics profiling on tissue from the orbitofrontal cortex (OFC), a brain region associated with heroin seeking, following 2 days of forced abstinence from self-administration of 0.03 mg/kg/infusion heroin or sucrose. Heroin self-administration resulted in a robust shift of the OFC miRNA profile, regulating 77 miRNAs, while sucrose self-administration only regulated 9 miRNAs that did not overlap with the heroin-induced profile. Conversely, proteomics revealed dual regulation of seven proteins by both heroin and sucrose in the OFC. Pathway analysis determined that heroin-associated miRNA pathways are predicted to target genes associated with the term "prion disease," a term that was also enriched in the heroin-induced protein expression dataset. Lastly, we confirmed that a subset of heroin-induced miRNA expression changes in the OFC are regulated in peripheral serum and correlate with heroin infusions. These findings demonstrate that peripheral blood samples may have biomarker utility for assessment of drug-induced miRNA pathway alterations that occur in the brain following chronic drug exposure.

KEYWORDS

microRNA, heroin, opioid, biomarker, self-administration

Introduction

Misuse of opioid drugs is associated with a high risk of overdose death [1]. A drastic increase in the incidence of misuse and overdose of opioids has occurred in the United States over the past two decades [2] and represents a major public health concern. In 2021, opioids were involved in more than 70% of the 100,000+ overdose deaths that occurred in the United States [3]. These epidemiological patterns emphasize that critical efforts are required to reduce drug overdose deaths and aid in maintenance of abstinence behavior from opioid use. Because many patients recovering from opioid use disorder (OUD) continue to experience motivation to seek opioids, despite abstinence or FDA-approved OUD medications [4, 5], elucidation of the molecular signaling patterns in the drug-free period following cessation of drug use may provide insight into the pathways that can be targeted for reduction of drug seeking behavior.

Rodent models of drug self-administration provide an excellent tool to model drug seeking behavior and interrogate the molecular neuroadaptations that arise in discrete brain areas following chronic drug exposure. Previous studies from our labs and others have demonstrated that chronic self-administration of opioids, such as morphine or heroin, induces drug seeking behavior that is both immediate and long lasting in the absence of drug access [6–9]. Such behaviors are accompanied by regulation of a class of small noncoding RNAs called microRNAs (miRNAs) that are ~18–24 nucleotides long [10]. miRNAs can regulate gene expression by inhibiting translation of a "target" mRNA to protein [10]. The short sequence of miRNAs allows them to accomplish this process by binding to the 3′-UTR of a target mRNA with sequence complementarity and inducing deadenylation of poly-A mRNA [10]. miRNAs bind to their targets within a short 6–8 nucleotide "seed" region, which theoretically permits an individual miRNA to target 100s, even 1000s of mRNA sequences [11]. Because of this, miRNA-mediated inhibition of protein translation is an essential regulatory mechanism for modulation of gene expression and the proteome [11]. Exposure to all classes of drugs can induce long-lasting alterations to brain miRNA expression profiles and regulation of miRNA function can modulate drug seeking behavior [7, 12–24]. Manipulation of individual miRNA expression or functional capabilities has been reported to regulate seeking for the opioids morphine and heroin, as well as psychostimulants and alcohol [14, 17, 20, 21, 23, 24]. In our recent publication, we reported the regulation of miRNAs and their associated downstream proteins in the orbitofrontal cortex (OFC) of rats following late abstinence (21 days) from self-administration of two heroin dose, 0.03 mg/kg/infusion or 0.075 mg/kg/infusion [24]. OFC-specific manipulation of the heroin-associated miRNA miR-485-5p resulted in regulation of long-lasting heroin seeking behavior [24]. The OFC has been identified as a key brain region that is active during incubation of heroin craving [25] and humans that have used heroin chronically display elevated blood flow to the OFC in imaging studies during a craving experience [26].

More than 700 miRNAs have been detected in the rodent brain [27], yet, less than <1% of brain-derived miRNAs have been explored to determine their association with drug seeking. Moreover, investigation of miRNA expression in serum exosomes derived from peripheral blood represents an intriguing avenue for biomarkers associated with drug craving. However, the profile of miRNAs in discrete brain regions has not been compared to blood miRNAs levels following heroin exposure, nor have blood miRNA levels been correlated to opioid seeking behavior. Thus, identifying miRNAs and their associated downstream protein pathways that are regulated in the brain as a result of chronic opioid exposure represents a novel strategy for determining previously understudied mechanisms that may have therapeutic relevance for the reduction of opioid seeking in OUD. Brain-region specific and drug dose-dependent regulation of miRNAs occurs [7], which necessitates the need to uncover the miRNA profile that results following a wide range of drug exposure protocols. In the present study, we have begun addressing these critical issues by performing small RNA sequencing of miRNAs and protein profiling on the OFC of rats that self-administered heroin at a dose of 0.03 mg/kg/infusion and underwent forced abstinence for 2 days (early abstinence). We chose to study miRNAs associated with heroin seeking behavior due to the association of miRNA expression with heroin dependence in human subjects [28–32]. Our results have uncovered a unique profile of drug-specific and sucrose-specific OFC miRNA and protein regulation in the acute abstinence period. We report select blood miRNA patterns may be robustly responsive to heroin self-administration and provide insight into drug-induced miRNA expression that has utility for biomarker measurement of heroin-taking behavior.

Methods

Subjects

35 adult male Sprague Dawley rats (Charles River) were used in this study. Rats were ~240 g and 8 weeks old on arrival. All animals were pair-housed on a reverse light/dark cycle and provided food *ad libitum*, except where noted. Animals were acclimated to the facility for at least 5 days prior to beginning behavioral testing. All procedures were approved by Temple University's Institutional Animal Care and Use Committee and followed the National Institute of Health's Guide for the Care and Use of Laboratory Animals.

Reagents

Heroin hydrochloride was obtained from the NIDA Drug Supply Program and dissolved in 0.9% sterile saline. 45 mg

chocolate-flavored sucrose pellets were obtained from Bio-Serv (Flemington, NJ, USA).

Self-administration

Self-administration of 0.03 mg/kg/infusion heroin and sucrose on an FR1 schedule was performed as previously reported [6, 24, 33]. Self-administration data for heroin animals was previously reported [24]. Drug-naïve animals were handled daily but did not undergo self-administration of any substance. 48-hours after the last heroin or sucrose session, animals were euthanized with 5% isoflurane and rapidly decapitated. Brains were immediately frozen in ice-cold liquid isopentane on dry ice and stored at −80°C until dissection.

Blood & serum collection

Trunk blood was collected immediately following decapitation into 50 mL tubes and stored +4°C for ~12 h. Following coagulation, blood was centrifuged at 2,000 rpm for 10 min. The serum supernatant was collected and stored at −80°C until RNA extraction.

RNA extraction

Bilateral tissue punches of the OFC were collected from each animal. The regions of the OFC dissected were the ventral OFC and lateral OFC subregions. For extraction of total RNA from OFC tissue, the miRVANA PARIS RNA extraction kit (Life Technologies, Carlsbad, CA) was used, as we have previously reported [7, 24, 34]. Exosomal RNA was extracted from blood serum using the SeraMir Exosome RNA Amplification Kit (System Biosciences, Palo Alto, CA), according to the manufacturer's instructions.

Small-RNA sequencing

Library preparation and small-RNA sequencing of miRNAs was performed on individual biological replicate samples, 4 per group, by BGI Genomics (BGI Americas Corp, Cambridge, MA, United States), as we have previously described [24]. Briefly, RNA integrity >7.5 and 28S/18S>1.3 for each sample was confirmed with Bioanalyzer prior to library preparation. Small RNAs were size selected by PAGE gel, ligated with 3′ and 5′ adaptors and reverse transcribed to cDNA for PCR amplification with high-ping polymerase. Following PAGE gel separation, PCR products were purified and quantified by single strand DNA cyclization then DNA nanoballs were by rolling circle replication. DNA nanoballs were sequenced on the BGISEQ-500 and raw sequencing reads were filtered to yield clean reads without contamination. Clean reads were aligned to the reference genome with Bowtie2 [35]. The small-RNA seq yielded approximately 40 million reads per sample. Small RNA expression was calculated as transcripts per kilobase million (TPM). The open-access software miRPATH from DIANA was used to predict putative pathways of target genes impacted by heroin- or sucrose-associated miRNAs [36]. Raw sequencing data are available in the SRA and Gene Expression Omnibus repositories (Accession # PRJNA949640 and GSE237409). A list of OFC miRNA statistics between heroin, sucrose and naïve animals can be found in Supplementary Tables SE1–SE3.

Proteomics

For proteomic profiling of OFC proteins following heroin or sucrose self-administration, dissected OFC tissue punches were obtained from 2 to 3 individual animals per group and submitted to the Core Research Facility at Yale University. Samples were processed and differential proteins were calculated, as we have previously reported [24]. Briefly, chloroform-methanol precipitation, dual enzymatic digestion with lysine and trypsin, acidification with 20% trifluoroacetic acid and desalting were performed on protein tissue samples prior to Label-Free Quantification with an Orbitrap Fusion Mass Spectrophotometer (ThermoFisher Scientific). Only proteins that were present in all samples were considered for comparison between two groups. KEGG pathway analysis of differentially regulated proteins between two comparisons were performed using DAVID (NIH) [37, 38]. Lists of protein expression values for and statistics of differentially expressed proteins between heroin, sucrose or drug-naïve animals is available in Supplementary Tables SE4–SE7. For overlap of miRNA data with proteomics, the microTCDS software from DIANA was used to identify putative targets of the heroin-regulated miRNAs [39].

qPCR analysis

For measurement of serum miRNAs with qPCR, 20 ng of RNA was reverse transcribed into cDNA using the miRCURY LNA RT KIT (Qiagen), according to the manufacturer's instructions, as we have previously reported [7, 24]. cDNA was diluted 1:60 and used as a template for qPCR with the miRCURY LNA SYBR Green PCR Kit (Qiagen) and the following LNA miRCURY SYBR green assays (Qiagen): rno-miR-877-5p (Assay ID: YP00205626); rno-miR-376a-3p (Assay ID: YP00205059); rno-miR-29c-3p (Assay ID: YP00204729); rno-miR-379-5p (Assay ID: YP00205658); rno-miR-186-5p (Assay ID: YP00206053); rno-miR-107-3p (Assay ID:

YP00204468); rno-miR-219a-5p (Assay ID: YP00204780); rno-miR-451-5p (Assay ID: YP02119305); rno-miR-135a-5p (Assay ID: YP00204762); rno-miR-218b (Assay ID: YP02101069). rno-miR-320-3p (Assay ID: YP00206042) and rno-mir-191a-5p (Assay ID: YP00204306) were used as endogenous control genes because they were not regulated in the small-RNA sequencing analysis. Expression levels were calculated using $2^{-\Delta\Delta CT}$ method [40].

Statistical analysis

Two-tailed Mann-Whitney tests were used to confirm a significant preference of the reward-paired active lever during self-administration, compared to the inactive lever. For small-RNA sequencing, DEseq2 [41] was used to determine miRNAs differentially expressed between two groups, with the Benjamini and Hochberg method applied to correct for multiple comparisons [42]. miRNAs were considered statistically significant if the adjusted *p*-value between two groups was <0.05. For proteomics and miRNA qPCR, unpaired t-tests were used to determine differentially expressed proteins or miRNAs between treatment groups with normal distribution, with $p < 0.05$ considered significant. Two-tailed Mann-Whitney tests were used to compare miRNA expression when data was not normally distributed. Shapiro-Wilk normality tests were used to determine the distribution of data. Outliers were defined as values exceeding the mean by >2.5 times the standard deviation. Pearson correlations were used to compare the relationship between miRNA expression and drug-seeking behavior. All statistical analyses were performed using Graphpad Prism (Prism version 9, San Diego, CA, USA).

Results

Our lab and others have demonstrated that self-administration of 0.03 mg/kg/infusion of heroin results in perseverant heroin-seeking behavior [6, 43], defined as a significant preference for the active, drug-paired lever compared to the inactive lever during cue-induced relapse sessions. Furthermore, such a protocol induces biochemical changes in the brain that recapitulate heroin-induced neuroadaptations observed in human subjects [43–46]. We sought to further characterize the neurobiological consequences of heroin self-administration at this dose by profiling miRNAs and proteins in the OFC, a brain region critical for opioid-seeking behavior [24, 25, 47, 48]. Results were compared to a separate group of rats that only self-administered sucrose pellets. Adult male Sprague Dawley rats self-administered heroin or sucrose pellets on an FR1 schedule for 10 days (Figure 1A). Rats in both heroin and sucrose groups demonstrated a significant preference for the active reward-paired lever compared to an inactive lever (Mann-Whitney test, heroin: $U = 6$, $p < 0.0001$; sucrose: $U = 0$, $p < 0.0001$; Figure 1B). Two days after the last self-administration session, animals were euthanized for small-RNA sequencing of OFC miRNAs or proteomic analysis of OFC proteins. Self-administration of heroin or sucrose resulted in differential expression of miRNAs in the OFC (Figures 1C–E; Supplementary Tables S1–S3). Exposure to heroin regulated 77 OFC miRNAs compared to drug-naïve animals, while sucrose only regulated 9 (Figures 2A, B). None of the sucrose-associated miRNAs were commonly regulated by heroin. The top 5 most regulated miRNAs in each comparison can be found in Table 1. Most heroin-regulated miRNAs were downregulated, suggesting a relief of miRNA inhibition of protein expression (Figure 2A). ~75% of the OFC miRNAs regulated between heroin and naïve animals were also regulated between heroin and sucrose animals, demonstrating that heroin induces a unique profile of OFC expression beyond that observed with an appetitive reward (Figure 2B). Because miRNAs regulate mRNA translation into protein, we performed bioinformatic analysis to determine the putative pathways that are regulated by heroin- or sucrose-associated miRNAs. Predicted targets of heroin-associated miRNAs are involved in signaling pathways related to "Prion diseases," "N-Glycan biosynthesis," "Proteoglycans in cancer," and "TGF-beta signaling," among others (Figure 2C). Only one pathway was enriched for predicted target genes of the 9 sucrose-associated miRNAs: "Mucin type O-Glycan biosynthesis" (Figure 2D). Pathways predicted to be targeted by miRNAs significantly regulated between heroin and sucrose animals were largely overlapping with heroin-associated miRNAs and included the most significant pathway, "Prion diseases" (Figure 2E). Genes predicted to be targeted by miRNAs in this pathway included many with known links to opioid exposure, including *Elk1*, *Egr1*, and *Erk1* (Table 2) [44, 49–54].

To provide more insight into both the reproducibility of our initial miRNA sequencing findings as well as determine the potential miRNA-mediated protein pathways that are associated with heroin or sucrose self-administration, we performed parallel proteomics profiling on OFC tissue from separate animals that self-administered heroin or sucrose (Figure 3). More than 2,000 proteins were detected in the OFC with label-free mass spectrometry and heroin regulated expression of 43 OFC proteins relative to naïve animals and 60 OFC proteins relative to sucrose animals, while sucrose regulated expression of 33 OFC proteins relative to naïve animals (Figures 3A–D; Supplementary Tables S4–S7). 36 proteins were specifically regulated by heroin and not sucrose when compared to drug-naïve animals, while 57 proteins were specifically regulated by heroin and not sucrose when comparing to only sucrose animals (Figure 3D). 23 proteins were regulated by sucrose alone and not overlapping with heroin-exposed animals (Figure 3D). ~60% of heroin-associated proteins were upregulated

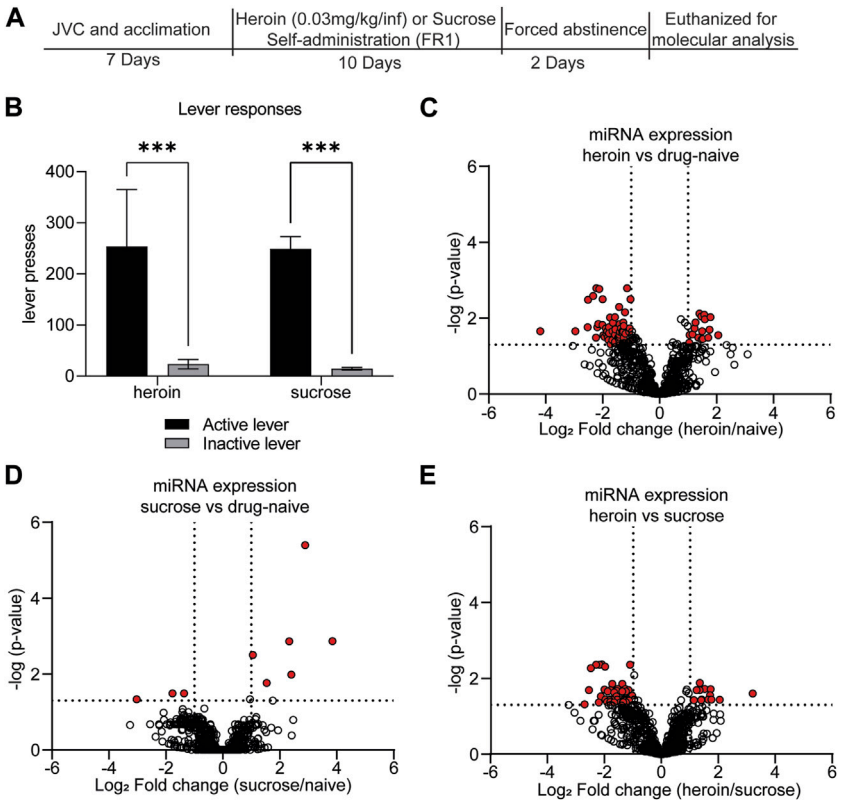

FIGURE 1
Self-administration of rewarding substances induces differential regulation of OFC miRNAs. **(A)** Experimental overview. Animals underwent acclimation and/or jugular vein catheterization (JVC). Seven days later, animals self-administered either heroin (0.03 mg/kg/infusion) for 6 h per day or sucrose pellets for 2 h per day for a total of 10 days. Animals underwent 2 days forced abstinence and were euthanized for molecular analysis of OFC and blood expression. **(B)** The average number of active or inactive lever responses across 10 days of self-administration of heroin or sucrose. $N = 11–12$/group. $^{***}p < 0.001$. Error bars depict ± the standard error of the mean (SEM). **(C–E)** Volcano plots depicting miRNA expression in the OFC for heroin vs. drug-naïve animals **(C)**, sucrose vs. drug-naïve animals **(D)**, or heroin vs. sucrose animals **(E)**. Red dots indicate miRNAs that were significantly regulated in each of the comparisons. Dotted lines indicate the threshold for significance based on p-value (horizontal) or $\log_2$ fold change (vertical).

(Figures 3A, C), in contrast to the large downregulation of OFC miRNAs, suggesting that heroin may repress expression of some miRNAs to allow for positive gene expression regulation. The top 5 proteins regulated in each comparison can be found in Table 3. None of the proteins regulated in the comparison of heroin to naïve animals were overlapping in the comparison of heroin to sucrose animals. However, 7 proteins were commonly regulated by both heroin and sucrose when each was compared to drug-free naïve animals (Figure 3D; Table 4). The pathways of the heroin-regulated proteins included "Proteosome," and several neurodegenerative pathways that all contained the similar proteins, such as "Amyotrophic lateral sclerosis," "Parkinson disease" and "Prion disease," "Huntington disease" and "Alzheimer disease" (Figure 3E). The only pathway significantly enriched for sucrose-associated OFC proteins was "Metabolic pathways" (Supplementary Figure S1). Proteins regulated by heroin compared to sucrose were significantly enriched in terms such as "Amyotrophic lateral sclerosis," "Mineral absorption," "Tight junction" and "Huntington disease" (Supplementary Figure S1). We overlapped the heroin-regulated OFC proteomics dataset with the small-RNA sequencing data of OFC miRNAs regulated following 2D forced abstinence from heroin and observed a high degree of overlap between the datasets (Figure 3F). Nearly two-thirds of the heroin-induced proteins are predicted to be regulated by a miRNA-mRNA interaction and approximately half of the heroin-regulated miRNAs targeted at least one mRNA for a heroin-associated protein (Figure 3F). This data indicates that heroin regulates OFC miRNA pathways.

To provide insight into the potential biomarker utility of heroin-associated OFC miRNAs, we examined the expression patterns of a subset of these miRNAs in

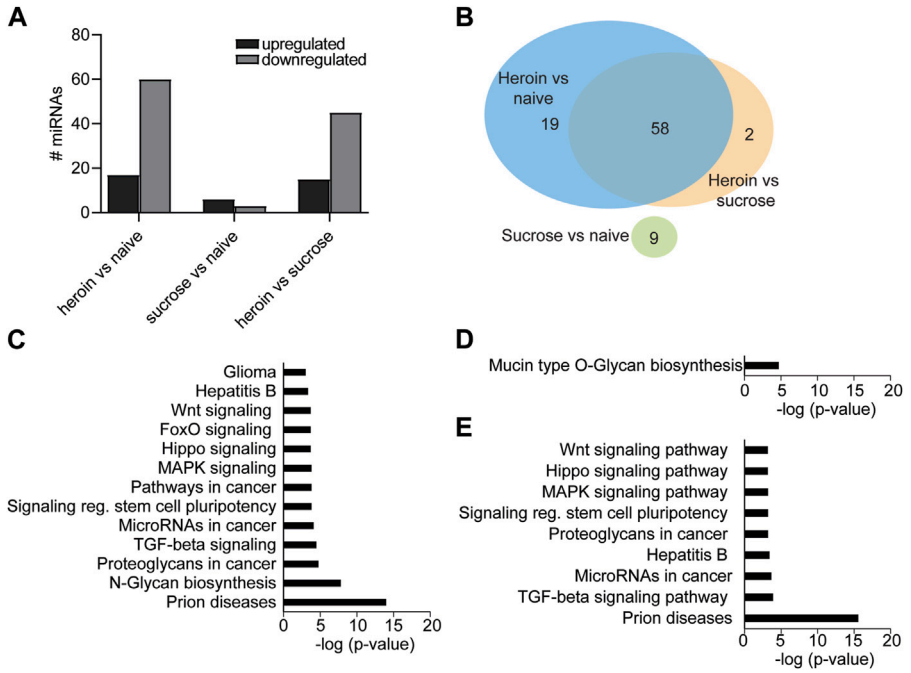

FIGURE 2
miRNA pathways in the OFC are regulated by acute withdrawal from heroin self-administration. **(A)** Number of miRNAs upregulated or downregulated following heroin or sucrose self-administration. **(B)** Venn diagram depicting the number of miRNAs that were overlapping or unique in the comparisons between heroin, sucrose, and naïve animals. **(C–E)** KEGG pathway terms of genes predicted to be targeted by miRNAs that were significantly enriched between heroin and naïve animals **(C)**, sucrose and naïve **(D)**, or heroin and sucrose **(E)**.

peripheral blood samples. Using RNA extracted from exosomes in serum blood samples, we performed qPCR to measure expression of 10 miRNAs that were regulated in the OFC: miR-107-3p; miR-135a-5p; miR-186-5p; miR-218b; miR-219a-5p; miR-29c-3p; miR-376a-3p; miR-379-5p; miR-451-5p; miR-877-5p (Figure 4A). These miRNAs were chosen based on their robust expression values in the central nervous system as well as their high fold change values in the OFC. Three of the miRNAs, miR-135a-5p, miR-218b, and miR-376a-3p, had very low expression in serum samples and were not able to be quantified. Of the remaining 7 miRNAs we examined, miR-186-5p was significantly downregulated (t [12] = 2.179; p = 0.050) and both miR-29c-3p and miR-877-5p were significantly upregulated (miR-29c-3p: Mann-Whitney U = 5, p = 0.006; miR-877-5p: unpaired t-test: t [13] = 5.115; p = 0.0002) (Figure 4A). The regulation of miR-186-5p and miR-877 mirrored the opioid-induced differential regulation of these two miRNAs observed in the OFC. Expression levels of three miRNAs positively correlated with heroin infusions administered on the last day of self-administration: miR-107-3p (Pearson r = 0.754; p = 0.050), miR-186-5p (Pearson r = 0.785; p = 0.036) and miR-219a-5p (Pearson r = 0.805; p = 0.029) (Figures 4B–D). These data demonstrate that blood miRNA levels may, in some instances, reflect heroin-induced regulation of OFC miRNAs.

Discussion

Opioid exposure results in brain-region specific regulation of the miRNA profile. Our results demonstrate that acute abstinence from heroin self-administration results in a robust regulation of both miRNAs and proteins in the OFC. In a prior study, we determined that heroin self-administration induces lasting regulation of OFC miRNAs that may be manipulated to modulate long-lasting heroin seeking behavior [24]. The present work identified a unique profile of OFC miRNA regulation during acute abstinence that greatly differed from that observed in the OFC following late abstinence. This data demonstrate that the brain undergoes neuroadaptations following cessation of drug use and the best miRNA pathways to target pharmacologically for reduction of drug seeking behavior may be dynamically regulated in a time-dependent manner, as we have previously observed for morphine exposure [7]. Of the 77 heroin-associated miRNAs that were identified as differentially regulated in the OFC between heroin and naïve animals, we determined that none of the miRNAs were overlapping with the OFC profile following between sucrose self-administration and naive. However, we identified 7 proteins commonly regulated in the OFC following heroin or sucrose self-administration relative to naïve animals. These data suggest that the profile of heroin-associated miRNAs we identified is

TABLE 1 Top miRNAs regulated by heroin and sucrose.

Top 5 miRNAs regulated by heroin relative to naïve animals

miRNA	miRBase Accession	*p*-value, adj	Log2FC
rno-miR-10b-5p	MIMAT0000783	0.022	−4.192
rno-miR-19a-3p	MIMAT0000789	0.022	−2.964
rno-miR-764-3p	MIMAT0017370	0.017	−2.527
rno-miR-29c-3p	MIMAT0000803	0.003	−2.516
rno-miR-377-3p	MIMAT0003123	0.003	−2.338

Top 5 miRNAs regulated by sucrose relative to naïve animals

miRNA	miRBase Accession	*p*-value, adj	Log2FC
rno-let-7a-5p	MIMAT0000774	0.046	−3.031
rno-miR-214-3p	MIMAT0000885	0.001	2.331
rno-miR-196a-5p	MIMAT0000871	0.010	2.403
rno-miR-133a-3p	MIMAT0000839	<0.001	2.888
rno-miR-196b-5p	MIMAT0001082	0.001	3.849

Top 5 miRNAs regulated by heroin relative to sucrose animals

miRNA	miRBase Accession	*p*-value, adj	Log2FC
rno-miR-19a-3p	MIMAT0000789	0.048	−2.707
rno-miR-764-3p	MIMAT0017370	0.020	−2.557
rno-miR-29c-3p	MIMAT0000803	0.005	−2.490
rno-miR-377-3p	MIMAT0003123	0.004	−2.302
rno-miR-183-5p	MIMAT0000860	0.025	3.193

TABLE 2 miRNA-mediated protein pathways enriched for 'Prion Disease' in heroin animals, relative to both naïve and sucrose comparisons.

Putative miRNA-targeted genes in "Prion Disease" pathway, commonly regulated by heroin vs. naïve or sucrose

Ensembl ID	Gene name	miRNA
ENSRNOG00000007697	*C8a*	rno-miR-764-3p
ENSRNOG00000019422	*Egr1*	rno-miR-300-3p
ENSRNOG00000010171	*Elk1*	rno-miR-495, rno-miR-873-5p
ENSRNOG00000000596	*Fyn*	rno-miR-495
ENSRNOG00000018294	*Hspa5*	rno-miR-495, rno-miR-379-5p
ENSRNOG00000004575	*Il1a*	rno-miR-495, rno-miR-30e-5p, rno-miR-543-3p, rno-miR-758-3p
ENSRNOG00000002680	*Lamc1*	rno-miR-340-5p, rno-miR-764-3p, rno-miR-29a-3p, rno-miR-29b-3p, rno-miR-29c-3p
ENSRNOG00000019601	*Mapk3 (Erk1)*	rno-miR-15a-5p
ENSRNOG00000031890	*Ncam1*	rno-miR-466b-5p
ENSRNOG00000002126	*Ncam2*	rno-miR-340-5p, rno-miR-127-5p
ENSRNOG00000019322	*Notch1*	rno-miR-340-5p
ENSRNOG00000003696	*Prkx*	rno-miR-495, rno-miR-873-5p, rno-miR-3065-5p
ENSRNOG00000021259	*Prnp*	rno-miR-107-5p, rno-miR-466b-5p
ENSRNOG00000021164	*Stip1*	rno-miR-340-5p

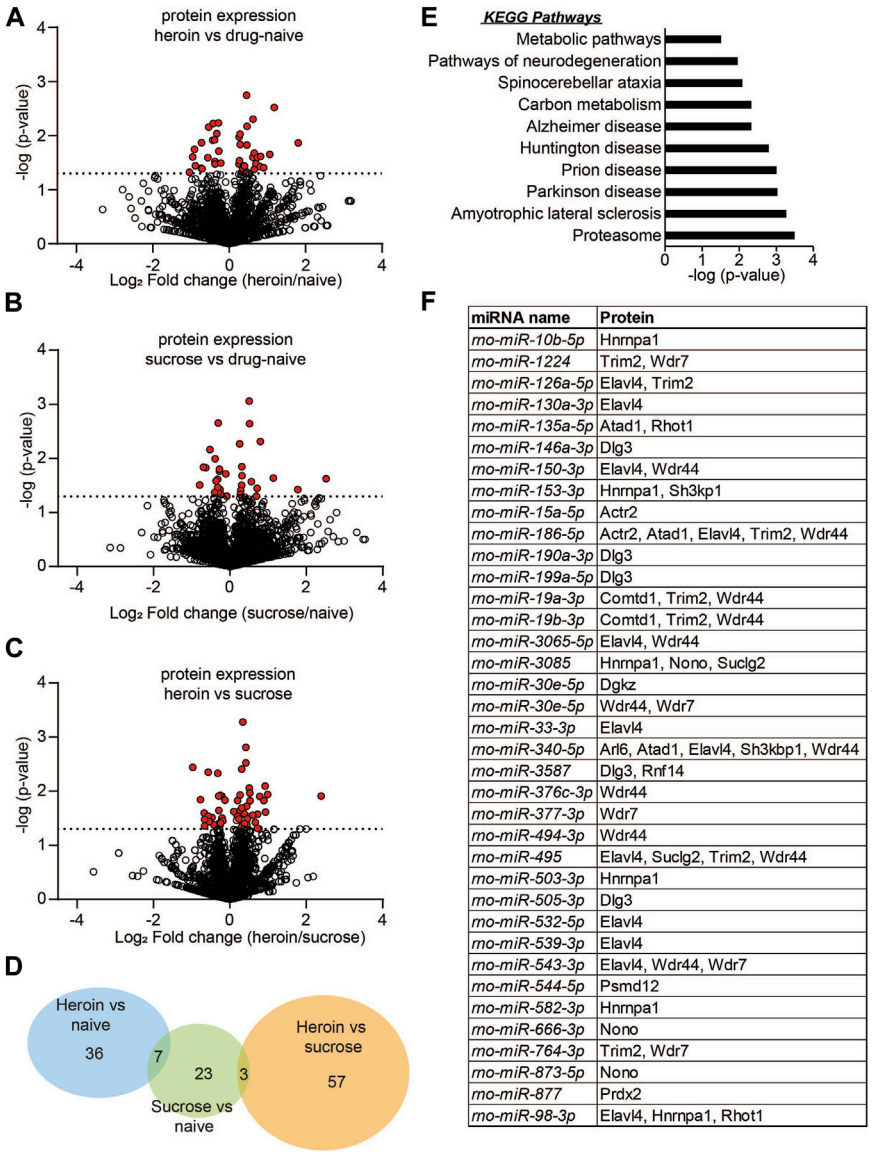

miRNA name	Protein
mo-miR-10b-5p	Hnrnpa1
mo-miR-1224	Trim2, Wdr7
mo-miR-126a-5p	Elavl4, Trim2
mo-miR-130a-3p	Elavl4
mo-miR-135a-5p	Atad1, Rhot1
mo-miR-146a-3p	Dlg3
mo-miR-150-3p	Elavl4, Wdr44
mo-miR-153-3p	Hnrnpa1, Sh3kp1
mo-miR-15a-5p	Actr2
mo-miR-186-5p	Actr2, Atad1, Elavl4, Trim2, Wdr44
mo-miR-190a-3p	Dlg3
mo-miR-199a-5p	Dlg3
mo-miR-19a-3p	Comtd1, Trim2, Wdr44
mo-miR-19b-3p	Comtd1, Trim2, Wdr44
mo-miR-3065-5p	Elavl4, Wdr44
mo-miR-3085	Hnrnpa1, Nono, Suclg2
mo-miR-30e-5p	Dgkz
mo-miR-30e-5p	Wdr44, Wdr7
mo-miR-33-3p	Elavl4
mo-miR-340-5p	Arl6, Atad1, Elavl4, Sh3kbp1, Wdr44
mo-miR-3587	Dlg3, Rnf14
mo-miR-376c-3p	Wdr44
mo-miR-377-3p	Wdr7
mo-miR-494-3p	Wdr44
mo-miR-495	Elavl4, Suclg2, Trim2, Wdr44
mo-miR-503-3p	Hnrnpa1
mo-miR-505-3p	Dlg3
mo-miR-532-5p	Elavl4
mo-miR-539-3p	Elavl4
mo-miR-543-3p	Elavl4, Wdr44, Wdr7
mo-miR-544-5p	Psmd12
mo-miR-582-3p	Hnrnpa1
mo-miR-666-3p	Nono
mo-miR-764-3p	Trim2, Wdr7
mo-miR-873-5p	Nono
mo-miR-877	Prdx2
mo-miR-98-3p	Elavl4, Hnrnpa1, Rhot1

FIGURE 3
Protein expression is regulated in the OFC following acute abstinence from heroin self-administration. **(A–C)** Volcano plots depicting protein expression in the OFC for heroin vs. drug naïve animals **(A)**, sucrose vs. drug-naïve animals **(B)**, or heroin vs. sucrose animals **(C)**. Red dots indicate proteins that were significantly regulated in each of the comparisons. Dotted line indicates the threshold for significance based on *p*-value. **(D)** Venn diagram depicting the number of proteins that were regulated in each comparison of **(A–C)**. **(E)** KEGG pathway terms of proteins that were significantly enriched between heroin and naïve animals. **(F)** Overlap of miRNA sequencing data with proteomics to depict the significantly regulated miRNAs that are predicted to target significantly regulated proteins following chronic heroin.

likely due to drug exposure and not learning a rewarding task. In addition, the common proteins regulated by both sucrose and heroin may be due to miRNA-independent pathways, or the unique profile of miRNAs regulated by sucrose and heroin commonly target the same OFC proteins.

In comparison with our previously published study that examined miRNA regulation associated with long-lasting heroin seeking behavior following 21D forced abstinence from either 0.03 mg/kg/infusion or 0.075 mg/kg/infusion heroin, we observed some overlap of heroin-regulated miRNA expression in the OFC. 5 miRNAs were commonly regulated following 2 or 21D forced abstinence from the 0.03 mg/kg/infusion heroin dose: miR-219a-5p, miR-299a-5p, miR-29c-3p, miR-666-3p and miR-764-3p. In addition to miR-219a-5p, miR-218b, miR-3065-5p, miR-338-3p, miR-379-5p and miR-503-3p, which were regulated in the present study following 2D forced abstinence from

TABLE 3 Top proteins regulated by heroin or sucrose.

Top 5 proteins regulated by heroin relative to naïve animals

Uniprot Accession	Protein Description	Protein Symbol	Log2FC
Q3ZAU6	RBR-type E3 ubiquitin transferase	Rnf14	−1.043
A0A0G2JSH9	Peroxiredoxin 2	Prdx2	−0.959
P40307	Proteasome subunit beta type-2	Psmb2	1.059
D3ZAF6	ATP syntdase subunit f, mitochondrial	Atp5mf	1.179
A0A0G2K707	Diacylglycerol kinase	Dgkz	1.806

Top 5 proteins regulated by sucrose relative to naïve animals

Uniprot Accession	Protein Description	Protein Symbol	Log2FC
P32232	Cystatdionine beta-syntdase	Cbs	−0.794
P11348	Dihydropteridine reductase	Qdpr	0.795
Q62785	28 kDa heat- and acid-stable phosphoprotein	Pdap1	1.138
Q6QIX3	Probable proton-coupled zinc antiporter	Slc30a3	1.777
M0R4L7	Histone Cluster 1 H2B Family Member L	Hist1h2bl	2.518

Top 5 proteins regulated by heroin relative to sucrose animals

Uniprot Accession	Protein Description	Protein Symbol	Log2FC
Q6QIX3	Probable proton-coupled zinc antiporter	Slc30a3	−0.970
F1MAH8	CAP-Gly domain-containing linker protein 1	Clip1	0.923
Q6MGC4	H2-K region expressed gene 2, rat ortdologue	Pfdn6	0.933
A0A0G2K4W2	Transcription factor BTF3	Btf3	0.990
Q6IRG7	Claudin	Cldn11	2.388

TABLE 4 Proteins commonly regulated by heroin or sucrose comparisons.

Commonly regulated by sucrose relative to drug-naïve or heroin animals

Uniprot Accession	Protein Description	Protein Symbol	Length
D3ZAN3	Alpha glucosidase 2 alpha neutral subunit (Predicted)	Ganab	797 AA
Q920Q0	Paralemmin-1	Palm	383 AA
Q6QIX3	Probable proton-coupled zinc antiporter SLC30A3	Slc30a3	388 AA

Commonly regulated by heroin and sucrose relative to drug-naïve animals

Uniprot Accession	Protein Description	Protein Symbol	Length
P09117	Fructose-bisphosphate aldolase C	Aldoc	363 AA
B1WC73	ADP-ribosylation factor-like protein 6	Arl6	186 AA
A0A0H2UHI7	ATPase family, AAA domain containing 1	Atad1	403 AA
D3ZM21	Catechol-O-metdyltransferase domain containing 1	Comtd1	262 AA
P47942	Dihydropyrimidinase-related protein 2	Dpysl2	572 AA
A0A140TAF2	ELAV-like protein 4	Elavl4	385 AA
Q925Q9	SH3 domain-containing kinase-binding protein 1	Sh3kbp1	709 AA

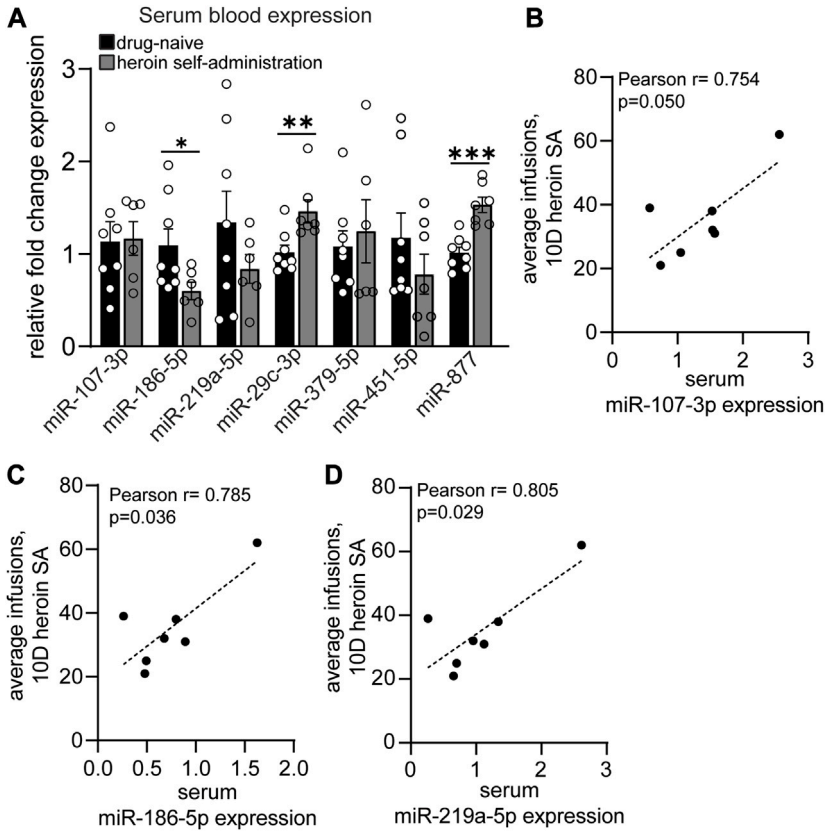

FIGURE 4
Acute withdrawal from heroin self-administration induces miRNA expression regulation in the blood that reflects the OFC profile. **(A–D)** Serum blood expression of heroin-associated miRNAs measured by qPCR in drug-naïve and heroin self-administration animals. **(B–D)** Correlations between serum miRNA expression and the average number of heroin infusions over the course of 10 days of self-administration. *N* = 6–8/group. $^{*}p < 0.05$. $^{**}p < 0.01$. $^{***}p < 0.001$. Error bars depict ± SEM.

0.03 mg/kg/infusion heroin, were also regulated in the OFC following 21D forced abstinence from a higher heroin dose of 0.075 mg/kg/infusion. The combination of these two studies demonstrates that some miRNAs, such as miR-219a-5p, are regulated by both high and low doses of heroin. Moreover, a subset of miRNAs are regulated immediately following heroin and remain altered for at least 21D following the last heroin self-administration session. This later finding demonstrates that miRNA regulation in the OFC is a long-lasting neuroadaptation that results from chronic heroin exposure. The dynamic responsiveness of miRNAs to opioids is likely dependent on drug dose, timepoint and region specificity. However, the present study is limited in that it does not address the contribution of the aforementioned variables on heroin-induced miRNA expression. Future studies that include animals of both sexes, additional timepoints following drug exposure, profiling of multiple brain regions and variable periods of drug exposure that may more accurately model physical dependence are likely to yield additional insight into the impact of heroin on miRNA expression. Validation of RNA-sequencing and proteomics with secondary measures will also help to narrow down the most relevant miRNAs for support of drug seeking behavior. While our study did not perform secondary validation with qPCR or western blots, the sequencing and proteomics datasets were obtained from separate groups of animals, yet we still observed overlap of putative heroin-regulated miRNA pathways with the proteomics data (Figure 3F).

The correspondence of the "Prion disease" pathway enriched for proteins regulated by heroin, as well as putative gene targets of miRNAs regulated by heroin, demonstrates the reproducibility of our findings. The genes predicted to be regulated in the "Prion disease" pathway by heroin-associated miRNAs included several transcription factors that have been demonstrated to regulate expression of proteins observed in our heroin-associated protein list, including Atp5pd (*Elk1*) and Uqcrfs1 (*Elk1*) [55]. These results are not surprising, given that the KEGG entry for the "Prion disease" pathway includes many genes known to be involved in drug-induced neuropathologies, including Erk1/2, CREB, Egr1, p38/JNK, GSK-3B, PKA, Fyn, and other genes involved in

proteosomal and mitochondrial function [43, 44, 49–51, 56–59]. However, by describing a pattern of genes regulated by heroin-associated miRNAs in the OFC, our study begins to fill in the molecular gap between heroin exposure and heroin-induced neuroadaptations. These findings suggest that miRNAs may function as key modulators of heroin-regulated proteins.

Published studies have reported differential regulation of miRNA expression in peripheral blood samples from humans exposed to opioids [28, 30, 60–64]. Demonstration of the utility of detecting miRNA expression in peripheral blood samples is evidenced by the observation that miRNAs may be predictive of need for hospitalization or pharmacological interventions in opioid-exposed infants [62]. However, it is unclear how the blood miRNA profile reflects brain-region specific miRNA expression induced by drugs. Only one such study has been performed with human samples, and this is likely due to the challenges of collecting blood and postmortem samples in a timely manner. Grimm et al reported the correspondence of frontal cortex brain and blood miRNA levels in postmortem human samples from OUD subjects and observed a large overlap in miRNA expression [65]. Of the miRNA profile measured in the BA9 region, the authors observed differential expression of hsa-miR-10b-5p, hsa-miR-337-3p, has-miR-340-5, hsa-miR-376a-3p, hsa-miR-376b-3p, hsa-miR-379-5p, hsa-miR-486-3p, hsa-miR-495-3p, and hsa-miR-758-3p [65], which were all dysregulated in the OFC of heroin-exposed rats in the current study. Investigation into the relationship between drug exposure and regulation of brain miRNAs that can also be detected in the periphery can be accomplished easily with rodent models of self-administration but has yet to be done. We report for the first time the regulation of two miRNAs, miR-186-5p and miR-877, in both the OFC and the serum of animals that have previously self-administered heroin. We identified three miRNAs that correlated with heroin infusions-miR-186-5p, miR-107-3p and miR-219a-5p-which suggests that miRNAs may have putative biomarker utility for understanding drug motivation or abstinence behavior. Indeed, miR-186-5p was significantly reduced in both the OFC and serum of heroin-exposed animals in our study, as well in peripheral blood samples obtained from humans that meet criteria for OUD [63]. We also identified miR-451-5p as a miRNA downregulated in the OFC following heroin self-administration and this miRNA was significantly downregulated in blood exosomal samples from human patients with heroin use disorder [64]. Additional studies to understand the responsiveness of blood miRNA expression as an indication of opioid craving or recovery from OUD may help to inform patient care in the clinic.

Data availability statement

The datasets presented in this study can be found in online repositories. The names of the repository/repositories and accession number(s) can be found in the article/Supplementary Material.

Ethics statement

The animal studies were approved by Temple Institutional Animal Care and Use Committee. The studies were conducted in accordance with the local legislation and institutional requirements. Written informed consent was obtained from the owners for the participation of their animals in this study.

Author contributions

Conceptualization, SS; methodology, SS, MZ, LS, and PM; formal analysis, SS, MZ, LS, and PM; data collection, MZ, LS, and PM; writing-original draft preparation, SS; writing-review and editing: SS, MZ, LS, and PM; supervision, SS; project administration, SS; funding acquisition, SS. All authors contributed to the article and approved the submitted version.

Funding

This work was supported by NIDA/NIH grants R00DA041469 (SS) and the NIDA P30 Core Grant DA013429 (Temple). The funders had no role in study design, data collection and analysis, decision to publish, or preparation of the manuscript.

Conflict of interest

The authors declare that the research was conducted in the absence of any commercial or financial relationships that could be construed as a potential conflict of interest.

Acknowledgments

Heroin was obtained from the NIDA Drug Supply Program. We thank Florine Collins and Rashaun Wilson at the Keck MS & Proteomics Resource at Yale University for mass spectrometry and proteomics. We acknowledge the Yale School of Medicine for providing mass spectrometers and biotechnology tools necessary for mass spectrometry, which is funded in part by National Institutes of Health grants S10OD02365101A1, S10OD019967, and S10OD018034.

Supplementary material

The Supplementary Material for this article can be found online at: https://www.frontierspartnerships.org/articles/10.3389/adar.2023.11668/full#supplementary-material

References

1. Buresh M, Stern R, Rastegar D. Treatment of opioid use disorder in primary care. *Bmj* (2021) 373:n784. doi:10.1136/bmj.n784

2. Hedegaard H, Miniño AM, Warner M. Drug overdose deaths in the United States, 1999-2015. *NCHS Data Brief* (2020) 394:1–8.

3. Hedegaard H, Miniño AM, Warner M. Co-involvement of opioids in drug overdose deaths involving cocaine and psychostimulants. *NCHS Data Brief* (2021) 406:1–8.

4. Grella CE, Lovinger K. 30-year trajectories of heroin and other drug use among men and women sampled from methadone treatment in California. *Drug Alcohol Depend* (2011) 118(2-3):251–8. doi:10.1016/j.drugalcdep.2011.04.004

5. Smyth BP, Barry J, Keenan E, Ducray K. Lapse and relapse following inpatient treatment of opiate dependence. *Ir Med J* (2010) 103(6):176–9.

6. Zanda MT, Floris G, Sillivan SE. Drug-associated cues and drug dosage contribute to increased opioid seeking after abstinence. *Sci Rep* (2021) 11(1): 14825. doi:10.1038/s41598-021-94214-4

7. Gillespie A, Mayberry HL, Wimmer ME, Sillivan SE. microRNA expression levels in the nucleus accumbens correlate with morphine-taking but not morphine-seeking behaviour in male rats. *Eur J Neurosci* (2022) 55(7):1742–55. doi:10.1111/ejn.15650

8. Shalev U, Morales M, Hope B, Yap J, Shaham Y. Time-dependent changes in extinction behavior and stress-induced reinstatement of drug seeking following withdrawal from heroin in rats. *Psychopharmacology (Berl)* (2001) 156(1):98–107. doi:10.1007/s002130100748

9. Mayberry HL, Bavley CC, Karbalaei R, Peterson DR, Bongiovanni AR, Ellis AS, et al. Transcriptomics in the nucleus accumbens shell reveal sex- and reinforcer-specific signatures associated with morphine and sucrose craving. *Neuropsychopharmacology* (2022) 47:1764–75. doi:10.1038/s41386-022-01289-2

10. Bartel DP. MicroRNAs: genomics, biogenesis, mechanism, and function. *Cell* (2004) 116(2):281–97. doi:10.1016/s0092-8674(04)00045-5

11. Friedman RC, Farh KK, Burge CB, Bartel DP. Most mammalian mRNAs are conserved targets of microRNAs. *Genome Res* (2009) 19(1):92–105. doi:10.1101/gr.082701.108

12. Bahi A, Dreyer JL. Striatal modulation of BDNF expression using microRNA124a-expressing lentiviral vectors impairs ethanol-induced conditioned-place preference and voluntary alcohol consumption. *Eur J Neurosci* (2013) 38(2):2328–37. doi:10.1111/ejn.12228

13. Chandrasekar V, Dreyer JL. microRNAs miR-124, let-7d and miR-181a regulate cocaine-induced plasticity. *Mol Cel Neurosci* (2009) 42(4):350–62. doi:10.1016/j.mcn.2009.08.009

14. Hollander JA, Im HI, Amelio AL, Kocerha J, Bali P, Lu Q, et al. Striatal microRNA controls cocaine intake through CREB signalling. *Nature* (2010) 466(7303):197–202. doi:10.1038/nature09202

15. Im HI, Hollander JA, Bali P, Kenny PJ. MeCP2 controls BDNF expression and cocaine intake through homeostatic interactions with microRNA-212. *Nat Neurosci* (2010) 13(9):1120–7. doi:10.1038/nn.2615

16. Kim J, Im HI, Moon C. Intravenous morphine self-administration alters accumbal microRNA profiles in the mouse brain. *Neural Regen Res* (2018) 13(1): 77–85. doi:10.4103/1673-5374.224374

17. Mavrikaki M, Anastasiadou E, Ozdemir RA, Potter D, Helmholz C, Slack FJ, et al. Overexpression of miR-9 in the nucleus accumbens increases oxycodone self-administration. *Int J Neuropsychopharmacol* (2019) 22(6):383–93. doi:10.1093/ijnp/pyz015

18. Most D, Salem NA, Tiwari GR, Blednov YA, Mayfield RD, Harris RA. Silencing synaptic MicroRNA-411 reduces voluntary alcohol consumption in mice. *Addict Biol* (2019) 24(4):604–16. doi:10.1111/adb.12625

19. Pittenger ST, Schaal VL, Moore D, Guda RS, Koul S, Yelamanchili SV, et al. MicroRNA cluster miR199a/214 are differentially expressed in female and male rats following nicotine self-administration. *Sci Rep* (2018) 8(1):17464. doi:10.1038/s41598-018-35747-z

20. Tapocik JD, Barbier E, Flanigan M, Solomon M, Pincus A, Pilling A, et al. microRNA-206 in rat medial prefrontal cortex regulates BDNF expression and alcohol drinking. *J Neurosci* (2014) 34(13):4581–8. doi:10.1523/JNEUROSCI.0445-14.2014

21. Xu W, Hong Q, Lin Z, Ma H, Chen W, Zhuang D, et al. Role of nucleus accumbens microRNA-181a and MeCP2 in incubation of heroin craving in male rats. *Psychopharmacology (Berl)* (2021) 238(8):2313–24. doi:10.1007/s00213-021-05854-3

22. Quinn RK, James MH, Hawkins GE, Brown AL, Heathcote A, Smith DW, et al. Temporally specific miRNA expression patterns in the dorsal and ventral striatum of addiction-prone rats. *Addict Biol* (2018) 23(2):631–42. doi:10.1111/adb.12520

23. Yan B, Hu Z, Yao W, Le Q, Xu B, Liu X, et al. MiR-218 targets MeCP2 and inhibits heroin seeking behavior. *Sci Rep* (2017) 7:40413. doi:10.1038/srep40413

24. Zanda MT, Floris G, Sillivan SE. Orbitofrontal cortex microRNAs support long-lasting heroin seeking behavior in male rats. *Transl Psychiatry* (2023) 13(1): 117. doi:10.1038/s41398-023-02423-4

25. Fanous S, Goldart EM, Theberge FR, Bossert JM, Shaham Y, Hope BT. Role of orbitofrontal cortex neuronal ensembles in the expression of incubation of heroin craving. *J Neurosci* (2012) 32(34):11600–9. doi:10.1523/JNEUROSCI.1914-12.2012

26. Sell LA, Morris JS, Bearn J, Frackowiak RS, Friston KJ, Dolan RJ. Neural responses associated with cue evoked emotional states and heroin in opiate addicts. *Drug Alcohol Depend* (2000) 60(2):207–16. doi:10.1016/s0376-8716(99)00158-1

27. Sillivan SE, Jamieson S, de Nijs L, Jones M, Snijders C, Klengel T, et al. MicroRNA regulation of persistent stress-enhanced memory. *Mol Psychiatry* (2019) 25:965–76. doi:10.1038/s41380-019-0432-2

28. Toyama K, Kiyosawa N, Watanabe K, Ishizuka H. Identification of circulating miRNAs differentially regulated by opioid treatment. *Int J Mol Sci* (2017) 18(9): 1991. doi:10.3390/ijms18091991

29. Xu W, Zhao M, Lin Z, Liu H, Ma H, Hong Q, et al. Increased expression of plasma hsa-miR-181a in male patients with heroin addiction use disorder. *J Clin Lab Anal* (2020) 34(11):e23486. doi:10.1002/jcla.23486

30. Gu WJ, Zhang C, Zhong Y, Luo J, Zhang CY, Wang C, et al. Altered serum microRNA expression profile in subjects with heroin and methamphetamine use disorder. *Biomed Pharmacother* (2020) 125:109918. doi:10.1016/j.biopha.2020.109918

31. Wang X, Sun L, Zhou Y, Su QJ, Li JL, Ye L, et al. Heroin abuse and/or HIV infection dysregulate plasma exosomal miRNAs. *J Neuroimmune Pharmacol* (2020) 15(3):400–8. doi:10.1007/s11481-019-09892-9

32. Shi X, Li Y, Yan P, Shi Y, Lai J. Weighted gene co-expression network analysis to explore the mechanism of heroin addiction in human nucleus accumbens. *J Cel Biochem* (2020) 121(2):1870–9. doi:10.1002/jcb.29422

33. Floris G, Gillespie A, Zanda MT, Dabrowski KR, Sillivan SE. Heroin regulates orbitofrontal circular RNAs. *Int J Mol Sci* (2022) 23(3):1453. doi:10.3390/ijms23031453

34. Sillivan SE, Jones ME, Jamieson S, Rumbaugh G, Miller CA. Bioinformatic analysis of long-lasting transcriptional and translational changes in the basolateral amygdala following acute stress. *PLoS One* (2019) 14(1):e0209846. doi:10.1371/journal.pone.0209846

35. Langmead B, Wilks C, Antonescu V, Charles R. Scaling read aligners to hundreds of threads on general-purpose processors. *Bioinformatics* (2019) 35(3): 421–32. doi:10.1093/bioinformatics/bty648

36. Vlachos IS, Zagganas K, Paraskevopoulou MD, Georgakilas G, Karagkouni D, Vergoulis T, et al. DIANA-miRPath v3.0: deciphering microRNA function with experimental support. *Nucleic Acids Res* (2015) 43(W1):W460–6. doi:10.1093/nar/gkv403

37. Huang d. W, Sherman BT, Lempicki RA. Systematic and integrative analysis of large gene lists using DAVID bioinformatics resources. *Nat Protoc* (2009) 4(1): 44–57. doi:10.1038/nprot.2008.211

38. Sherman BT, Hao M, Qiu J, Jiao X, Baseler MW, Lane HC, et al. David: a web server for functional enrichment analysis and functional annotation of gene lists (2021 update). *Nucleic Acids Res* (2022) 50:W216–W221. doi:10.1093/nar/gkac194

39. Tastsoglou S, Alexiou A, Karagkouni D, Skoufos G, Zacharopoulou E, Hatzigeorgiou AG. DIANA-MicroT 2023: including predicted targets of virally encoded miRNAs. *Nucleic Acids Res* (2023) 51(1):W148–W153. doi:10.1093/nar/gkad283

40. Livak KJ, Schmittgen TD. Analysis of relative gene expression data using real-time quantitative PCR and the 2(-Delta Delta C(T)) Method. *Methods* (2001) 25(4): 402–8. doi:10.1006/meth.2001.1262

41. Love MI, Huber W, Anders S. Moderated estimation of fold change and dispersion for RNA-seq data with DESeq2. *Genome Biol* (2014) 15(12):550. doi:10.1186/s13059-014-0550-8

42. Hochberg Y, Benjamini Y. More powerful procedures for multiple significance testing. *Stat Med* (1990) 9(7):811–8. doi:10.1002/sim.4780090710

43. Egervari G, Akpoyibo D, Rahman T, Fullard JF, Callens JE, Landry JA, et al. Chromatin accessibility mapping of the striatum identifies tyrosine kinase FYN as a therapeutic target for heroin use disorder. *Nat Commun* (2020) 11(1):4634. doi:10.1038/s41467-020-18114-3

44. Sillivan SE, Whittard JD, Jacobs MM, Ren Y, Mazloom AR, Caputi FF, et al. ELK1 transcription factor linked to dysregulated striatal mu opioid receptor signaling network and OPRM1 polymorphism in human heroin abusers. *Biol Psychiatry* (2013) 74(7):511–9. doi:10.1016/j.biopsych.2013.04.012

45. Egervari G, Landry J, Callens J, Fullard JF, Roussos P, Keller E, et al. Striatal H3K27 acetylation linked to glutamatergic gene dysregulation in human heroin abusers holds promise as therapeutic target. *Biol Psychiatry* (2017) 81(7):585–94. doi:10.1016/j.biopsych.2016.09.015

46. Brown TG, Xu J, Hurd YL, Pan YX. Dysregulated expression of the alternatively spliced variant mRNAs of the mu opioid receptor gene, OPRM1, in the medial prefrontal cortex of male human heroin abusers and heroin self-administering male rats. *J Neurosci Res* (2022) 100(1):35–47. doi:10.1002/jnr.24640

47. Reiner DJ, Lofaro OM, Applebey SV, Korah H, Venniro M, Cifani C, et al. Role of projections between piriform cortex and orbitofrontal cortex in relapse to fentanyl seeking after palatable food choice-induced voluntary abstinence. *J Neurosci* (2020) 40(12):2485–97. doi:10.1523/JNEUROSCI.2693-19.2020

48. Altshuler RD, Yang ES, Garcia KT, Davis IR, Olaniran A, Haile M, et al. Role of orbitofrontal cortex in incubation of oxycodone craving in male rats. *Addict Biol* (2021) 26(2):e12927. doi:10.1111/adb.12927

49. Ortiz J, Harris HW, Guitart X, Terwilliger RZ, Haycock JW, Nestler EJ. Extracellular signal-regulated protein kinases (ERKs) and ERK kinase (MEK) in brain: regional distribution and regulation by chronic morphine. *J Neurosci* (1995) 15(2):1285–97. doi:10.1523/jneurosci.15-02-01285.1995

50. Macey TA, Lowe JD, Chavkin C. Mu opioid receptor activation of ERK1/2 is GRK3 and arrestin dependent in striatal neurons. *J Biol Chem* (2006) 281(45): 34515–24. doi:10.1074/jbc.M604278200

51. Lyons D, de Jaeger X, Rosen LG, Ahmad T, Lauzon NM, Zunder J, et al. Opiate exposure and withdrawal induces a molecular memory switch in the basolateral amygdala between ERK1/2 and CaMKIIα-dependent signaling substrates. *J Neurosci* (2013) 33(37):14693–704. doi:10.1523/JNEUROSCI.1226-13.2013

52. Ferrer-Alcón M, García-Fuster MJ, La Harpe R, García-Sevilla JA. Long-term regulation of signalling components of adenylyl cyclase and mitogen-activated protein kinase in the pre-frontal cortex of human opiate addicts. *J Neurochem* (2004) 90(1):220–30. doi:10.1111/j.1471-4159.2004.02473.x

53. Kuntz-Melcavage KL, Brucklacher RM, Grigson PS, Freeman WM, Vrana KE. Gene expression changes following extinction testing in a heroin behavioral incubation model. *BMC Neurosci* (2009) 10:95. doi:10.1186/1471-2202-10-95

54. Kuntz KL, Patel KM, Grigson PS, Freeman WM, Vrana KE. Heroin self-Administration: II. CNS gene expression following withdrawal and cue-induced drug-seeking behavior. *Pharmacol Biochem Behav* (2008) 90(3):349–56. doi:10.1016/j.pbb.2008.03.019

55. Rouillard AD, Gundersen GW, Fernandez NF, Wang Z, Monteiro CD, McDermott MG, et al. The harmonizome: a collection of processed datasets gathered to serve and mine knowledge about genes and proteins. *Database (Oxford)* (2016) 2016:baw100. doi:10.1093/database/baw100

56. Besnard A, Bouveyron N, Kappes V, Pascoli V, Pagès C, Heck N, et al. Alterations of molecular and behavioral responses to cocaine by selective inhibition of Elk-1 phosphorylation. *J Neurosci* (2011) 31(40):14296–307. doi:10.1523/jneurosci.2890-11.2011

57. Caputi FF, Rullo L, Stamatakos S, Candeletti S, Romualdi P. Interplay between the endogenous opioid system and proteasome complex: beyond signaling. *Int J Mol Sci* (2019) 20(6):1441. doi:10.3390/ijms20061441

58. Calarco CA, Fox ME, Van Terheyden S, Turner MD, Alipio JB, Chandra R, et al. Mitochondria-related nuclear gene expression in the nucleus accumbens and blood mitochondrial copy number after developmental fentanyl exposure in adolescent male and female C57BL/6 mice. *Front Psychiatry* (2021) 12:737389. doi:10.3389/fpsyt.2021.737389

59. Sillivan SE, Black YD, Naydenov AV, Vassoler FR, Hanlin RP, Konradi C. Binge cocaine administration in adolescent rats affects amygdalar gene expression patterns and alters anxiety-related behavior in adulthood. *Biol Psychiatry* (2011) 70(6):583–92. doi:10.1016/j.biopsych.2011.03.035

60. Hsu CW, Huang TL, Tsai MC. Decreased level of blood MicroRNA-133b in men with opioid use disorder on methadone maintenance therapy. *J Clin Med* (2019) 8(8):1105. doi:10.3390/jcm8081105

61. Purohit P, Roy D, Dwivedi S, Nebhinani N, Sharma P. Association of miR-155, miR-187 and inflammatory cytokines IL-6, IL-10 and TNF-α in chronic opium abusers. *Inflammation* (2022) 45(2):554–66. doi:10.1007/s10753-021-01566-0

62. Mahnke AH, Roberts MH, Leeman L, Ma X, Bakhireva LN, Miranda RC. Prenatal opioid-exposed infant extracellular miRNA signature obtained at birth predicts severity of neonatal opioid withdrawal syndrome. *Sci Rep* (2022) 12(1): 5941. doi:10.1038/s41598-022-09793-7

63. Dai Q, Pu SS, Yang X, Li C, He Y, Liu X, et al. Whole transcriptome sequencing of peripheral blood shows that immunity/GnRH/PI3K-akt pathways are associated with opioid use disorder. *Front Psychiatry* (2022) 13:893303. doi:10.3389/fpsyt.2022.893303

64. Chen F, Xu Y, Shi K, Zhang Z, Xie Z, Wu H, et al. Multi-omics study reveals associations among neurotransmitter, extracellular vesicle-derived microRNA and psychiatric comorbidities during heroin and methamphetamine withdrawal. *Biomed Pharmacother* (2022) 155:113685. doi:10.1016/j.biopha.2022.113685

65. Grimm SL, Mendez EF, Stertz L, Meyer TD, Fries GR, Gandhi T, et al. MicroRNA-mRNA networks are dysregulated in opioid use disorder postmortem brain: further evidence for opioid-induced neurovascular alterations. *Front Psychiatry* (2022) 13:1025346. doi:10.3389/fpsyt.2022.1025346

ADAR

ADAR is the official journal of the International Drug Abuse Research Society and the International Narcotics Research Conference.

The journal aims to bring together drug and alcohol abuse scientists and clinicians from across the globe to share and discuss the current state of knowledge, challenges, and the future of drug addiction that continues to be a global problem.

Discover more of our Special Issues

See more →

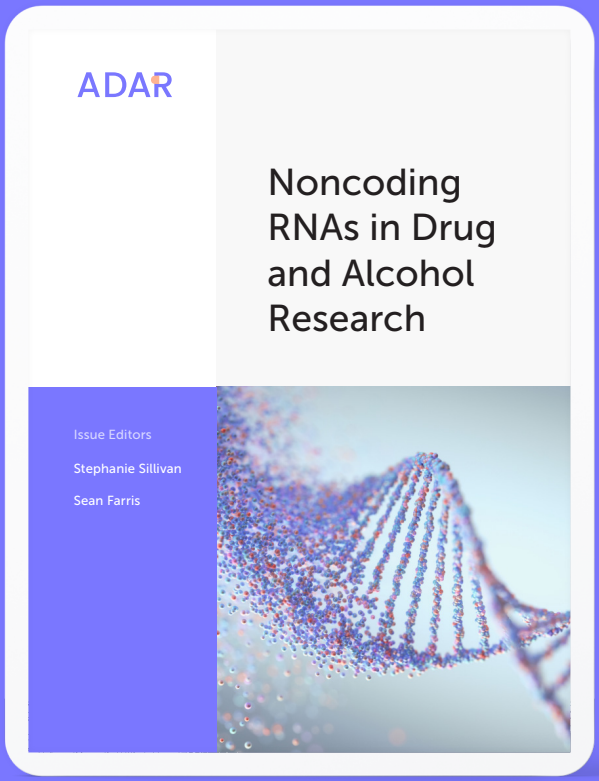

fro.ntiers.in/JPyM
frontierspartnerships.org

Contact
+41 (0) 21 510 17 40
adar@frontierspartnerships.org